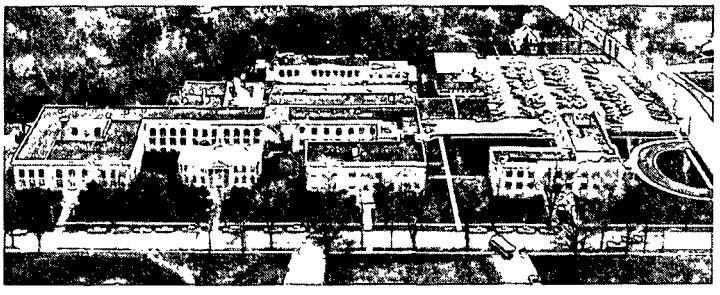

THE INSTITUTE OF PAPER CHEMISTRY, APPLETON, WISCONSIN

STATUS REPORTS

To The

PAPER PROPERTIES AND USES

PROJECT ADVISORY COMMITTEE

October 21-22, 1987
The Institute of Paper Chemistry
Continuing Education Center
Appleton, Wisconsin

NOTICE & DISCLAIMER

The Institute of Paper Chemistry (IPC) has provided a high standard of professional service and has exerted its best efforts within the time and funds available for this project. The information and conclusions are advisory and are intended only for the internal use by any company who may receive this report. Each company must decide for itself the best approach to solving any problems it may have and how, or whether, this reported information should be considered in its approach.

IPC does not recommend particular products, procedures, materials, or services. These are included only in the interest of completeness within a laboratory context and budgetary constraint. Actual products, procedures, materials, and services used may differ and are peculiar to the operations of each company.

In no event shall IPC or its employees and agents have any obligation or liability for damages, including, but not limited to, consequential damages, arising out of or in connection with any company's use of, or inability to use, the reported information. IPC provides no warranty or guaranty of results.

This information represents a review of on-going research for use by the Project Advisory Committees. The information is not intended to be a definitive progress report on any of the projects and should not be cited or referenced in any paper or correspondence external to your company.

Your advice and suggestions on any of the projects will be most welcome.

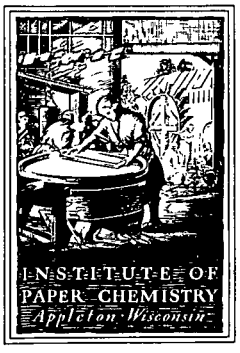

THE INSTITUTE OF PAPER CHEMISTRY
Post Office Box 1039
Appleton, Wisconsin 54912
Phone: 414/734-9251
Telex: 469289

October 2, 1987

TO: MEMBERS OF PAPER PROPERTIES AND USES PROJECT ADVISORY COMMITTEE

Attached for your review are the Status Reports for the Projects to be discussed at the Paper Properties and Uses PAC meeting scheduled for October 21-22, 1987, in Appleton. A meeting agenda can be found inside the booklet.

For those of you staying at the Continuing Education Center, the attached pink card gives the combination to the front door so that you may gain entrance if you arrive after the doors are locked. Room schedules are posted in the lobby. If you have not indicated whether you will be attending the meeting or have not yet reserved a room, please do so by notifying Sheila Burton at 414/738-3259.

We look forward to seeing you on October 21-22. Best regards.

Sincerely yours,

Gary A. Baum
Director
Paper Materials Division

GAB/sb
Enclosure

TABLE OF CONTENTS

AGENDA

PAPER PROPERTIES AND USES
PROJECT ADVISORY COMMITTEE

October 21-22, 1987
The Institute of Paper Chemistry
Continuing Education Center
Appleton, WI

Wednesday -- October 21

8:30 a.m.	Welcome/Introductions	Van Liew/Baum
8:45	OVERVIEW OF PROJECTS	Baum
9:15	PROJECT REVIEWS	
	Board Properties and Performance	Whitsitt/Halcomb/ Dees
10:30	COFFEE BREAK	
10:45	PROJECT REVIEWS	
	Process, Properties, Product Relationships	Baum/Habeger
12:00 noon	LUNCH (CEC Dining Room)	
1:00	TOUR OF PAPER MATERIALS DIVISION LABORATORIES	
2:15	PROJECT REVIEWS	
	Internal Strength Enhancement	Stratton
3:00	COFFEE BREAK	
3:15	PROJECT REVIEWS	
	Strength Improvement and Failure Mechanisms	Waterhouse
	On-Line Measurement of Paper Mechanical Properties	Hall/Habeger/Baum
5:15	SOCIAL TIME	
6:00	DINNER (CEC Dining Room)	
7:30	DISCUSSION OF RAC BRAINSTORMING MEETING	

Thursday -- October 22

7:15 a.m.	BREAKFAST (CEC Dining Room)	
8:00	DISCUSSION OF PROJECTS (Krannert 108/109)	Committee
10:00	DISCUSSION OF PROJECTS (continued)	
11:00	CLOSING COMMENTS	
	NEXT MEETING - March 23-24, 1988	
11:30	ADJOURNMENT/LUNCH (CEC Dining Room)	

PAPER PROPERTIES AND USES
PROJECT ADVISORY COMMITTEE

Dr. Gary Van Liew, Chairman -- 6/88*
Department Manager, Shipping
Container & Containerboard R&D
Weyerhaeuser Paper Company
WTC 2H42
Tacoma, WA 98477
(206) 924-6464

Mr. James E. Beatty -- 6/89
Technical Director
Amricon Corporation
800 South Lawe Street
P.O. Box 179
Appleton, WI 54912
(414) 733-3070

Dr. Robert L. Beran -- 6/89
Research Director
Westvaco Corporation
Covington Research Center
Washington Avenue
Covington, VA 24426
(703) 962-2111

Mr. Dennis Betz -- 6/89
Assistant Research Director
P. H. Glatfelter Co.
228 S. Main Street
Spring Grove, PA 17362
(717) 225-4711

Mr. Marvin D. Cooper -- 6/89
Resident Manager
Western Kraft Paper Group
Red River Mill
Willamette Industries, Inc.
P.O. Box 377
Campti, LA 71411
(318) 476-3392

Mr. Richard P. Grant -- 6/89
Senior Engineer
Eastman Kodak Company
1669 Lake Avenue
Bldg. 36
Rochester, NY 14650
(716) 477-6537

Dr. Peter F. Lee -- 6/88
Director, Pulp and Paper Technology
Mead Corporation
Central Research
8th and Hickory Street
Chillicothe, OH 45601
(614) 772-3528

Dr. James J. Nault -- 6/90
Assistant Papermill Superintendent
Stone Container Corporation
P.O. Box 201
Hopewell, VA 23860
(804) 541-9754

Dr. R. Heath Reeves -- 6/89
Sr. Research Associate
James River Corporation
Neenah Technical Center
1915 Marathon Avenue
Neenah, WI 54956
(414) 729-8148

Dr. Simon Salama -- 6/90
Group Leader
Union Camp Corporation
R&D Division
P.O. Box 3301
Princeton, NJ 08540-0148
(609) 896-1200

Mr. Lowell Schleicher -- 6/89
Director of Basic Research
Appleton Papers Inc.
P.O. Box 359
Appleton, WI 54912
(414) 735-8857

Mr. Robert L. Smathers -- 6/89
Manager, Technical Services
MacMillan Bloedel Inc.
P.O. Box 336
Pine Hill, AL 36769
(205) 963-4391

CONTINUED ON NEXT PAGE

*Date of retirement from committee.

PAC Project Advisory Committee continued.

Mr. Lynn D. Smeltzer -- 6/90
Quality Manager
Arkansas Kraft Corporation
P.O. Box 711
Morrilton, AR 72110
(501) 354-4521

Mr. David South -- 6/89
Director of Market Planning & Prod. Dev.
Chesapeake Corporation
P.O. Box 311
West Point, VA 23181
(804) 843-5252

Mr. Quinton W. Vancleave -- 6/90
Technical Manager
Kraft Paper and Paperboard Kraft
Georgia Pacific Corporatoin
133 Peachtree Street
Atlanta, GA 30303
404/521-5903

Mr. Gary W. White -- 6/89
Supervisor, Materials Development
Owens-Illinois, Inc.
One SeaGate - 25L-FP
Toledo, OH 43666
(419) 247-5786

9/87

THE INSTITUTE OF PAPER CHEMISTRY

Appleton, Wisconsin

Status Report

to the

PAPER PROPERTIES AND USES

PROJECT ADVISORY COMMITTEE

Project 3571

BOARD PROPERTIES AND PERFORMANCE

September 11, 1987

PROJECT SUMMARY

PROJECT NO. 3571: BOARD PROPERTIES AND PERFORMANCE September 11, 1987

PROJECT STAFF: W. J. Whitsitt, R. A. Halcomb, J. Dees

PROGRAM GOAL:

Develop relationships between critical paper and board property parameters and how they are achieved in terms of raw material selection, principles of sheet design, and processing conditions.

PROJECT OBJECTIVE:

- To develop relationships between container performance, combined board and component properties.

- To improve the performance/cost ratios of combined board (including medium).

- The short term goals are directed to (1) using structural models to assess the impact of papermaking factors on combined board and box performance and (2) improving liner and medium end-use and converting performance properties.

PROJECT RATIONALE, PREVIOUS ACTIVITY AND PLANNED ACTIVITY FOR FISCAL 1987-88 are on the Project Form that follows.

SUMMARY OF RESULTS LAST PERIOD: (October 1986 - March 1987)

(1) For similar papermaking conditions 40-lb mediums give 15-20% lower ECT strengths per weight of medium fiber than 26-lb mediums because they are damaged more in the fluting operation.

(2) Bulky sheets exhibit quite poor flat crush strengths per weight of medium fiber and this is particularly true at high basis weights. This is also a result of fluting damage.

(3) There should be opportunities to improve medium performance by achieving a better balance of ECT and flat crush strengths.

(4) Sheet porosity appears to be adversely affected by increasing fiber alignment in the machine direction.

Section 2. Runnability modeling.

(1) The wrap angle of the medium over the flute tips in the corrugating nip has been verified to be an important factor in our runnability model.

(2) The wrap angles for A-, B-, and C-flute profiles exhibit a sawtooth pattern depending on the relative position of the flute in the nip. This indicates that the medium is subjected to appreciable tension pulses even though the average brake tension is held constant.

(3) Corrugating trials showed that mediums run on B-flute rolls exhibited higher fracture speeds than when run on C-flute rolls.

(4) B-flute board generally gave fewer high-lows at a given speed than C-flute board.

(5) Good predictions of B-flute runnability were obtained using a wrap angle of 2.3 radians in our model. This compares with a wrap angle of 3.09 radians for C-flute.

Section 3 - ECT/Box Compression

(1) Models are being developed to optimize ECT, combined board flexural stiffness and box compression taking into account various papermaking changes in the manufacture of linerboard and medium.

(2) Improvements in liner compressive strength and elastic moduli improve ECT and flexural stiffness and, hence box compressive strength.

(3) Improvements in medium properties increase ECT and box compression but have small effects on flexural stiffness. However, stronger mediums should resist abuse in the distribution system which is a beneficial factor not taken into account as yet.

SUMMARY OF RESULTS THIS PERIOD: (March 1987 - October 1987)

Section 1 - Medium Improvement

(1) Medium performance can be improved by achieving a better balance of ECT and flat crush strengths.

(2) Mediums made with various degrees of wet pressing, MD/CD directionality and refining generally exhibited pin adhesion strengths which were about comparable.

(3) The differences in pin adhesion strengths for these mediums were not well related to any of the following properties: air porosity, water drop, smoothness, and sheet density. Similar results are being found in other work showing that better ways to characterize the bonding properties of liner and medium are needed.

Section 2 - Liner and Medium Improvement -- Surface Treatment

(1) As an alternative to wet end chemical treatments, we are planning to study the effects of chemical surface treatments on the converting and end-use properties of board.

Section 3 - Runnability Modeling

(1) In addition to four medium properties our runnability model incorporates the following factors: flute tip radius, total effective wrap angle in the corrugating nip and the medium brake tension.

(2) A sensitivity analysis of the above factors shows that for equal percentage changes the flute tip radius has a larger effect on high-lows than either the wrap angle or brake tension. Changes in wrap angle have greater effects on high-lows than brake tension but this may be misleading because the operator can change the tension over a wide range.

(3) Increasing the flute tip radius reduces high-lows. Reducing the wrap angle or medium brake tension reduces high-lows.

(4) An article describing development of our runnability model has been written and will be presented at the October TAPPI Corrugated Container Conference.

(5) Three modifications or applications of the modelling are under study.

Section 4 - ECT and Box Compression Relationships

(1) Two studies have been planned. One study is directed to checking our compression and flexural stiffness modeling using experimental linerboards combined with commercial mediums. The second study is directed to determining the effects of simulated service abuse on the box properties of board and using the information to evaluate ways to improve cost/performance ratios.

Section 5 - Flat Crush and Flute Formation Modeling

(1) A computer model was developed which quantitatively describes the flute shape in the corrugating labyrinth. Used in conjunction with a finite element analysis program, flute formation stresses in the medium are being studied.

(2) A laboratory study to determine the causes, extent and location of damage to the medium during flute formation has been planned. This information will be used in our flat crush and structural performance modeling as well as converting.

PROJECT TITLE: Board Properties and Performance

PROJECT STAFF: W. Whitsitt/R. Halcomb/J. Dees

PRIMARY AREA OF INDUSTRY NEED: Properties related to end uses.

PROGRAM AREA: Performance and Properties of Paper and Board

Date: 1/21/87
Budget: $160,000
Period Ends: 6/30/88
Project No: 3571

PROGRAM GOAL:

Develop relationships between critical paper and board property parameters and determine how they are achieved in terms of raw materials, sheet design, and processing conditions.

PROJECT OBJECTIVE/GOAL:

- To develop relationships between container performance, combined board properties, and component properties.
- To improve the performance/cost ratios of combined board, linerboard, and medium.
- The short term goals are to (1) use structural models to assess the impact of papermaking factors on combined board and box performance and (2) improve medium end-use and converting performance properties.

PROJECT RATIONALE:

There are many aspects of container and component performance which have not been adequately related to board properties through sound structural models. Such models would identify the critical board properties needed for end use performance. They would be used to select papermaking approaches to maintain or improve box performance at less cost. An important step is to incorporate the elastic stiffnesses of the board into such models, if possible. This will enable us to use our knowledge on how papermaking factors affect the elastic stiffnesses to make board improvements.

RESULTS TO DATE:

Past analyses of container failure under several types of load using Rayleigh-Ritz methods have shown that compressive strength (ECT) is the limiting property. Analysis of present ECT vs. component local buckling models indicates they fail to predict ECT performance when the liner or medium density is changed. Therefore new models have been developed which show that combined board ECT is primarily dependent on the compressive strength and/or elastic stiffnesses of the liners and medium. The bending stiffness of the liners appears to have only a minor effect on ECT. The importance of linerboard bending stiffness has been a point of concern to our industry and these results indicate that it is much less important than compressive strength. These results have been experimentally validated and are being extended to combined board flexural stiffness and box compression. Initial results show that basis weight/performance property ratios can be improved via densification and MD/CD changes.

In the case of medium we have shown that the compressive strength is lowered by high bending and shear stresses imposed during forming. These losses in strength lower flat crush and ECT. The losses are inversely related to the density and Z-direction elastic stiffness of the medium. Densification via wet pressing is one way to improve end-use performance of medium.

Our current forming models indicate that satisfactory high speed runnability on the corrugator is dependent on at least four medium properties as well as nip geometry and medium web tension. Better runnability is obtained as MD tensile strength and stretch are increased and the coefficient of friction of the medium and medium thickness are decreased.

PLANNED ACTIVITY FOR FY 1987-88:

As noted above, our short term objectives are directed to (1) using structural models to assess the impact of papermaking factors on combined board and box performance and (2) improving medium end-use and converting performance properties. The structural models we are developing show how the elastic stiffnesses and compressive strengths of the components will affect combined board compressive strength (ECT) and box compressive strength.

During 1987 we will expand these analyses to optimize strength-to-weight ratios. This will include consideration of the impact of papermaking changes on ECT, combined board flexural stiffness and box compression in relation to combined board basis weight. Both commercial and experimental boards will be used to validate the work. Another part of our structural research is directed to identifying the main medium properties affecting the flat crush load-deflection properties of combined board. For this purpose finite element techniques are being used to determine the stresses involved in forming the flute arch and their subsequent effects on converting and end-use performance.

In the converting area we have developed a model which reveals that critical speeds for flute fracture and high-lows depend on four properties of the medium, the nip geometry of the fluting rolls, and the medium web tension. During FY 1987-88 we plan to expand our model to consider other flute geometries and to study the potential effects of papermaking changes on both runnability and compressive strength. Currently data is being collected to determine how strength losses during fluting are related to the model stress predictions.

In another part of our fluting work power spectral techniques are being used to determine why high-lows tend to occur at periodic intervals and to relate the frequencies involved to machine elements. While a part of this work will be shifted over to FKBG, basic research on vibration phenomena as related to high-low generation will continue under this project.

Status Report

BOARD PROPERTIES AND PERFORMANCE

Project 3571

The objectives of this program are to: (1) develop relationships between container performance, combined board and component properties, and (2) determine ways to improve the cost/performance ratios of medium and linerboard. To fulfill these objectives both end-use performance and processing runnability on the corrugator are being considered. Our current work is divided into several parts, namely, (1) liner and medium improvement, (2) runnability modeling, (3) ECT and box compression performance, and (4) finite element analysis of flat crush and fluting stresses.

Medium Improvement

Corrugating medium requirements include both MD and CD strengths and stiffnesses. Good runnability is favored by high MD tensile and stretch, a low friction coefficient at high temperature, and low thickness. The medium must also be capable of being bonded at high corrugating speeds. In combined board the medium serves to keep the liners separated and maintain bending stiffness and directly contributes to ECT and box compression.

We have begun to develop information on ways to optimize medium properties considering end-use and runnability requirements. For this purpose experimental mediums have been made on the Formette former using combinations of pressing, refining and MD/CD directionality. After preparation of the sheets they were fabricated into combined board on the Institute's pilot corrugator. Corrugating speeds ranged from 400 to 800 fpm depending on the basis weight of the medium.

As discussed in past reports the results for the 26 and 40-lb mediums show that CD short span compression (STFI) results can vary widely at a given minimum Concora level depending on the papermaking conditions. For example, better wet pressing and more refining enhance both CD STFI and Concora as would be expected because of improved fiber-to-fiber bonding (Fig. 1). However at any given level of pressing or refining CD STFI can be enhanced at the expense of Concora by making a squarer sheet. Thus there should be opportunities to improve ECT strengths while maintaining adequate flat crush levels, particularly for mediums at higher basis weight levels.

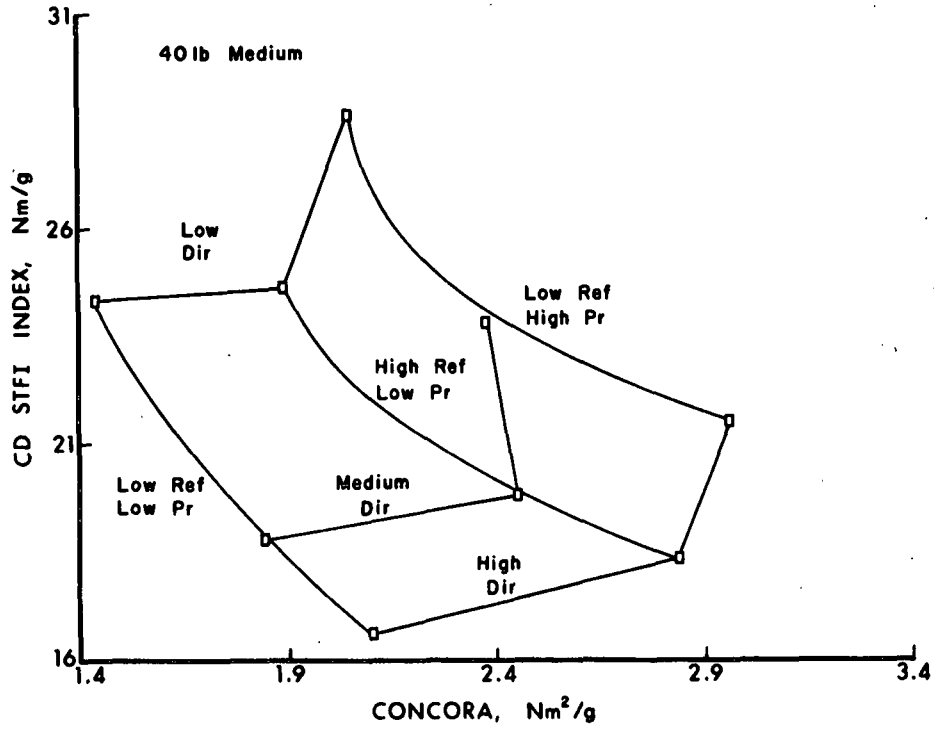

Figure 1. Relationships between CD STFI compressive strength and Concora for 40-lb mediums.

As a brief comment, MD/CD ratios are affected by fiber orientation and by drying restraints, specifically the paper machine draws. Past work has shown that MD compressive strength retention in the fluting process is dependent on

the in-plane and out-of plane elastic stiffnesses of the sheet as well as thickness or density (Fig. 2). Better retention of strength is favored by a high density achieved by better fiber bonding and a high out-of-plane elastic stiffness. However, Fig. 3. shows that increasing the draw on the paper machine will drastically lower the Z-direction elastic modulus according to the work by Baum, Habeger and Fleischman[1]. The above indicates that trying to achieve higher Concora levels by increasing the draws on the paper machine will adversely affect the compressive strength retained after fluting.

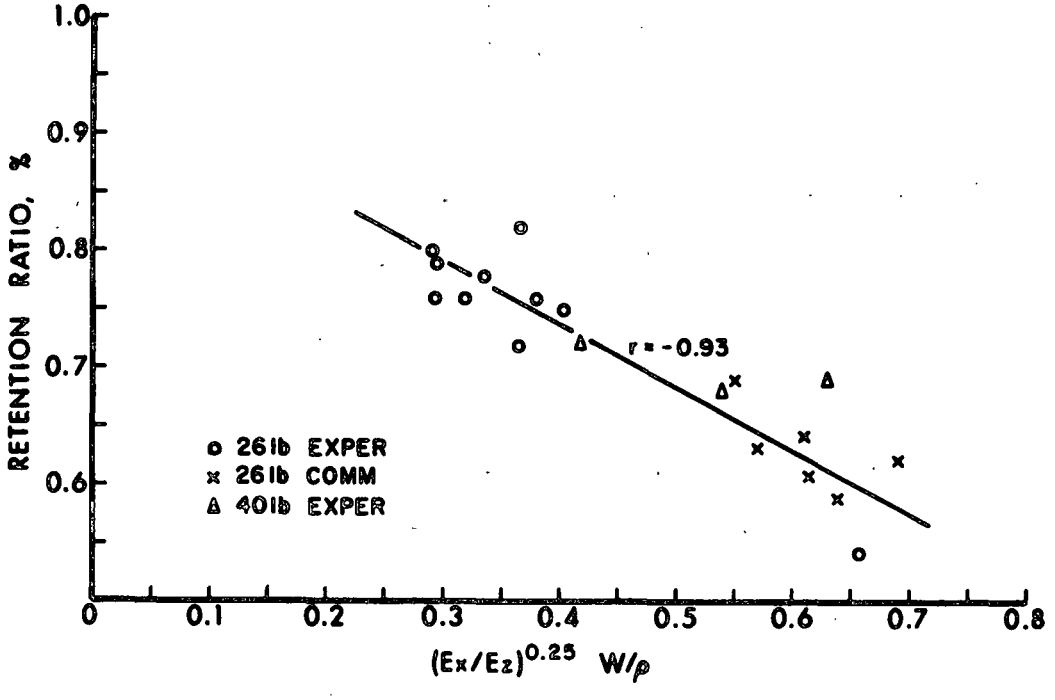

Figure 2. Retention of compressive strength during fluting depends on elastic stiffnesses, (E_X/E_Z), basis weight (W) and density (ρ).

For 40-lb mediums Fig. 4 shows that ECT strengths per weight of medium fiber ranged from 1.26 to 1.68 lb/in./lb, a difference of about 25% (see also Table 1). The sheets with the lower directionality and higher fiber-to-fiber

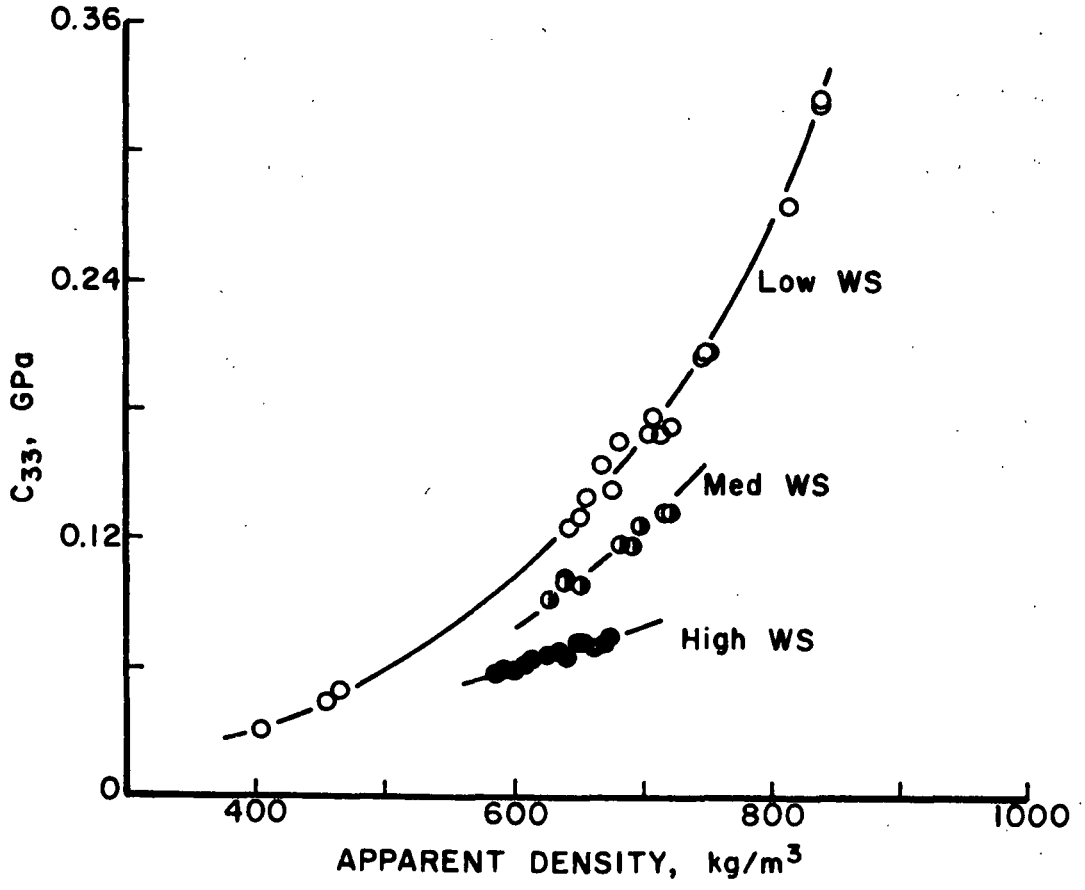

Figure 3. Wet straining markedly reduces the transverse elastic stiffness, C_{33} (almost equal to E_z).

bonding gave the higher ECT/strength ratios. Thus more efficient use of fiber in terms of ECT is achieved by higher wet pressing.

Figure 5 shows that flat crush strengths per weight of medium fiber ranged from 0.8 to 1.99 psi/lb for 40-lb mediums. Both wet pressing and refining increased the strength/weight ratios as expected but increase wet pressing was more effective because of the accompanying great reductions in caliper.

The 26-lb mediums were corrugated at speeds of 600 and 800 fpm; the speeds for the 40-lb mediums were 400 and 600 fpm. None of the mediums fractured at these speeds. All of the mediums corrugated at the selected speeds without any major glueing problem. The pin adhesion results on the 600 fpm single-faced board samples are shown on Table 1.

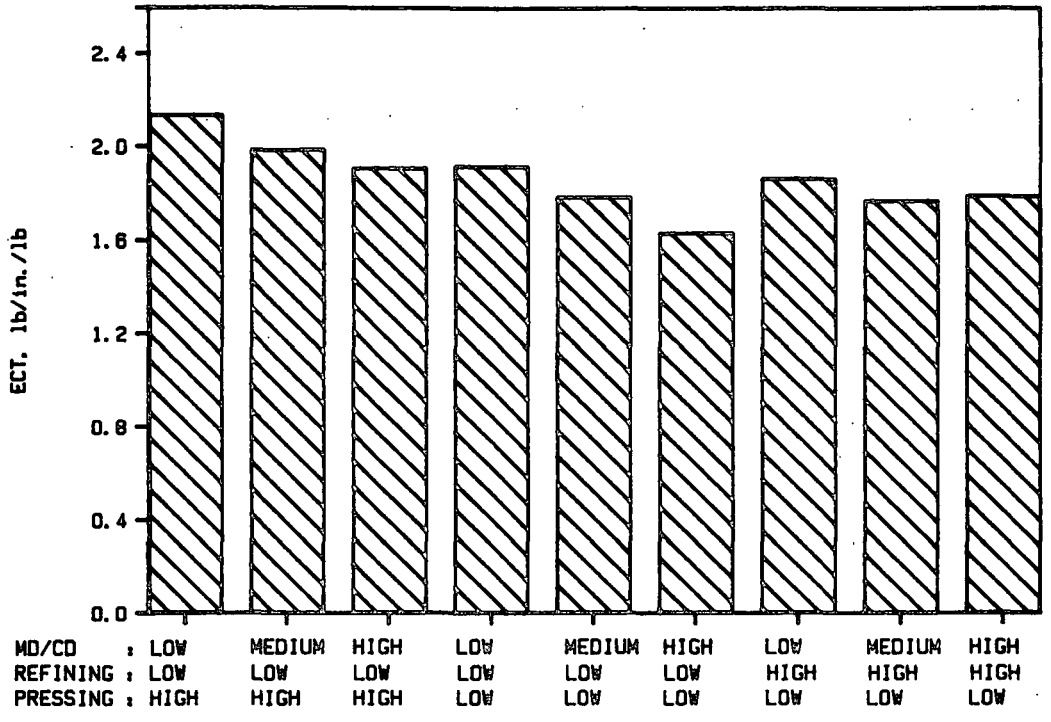

Figure 4. For 26-lb mediums ECT strength per mass of medium fiber increase with more wet pressing, refining and lower directionality.

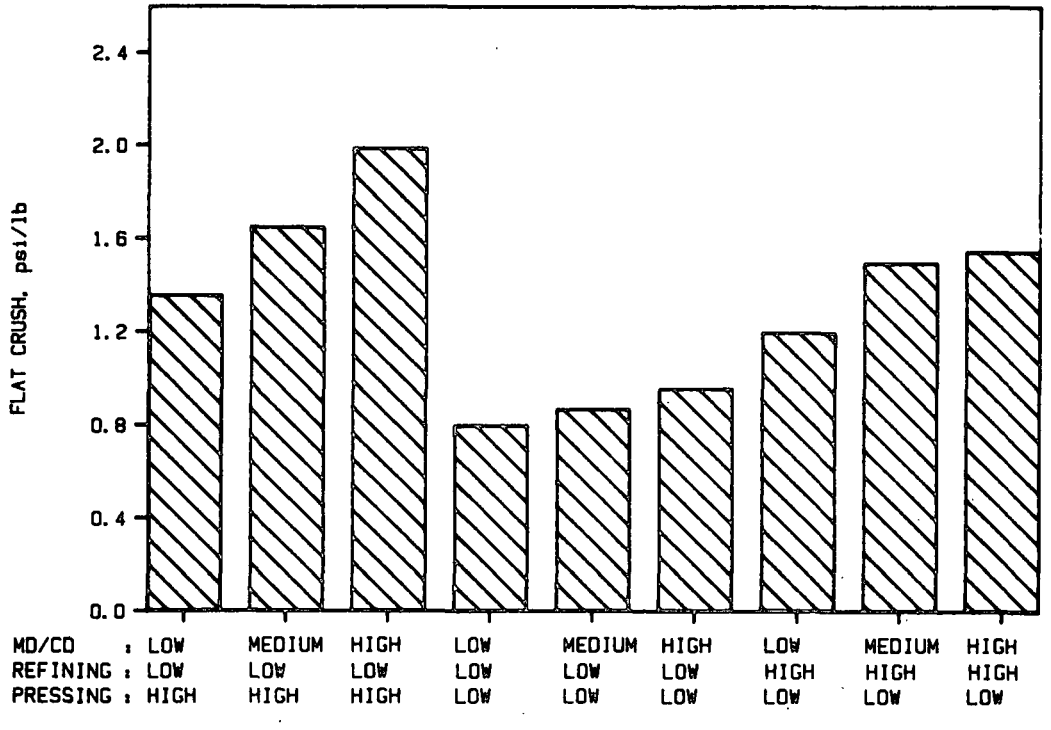

Figure 5. Flat crush strength per mass of medium fiber of 40-lb mediums show same trends as 26-lb mediums.

Table 1. Summary of combined board test properties.

Lot No.	Test Factors: Wet Pressing	MD/CD	Refining	Medium Basis Wt., g/m^2	Medium, Density, kg/m^3	Basis Weight, lb/M sq ft	Caliper mil	MD Stiffness lb-in.	CD Stiffness lb-in	Geom. Mn. Stiff., lb-in.	Flat, Crush, psi	Flat, Crush, psi/lb	ECT, lb/in.	ECT lb/in./lb	Pin Adhes., lb
3761-43	High	Low	Low	125.8	742	124.2	168.3	140.8	60.7	92.4	35.5	1.38	55.1	2.14	50.6
3671-45	High	Medium	Low	130.1	759	125.6	168.7	139.3	57.7	89.7	47.9	1.80	53.0	1.99	57.8
3761-46	High	High	Low	131.7	755	127.9	169.4	140.6	56.6	89.2	56.0	2.08	51.5	1.91	68.6
3761-34	Low	Low	Low	125.0	524	124.3	167.1	136.0	58.6	89.3	27.7	1.08	49.1	1.92	42.0
3761-36	Low	Medium	Low	127.0	540	126.8	168.6	137.3	55.9	87.6	37.8	1.45	46.5	1.79	43.6
3761-37	Low	High	Low	133.2	550	126.8	168.3	137.2	54.4	86.4	43.0	1.57	44.6	1.63	63.4
3761-24	Low	Low	High	141.0	560	128.7	168.4	141.1	60.4	92.3	38.9	1.35	53.9	1.87	
3761-27	Low	Medium	High	133.6	586	127.5	168.7	140.4	55.5	88.3	47.9	1.75	48.5	1.77	58.0
3761-28	Low	High	High	128.6	589	125.0	168.2	141.3	55.3	88.4	51.2	1.94	47.2	1.79	57.2
3761-48	High	Low	Low	197.4	703	144.8	169.6	140.1	66.4	96.4	55.0	1.36	68.0	1.68	58.0
3761-50	High	Medium	Low	201.8	729	144.3	170.0	144.5	61.0	93.9	68.4	1.65	62.9	1.52	94.2
3761-51	High	High	Low	204.4	735	146.4	170.4	143.0	58.0	91.1	83.3	1.99	60.2	1.44	61.6
3761-39	Low	Low	Low	193.6	526	144.6	169.9	139.1	63.1	93.7	31.8	0.80	58.5	1.48	67.8
3761-41	Low	Medium	Low	197.0	553	145.1	169.5	137.1	57.1	88.4	35.1	0.87	52.7	1.31	71.8
3761-42	Low	High	Low	205.7	563	148.2	170.1	139.2	56.6	88.7	40.4	0.96	53.0	1.26	79.2
3761-29	Low	Low	High	187.9	545	143.1	170.1	143.6	64.4	96.1	46.2	1.20	59.7	1.55	64.0
3761-31	Low	Medium	High	191.8	562	144.3	170.0	140.0	60.4	92.0	58.9	1.50	56.5	1.44	80.4
3761-33	Low	High	High	197.0	580	144.7	170.6	140.6	57.4	89.8	62.5	1.55	53.7	1.33	72.4

Figure 6 shows that the various degrees of refining and wet pressing did not greatly affect the pin adhesion strengths of the 26-lb mediums. While both wet pressing and refining made the medium less porous and sometimes less receptive to water, there was little effect on bonding strength on the corrugator. The results for the 40-lb mediums were similar but more erratic than the results for the 26-lb mediums (Fig. 7).

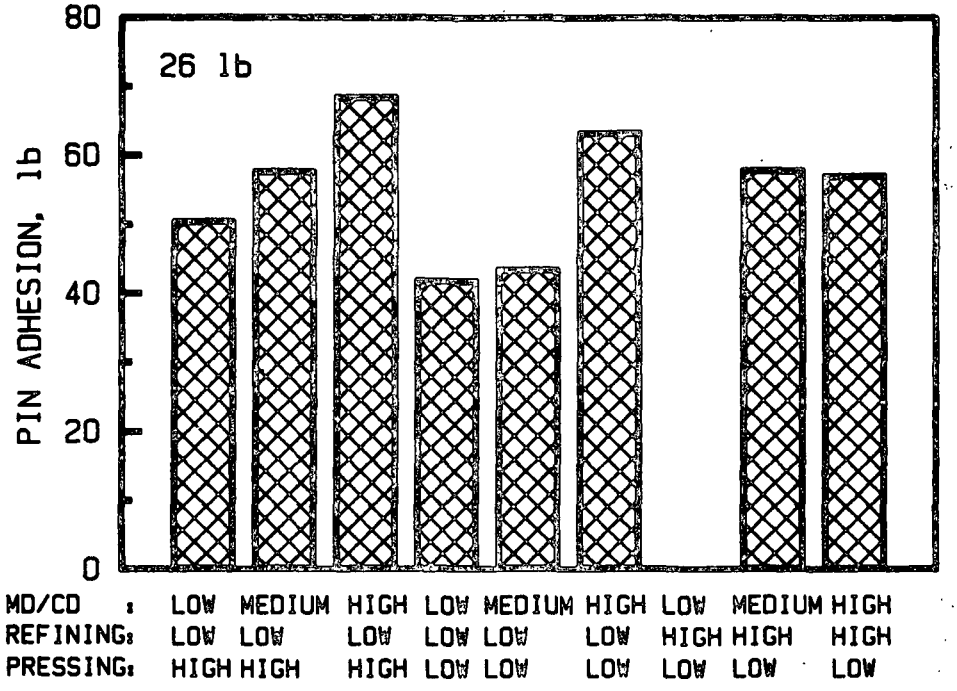

Figure 6. Pin Adhesion results for 26-lb mediums were not affected by changes in wet pressing and refining.

The pin adhesion results were not well related to sheet porosity for either the 26-lb (Fig. 8) or 40-lb mediums (Fig. 9). Bendtsen porosity values ranged from about 200 mL/min to nearly 1200 mL/min with the lower values being obtained on the more highly refined or wet pressed sheets. Despite this range in air porosity the less porous sheets (low test values) gave comparable adhesion strengths.

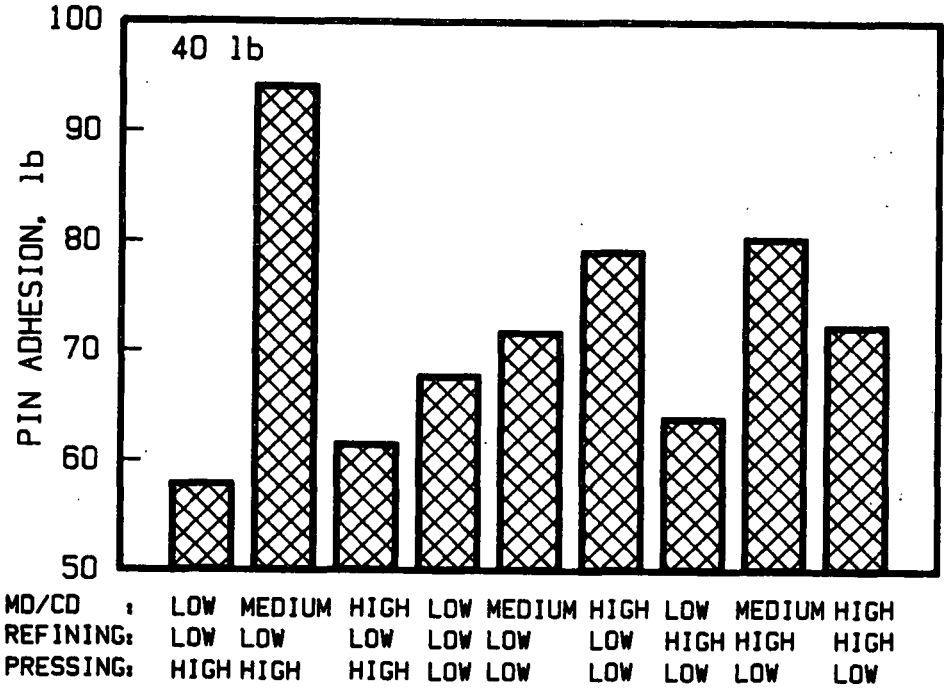

Figure 7. Pin adhesion results for 40-lb mediums were not consistently affected by changes in wet pressing or refining.

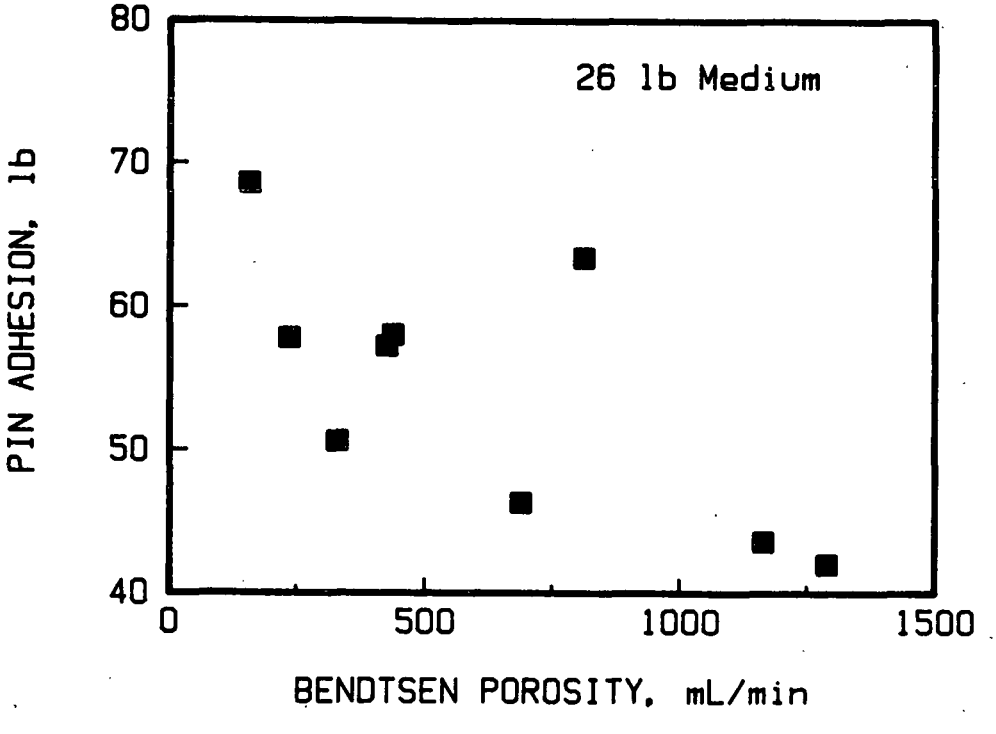

Figure 8. Pin adhesion results on 26-lb mediums were not well related to medium porosity.

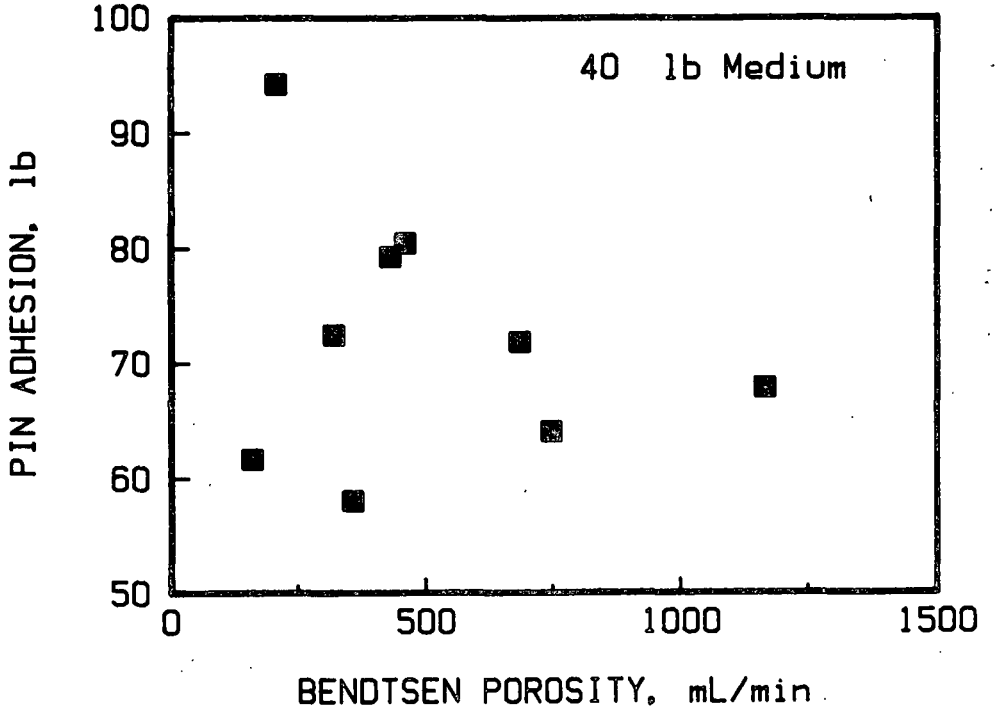

Figure 9. Pin adhesion results on 40-lb mediums show no relationship to medium porosity.

The water receptivity characteristics of medium are commonly measured using water drop tests following TAPPI method T819. Figure 10 and 11 show that pin adhesion strengths were not well related to water drop tests on either the 26 or 40-lb mediums. This held true even though the water drop values ranged from 35 to over 200 seconds for the 26-lb mediums. Some of the higher pin adhesion values were obtained on mediums with the higher water drop.

Figure 12 shows that the pin adhesion values were not well related to the smoothness of the medium. Medium density was also not well related to the single-face pin adhesion strengths (Fig. 13 and 14).

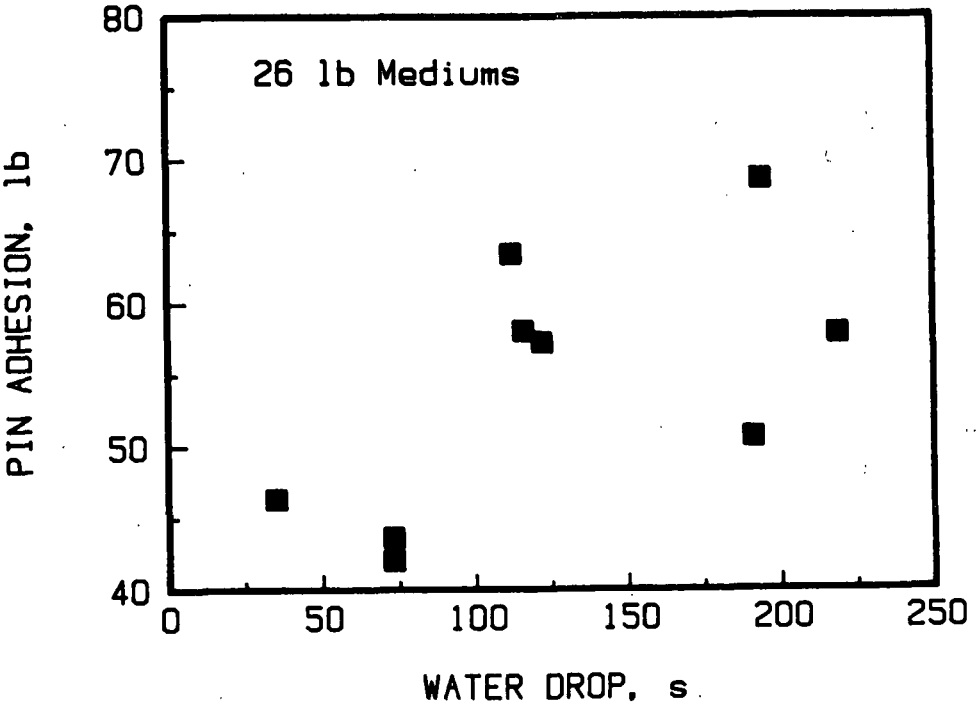

Figure 10. Pin adhesion test on 26-lb mediums were not related to water drop tests on the uncorrugated medium.

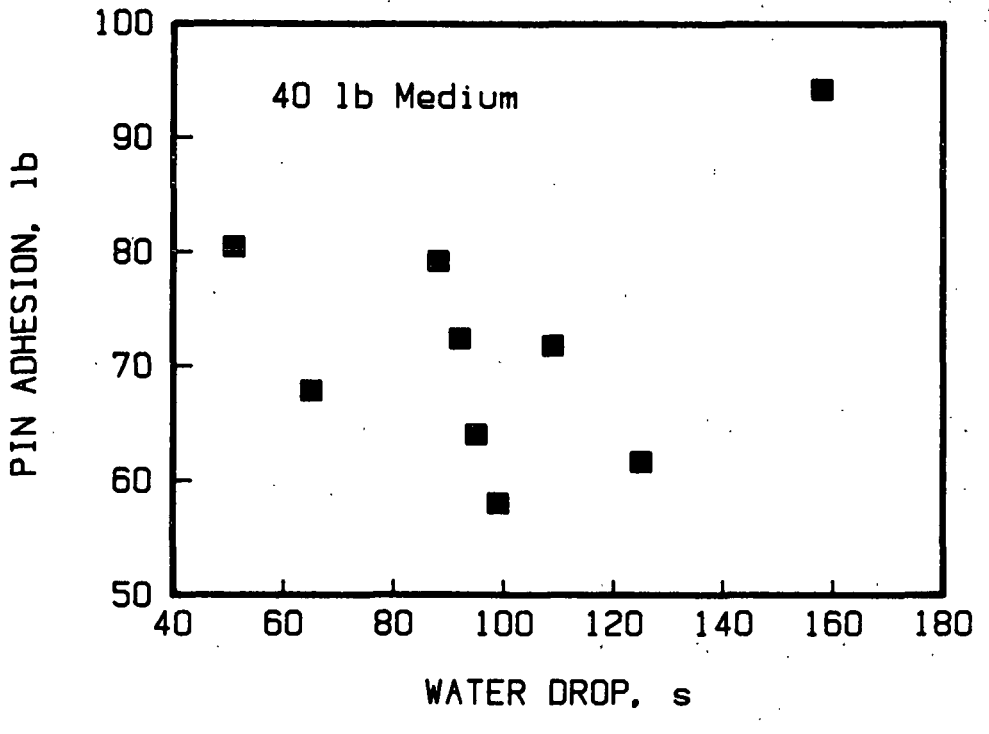

Figure 11. Pin adhesion tests on 40-lb mediums were not well related to water drop tests on the uncorrugated medium.

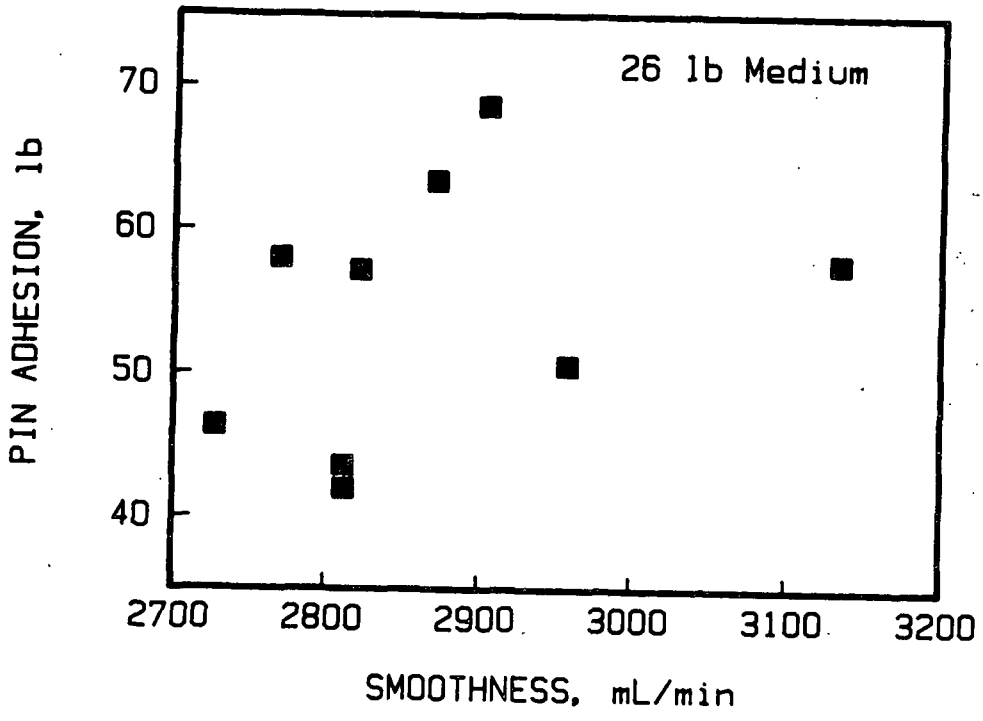

Figure 12. Pin adhesion strengths were not related to medium smoothness tests.

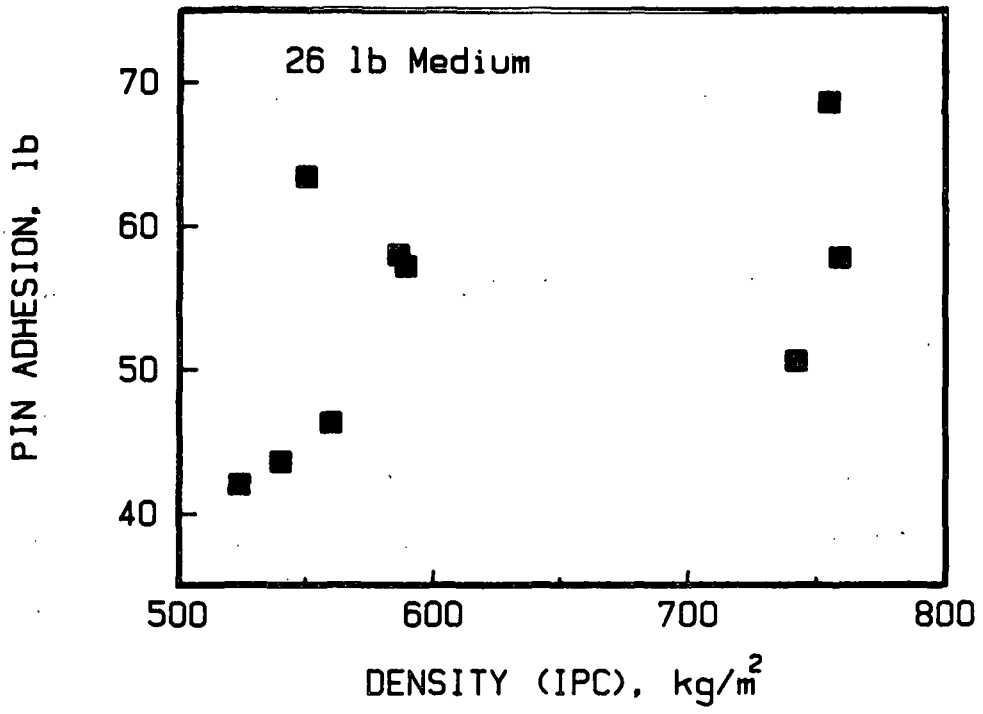

Figure 13. Sheet densities were not well related to single-face pin adhesion results on 26-lb mediums.

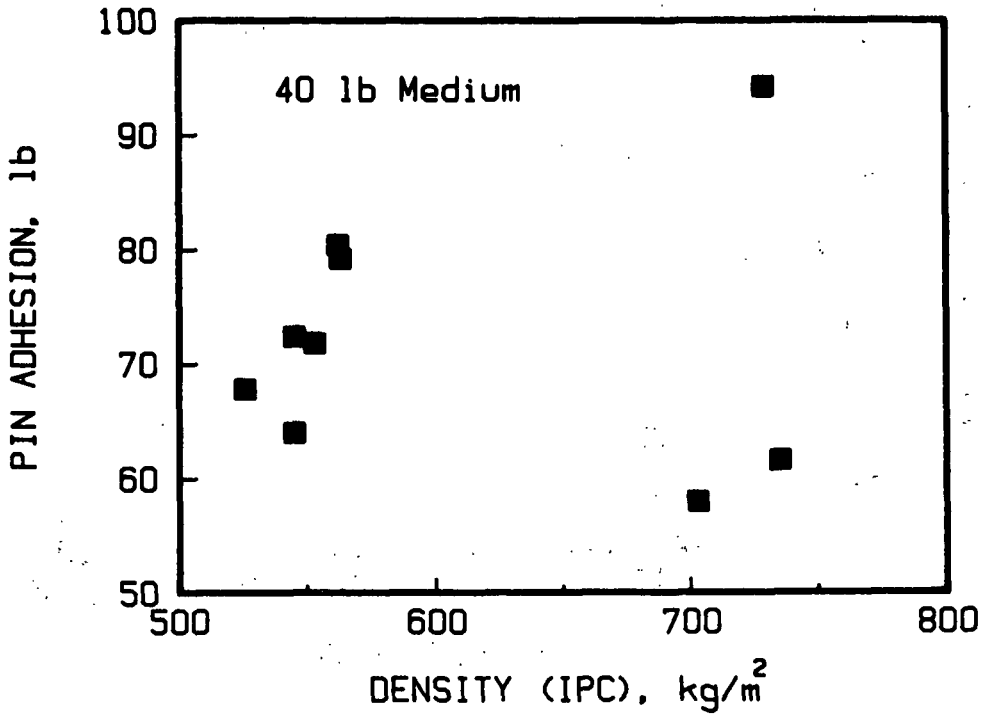

Figure 14. Sheet densities were not well related to single-face pin adhesion results for 40-lb mediums.

The poor relationships between pin adhesion strengths and such medium properties as porosity, water drop, smoothness and density is not unexpected. In past and current work on high speed bonding on the corrugator we have not been able to find strong relationships between single-face pin adhesion and such commonly measured tests. This is not surprising because bonding on the corrugator must develop in a few milliseconds whereas water drop times are orders of magnitude higher. Porosity and smoothness test are air leak methods and must differ somewhat from what occurs with liquid wetting and penetration. The Bristow tester which measures the volumetric roughness, fluid absorption and delay time of paper substrates may provide a better way to measure the glueability properties of linerboard and medium. One of the challenges will be

to find ways to adapt such tests to mill purposes. A part of our future plans in the corrugating area is to study ways to model the bonding process in the corrugator and define the paperboard properties needed for high speed operation.

Liner and Medium Improvement -- Surface Treatment

In Project 3526 various wet end additives are under study as a means to increase fiber bonding strength under normal and humid conditions. As an alternative to wet end addition we are planning to study the merits of a chemical surface treatment of board (linerboard or medium) on converting and end-use corrugated board performance. For this purpose narrow width webs or sheets will be treated with solutions of such agents as PAE, starch, and starch/PAE blends. Target pick-ups of the agents will range up to 2 to 3%. Care will be taken to avoid excessive shrinkage during drying.

As an initial step we plan to treat medium to determine if such treatment affect fluting damage, runnability and end-use performance of the combined board. The treated medium will be single-faced at a series of corrugating speeds ranging up to 1000 fpm, assuming no fractures or bonding deficiencies occur.

The single-faced boards will be tested for ECT, flat crush, adhesion and high-lows at 50% RH. ECT and flat crush tests will be carried out at 85-90% RH.

Runnability Modeling

Our runnability model shows that flute fracture and high-lows are dependent on medium properties, nip geometry and operational factors. Higher MD tensile strength and stretch and lower medium friction and thickness promote fluting with fewer high-lows and less chance of flute fracture. The nip

geometry factors are: (1) the total wrap angle in the labyrinth, and (2) the radius of the flute tip of the corrugating roll. We will present a paper at the 1987 TAPPI Corrugated Container Conference discussing development of the model. A copy of the paper is appended.

In past reports a sensitivity analysis was carried out for the four medium properties used in the model. Figure 15 compares the effects of the four properties on the maximum corrugating speed attainable before exceeding 10% high-lows greater than 4 mils. At a constant high-low level changes in MD stretch and thickness have the greatest effect. Changes in the hot friction coefficient and MD have significant but slightly lesser effects than the other two properties. These results illustrate that papermaking factors which give higher stretch and tensile strength and lower friction and thickness will promote operation at higher speed with less high-lows.

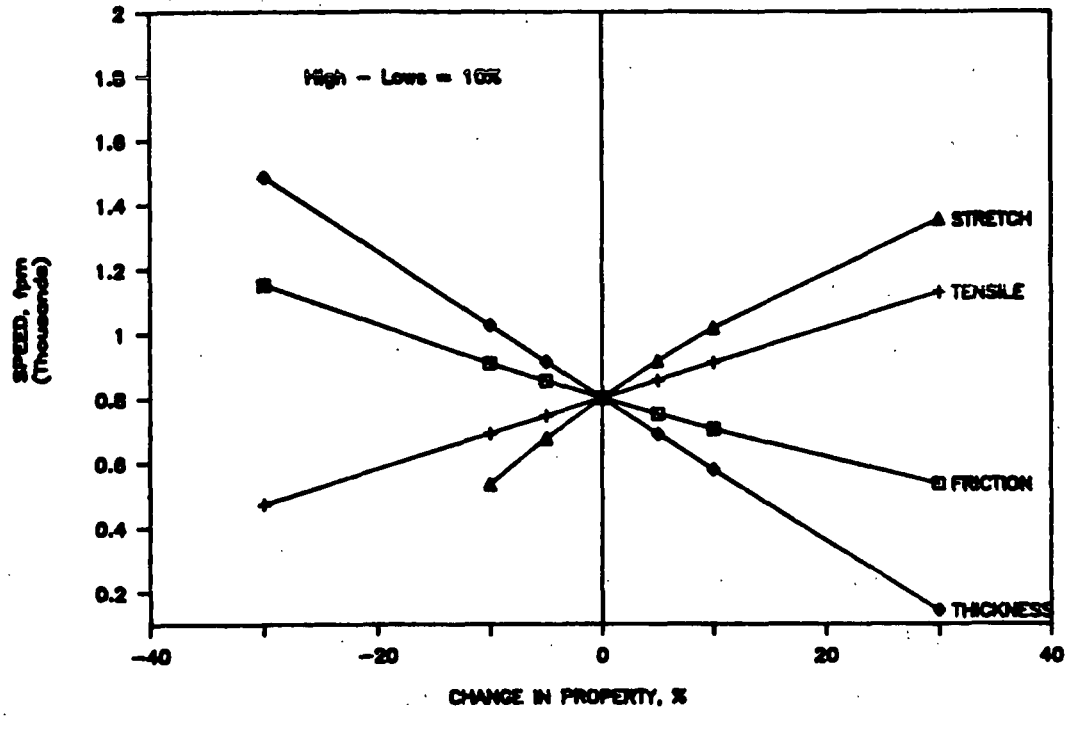

Figure 15. Effects of changes in medium properties on the speed at which high-lows equal 10%.

Recently a similar sensitivity analysis was carried out for the nip geometry and medium brake tension factors in the model (Fig. 16). At a constant high-low level of 10%, increasing the tip radius of the flute allows higher operating speeds before exceeding the 10% high-low level. The tip radius has a larger effect than either the wrap angle or the medium brake tension for equal percentage changes. Increases in either the brake tension or the wrap angle decrease the allowable speed for 10% high-lows as would be expected from past work. Of the two changes in wrap angle have greater effects than brake tension for equal percentage changes. However this may be misleading because there is no way for the operator to change the wrap angle or tip radius whereas he can change the medium brake tension over wide ranges.

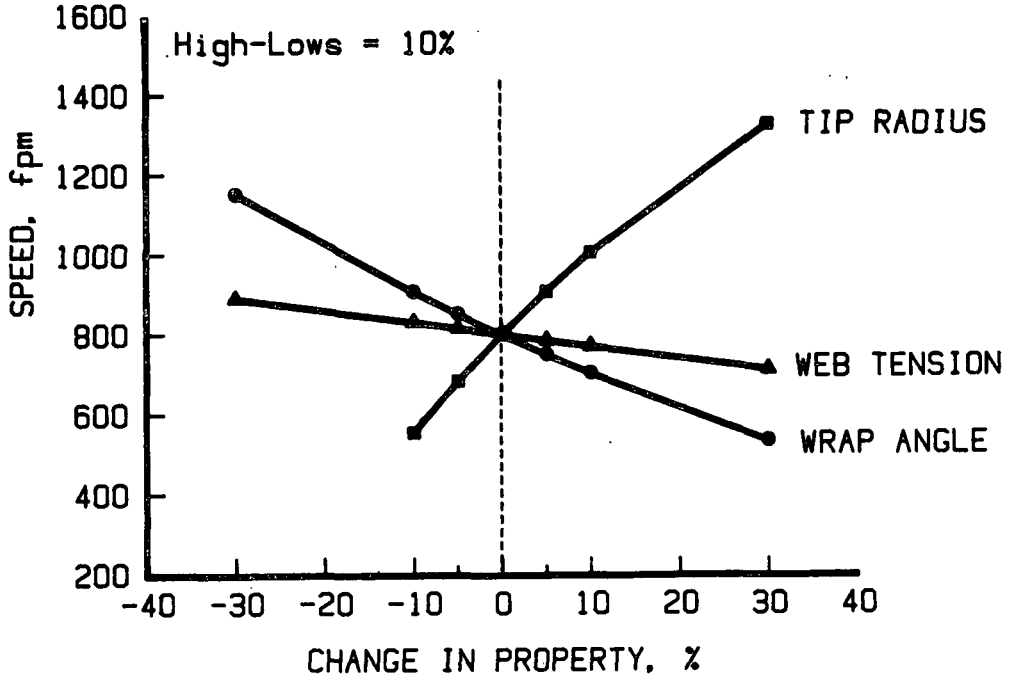

Figure 16. Effect of changes in flute geometry and medium brake tension on the speed at which high-low exceed 10%.

Figure 17 illustrates the sensitivity of these factors in terms of the high-low levels greater than 4 mil which would be obtained at a constant speed of 800 fpm. Increasing the tip radius of the profile greatly lower the high-low levels. Increasing the wrap angle or the medium brake tension can greatly increase high-lows.

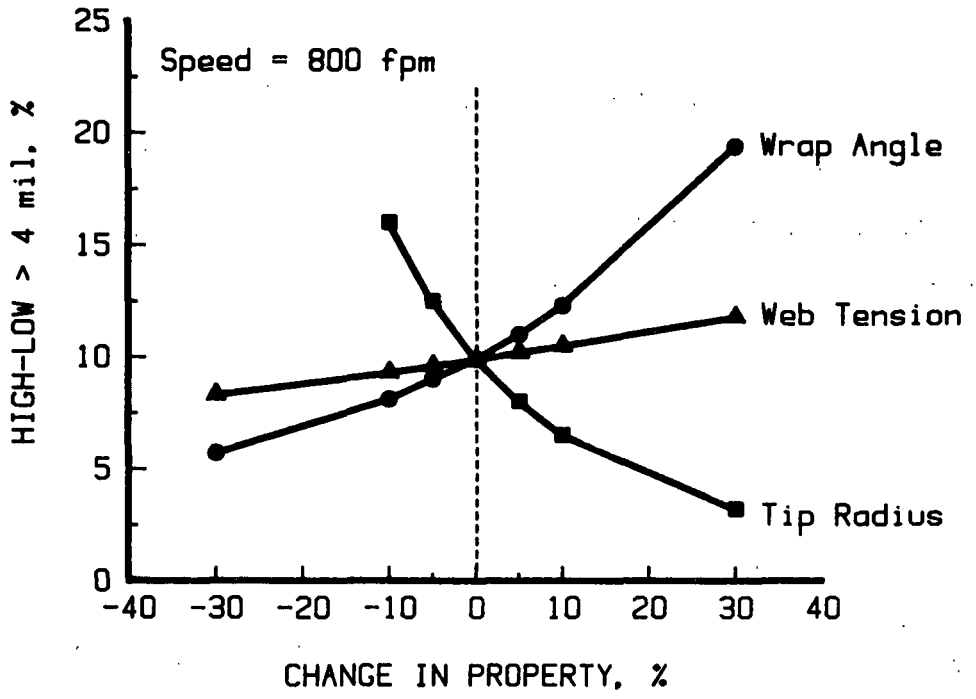

Figure 17. Effect of changes in flute geometry and medium brake tension on the high-low levels obtained at a speed of 800 fpm.

Three other topics related to our runnability modeling are being studied.

1. The potential effects of high strain-rate effects during corrugating on the tensile and stretch properties of medium are being studied using models based on mechanical systems comprised of springs and viscous dashpots.

2. The computer models originally developed for the runnability model are being used to study the effects of the fluting stresses on the strength properties of the medium. This information is needed for our finite element analyses of structural performance of the combined board after fluting. For example, flat crush performance will be affected by how much compressive strength loss occurs in the fluting process. This analysis is discussed in the later section concerned with finite element analysis of flat crush.

3. Our computer models of the fluting nip permit analysis of the clearances between upper and lower corrugating rolls. We speculate that the lack of sufficient clearance where the lower roll begins driving the upper roll can damage the medium and cause flute fracture. We are beginning to try and use this approach to trouble-shoot corrugating problems.

ECT and Box Compression Relationships

Our work is centered around modeling ECT, flexural stiffness and box compression strength. In our past work we developed an ECT model based on Von Karman's miniature plate approach. A combined board flexural stiffness model was also developed using an elliptic integral to account for the contribution of the medium. After simplification of both models, we have used them to predict the effects of changing the properties of the liners and medium on box compressive strength. Our current work is directed to checking the accuracy of the predictions and starting efforts to take into account the effects of moisture and handling abuse on board optimization.

To provide a check on our compression modeling we plan to fabricate and test combined board and tube structures made therefrom using experimental and commercial materials. As a first step experimental sheets have been made

on the Formette former to allow fabrication of the combined boards shown in Table 2.

The linerboard components have been made using two levels of wet pressing and MD/CD ratios at basis weights of 33, 38 and 42 lb. These linerboards are being combined with 26 and 33 lb commercial mediums as shown in Table 2.

Table 2. Board combinations.

Total C. B. Wt., lb	C. B. Combination	Experimental Liners Wt.	Approx. Density	MD/CD	Relative Total Wt., lb	Predicted ECT*
103	33-26-33	33	700	2.0	85	87
113	38-26-38	38	700	2.0	93	94
121*	42-26-42	42	700	2.0	100	100
103	33-26-33	33	850	2.0	85	93
113	33-33-33	33	850	2.0	93	103
113	38-26-38	38	850	2.0	93	102
123	38-33-38	38	850	2.0	102	111
113	38-26-38	38	850	1.25	93	112+
113	38-26-38	38	700	1.25	93	112

*Predicted ECT and relative total weights are compared to the 42-26-42 combination as 100.

The experimental linerboards and the commercial mediums are being tested. The combined boards will be tested as soon as the fabrication is complete. We plan to make small size rectangular tube structures from each material combination. These will be tested in compression. The test information will allow us to check our ECT and flexural stiffness model predictions. Using a modified form of the McKee box formula it will be possible to compare the tube compression results with predictions from the ECT and flexural stiffness models. Other experimental factors could be tested in future work.

One of the disadvantages of this approach is that only limited amounts of material can be practically made and the rectangular tube size is relatively small. Thus other use factors such as RH and combined board crushing effects cannot be systematically studied and incorporated in our modeling. For these reasons additional work has been scheduled as described below.

As discussed in past PAC meetings there is need to extend our work to commercial materials and to take conversion and distribution abuse in consideration along with RH effects. The planned work will be directed to:

1. Checking our ECT and flexural stiffness models on commercial board and large "compression" size boxes.

2. Determine effects of simulated service abuse on the box properties of boards made using a range of component weights and qualities.

3. Evaluate fiber savings potentials of high compression strength components.

For this work combined board and boxes will be tested at RH levels of 50, 75 and 85-90%RH. At each RH level the boxes and combined board will be subjected to 4 levels of crushing to simulate conversion and transportation damage. The crushed boards and boxes will also be tested at each RH level. If necessary boxes treated as above will be creep tested for several weeks after which compression tests will be carried out.

To assess the importance of the simulated abuse conditions and to develop techniques for later phases of the work an exploratory study is planned using 2-3 box combinations as follows:

1. 42-33-42
2. 69-33-69
3. 69-26-69

We are trying to obtain about 200 boxes of each combination for this work. A box size of 22.5 x 15 x 20 inches will be used. This work will be started as soon as the boxes are available. Following the above work it is planned to use the techniques developed to evaluate boxes made with liners and medium of different compression quality.

Flat Crush and Flute Formation Modeling

This portion of the project is directed toward improving the strength retention of the medium after corrugating. Past research has produced evidence that the medium experiences considerable damage to its physical properties (especially to its MD compression strength) during flute formation[2]. The damage adversely affects the flat crush yield point and ultimate strength. Also, the damage decreases the combined board edgewise compression strength, flexural stiffness and therefore the overall box compression strength.

Because the compression strength of the medium determines the board's ability to resist flat crush loads, a study is being conducted of the stresses applied to the medium during flute formation and the resulting damage. This study includes both an analysis of the stresses using finite element techniques and a laboratory investigation of the extent and location of damage to the medium during flute formation. Determining the factors which would minimize strength losses during flute formation requires an understanding of the complete history of applied stress and the resulting damage to the medium. It is anticipated that with this understanding will come directions in which to improve the strength retention of the medium after corrugating. Increased strength retention will produce boards with greater flat crush and box compression strength without increased material usage.

Presently there are two approaches to minimize strength losses during flute formation and they are as follows:

1) Alter the properties of the medium during manufacturing so that it can be formed with less damage. One effective alteration is a densification of the sheet before corrugating[3].
2) Alter the properties of the medium just prior to corrugating by making effective use of heat and steam preconditioning.

The ability to determine the stresses in the medium during flute formation would add a third option to minimizing strength losses, by possible changes in flute profile.

In the corrugating labyrinth, the medium is subjected to a variety of stresses which include tension, bending, shear and thickness direction compression. Previous research has indicated that the flute formation process results in an extensive reduction in the MD compressive strength of the medium[2]. The average reduction in MD STFI compression strength was approximately 40%, however, compression strength reductions were greatest at the flute tips and somewhat less at the flanks of the flute. Flexing of the medium around a radius similar to that of a flute tip (0.06 inches) resulted in a similar reduction (approximately 50%) in the medium compression strength. Initial prestressing of the medium in tension to failure did not have a significant effect on the subsequent compression strength. This suggested that the compression strength losses in the medium resulted primarily from excessive bending stresses generated during the flute formation process. The bending stresses apparently exceed the elastic range on the compression side (concave side) of the flexed medium with yielding and permanent compression strength losses to that side of the medium. The bending stresses usually do not exceed the ultimate strength of

the medium on the tension side (convex side), since flute fractures do not necessarily occur under normal corrugator operating conditions.

Formation and retention of the fluted shaped requires the stresses in the medium to exceed the elastic range on the compression side of each flute tip. A simple flexural analysis of a typical 26-lb medium which is bent over a flute tip will illustrate this point. It will be assumed that the tension and compression properties of the medium remain in the elastic range for this example. The following equation can be used to determine the approximate maximum tensile and compressive strain during bending.

$$\varepsilon_{max} = \pm \frac{t}{2R} = \pm = 8.3\%$$

where: ε_{max} = maximum bending strain (tensile strain (+) on the convex side of the flute tip and compression (-) on the concave side of the tip).

t = medium thickness (assume t = 0.010 in.)

R = radius of curvature of flute tip (assume equal to that of a C-flute tip, R = 0.060 in.)

This level of strain is significantly larger than both the MD tensile strain at failure (usually between 1% to 2%) and the CD compressive strain (estimated to be considerably less than the tensile strain at failure). Thus the medium apparently experiences strains which may be greater than ten times the yield point on the concave side of the flute tip.

If the stress-strain diagram would remain linear at this level of strain, the following equation could be used to calculate the stresses in the medium due to bending around a flute tip:

$$\sigma_{max} = \pm \frac{Et}{2R} = \pm 83{,}000 \text{ psi}$$

where: σ_{max} = maximum bonding stress (tension stress (+) and compression stress (-))

E = modulus of elasticity (assume $E = 1.0 10^6$ psi)

t = medium thickness (assume $t = 0.010$ in.)

R = radius of curvature of C-flute tip ($R = 0.060$ in.)

This level of stress is substantially greater than the typical ultimate MD tensile strength (6,000 psi) or the STFI MD compression strength (3,000 psi) for a 26-lb medium.

Apparently the medium has a much greater capacity for deformation into the inelastic range in compression than in tension. A portion of this study involves investigating the flexural aspect of flute formation, focusing on the extent of the compression side damage in the medium.

To date, the analysis of the stresses imposed on a medium during flute formation have been limited to the rather simplistic approach used above. This type of analysis does not provide a history of the stresses imposed on the medium during the flute formation process. Particularly absent is any indication of the stresses imposed on the flanks of the medium during corrugating. This is especially necessary information because the flat crush strength, to a large degree, is determined by the flanks of the flute. In the past, a lack of specific information about the geometric history of the medium during flute formation and insufficient analysis techniques made the study of flute formation stresses nearly impossible. Recent software developments have made a more accurate stress analysis of the medium during flute formation possible.

A computer model has been developed to simulate the shape of the medium web in the corrugating labyrinth. With this simulation, it is possible to track the movement and deformation of a segment of medium during the flute forming process. Used in conjunction with a finite element analysis program, flute formation stresses can be studied. The simulation is based on the following simplifying assumptions.

1) The web is not allowed to stretch in the machine direction.

2) The web conforms without resistance to the surface of the teeth tips.

3) The centers of both the upper and lower corrugating rolls are held fixed.

4) The upper and lower rolls are placed synchronously with respect to rotation and no attempt is made to account for the bottom roll driving the top roll.

Input parameters to the simulation include:

1) the number of teeth on a roll,

2) the outer roll radius,

3) the inner roll radius,

4) the tooth tip radius,

5) the separation distance between upper and lower rolls,

6) the rotational position of the rolls.

The program is capable of tracking discrete points on the web through various rotational positions. The resulting information can be presented in tabular or graphical form. An example of the simulation's graphical output is shown in Fig. 18 as the solid line. The upper and lower roll profiles indicated by the dotted lines have been added to the figure from a companion program. The heavy segment of the solid line represents a portion of the web which will be

formed into one complete flute. Figures 19a and 19b follow the same segment of web as it progresses further into the labyrinth and Fig. 19c shows the segment in its final flute shape.

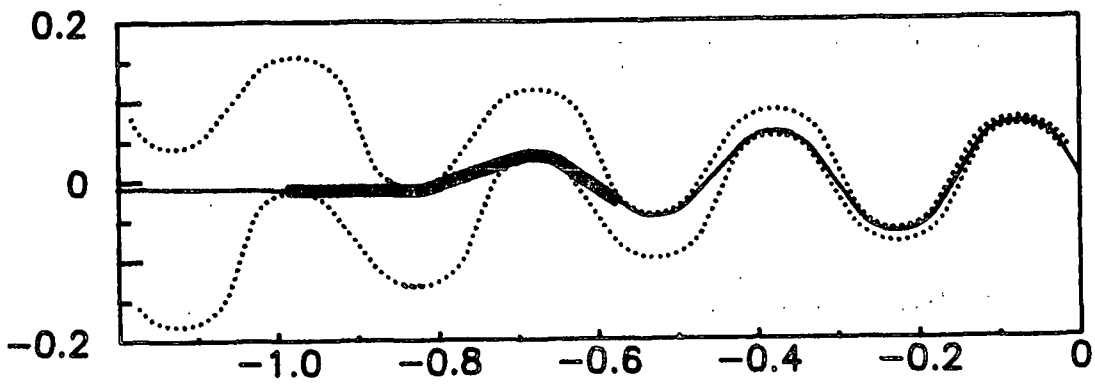

Figure 18. Simulation of web and corrugating rolls.

While it is not apparent from these 4 illustrations, an examination of the simulations reveals that (1) the pieces of web which end up as straight flute flanks are actually bent around the teeth tips in the process of the flute being formed and (2) the leading and trailing shoulders of a flute tip undergo rather different histories in the forming process.

The finite element analysis program, which we are presently using, is capable of a large deflection analysis such as flute formation using an iterative approach. However, it is only capable of linear elastic analysis. Although the flute formation process is a highly non-linear event, some useful information can be obtained from an elastic analysis. Presently, we are searching for a finite element program which will have the capability for non-linear material analysis. This will provide a more accurate analysis for the medium stresses during corrugating.

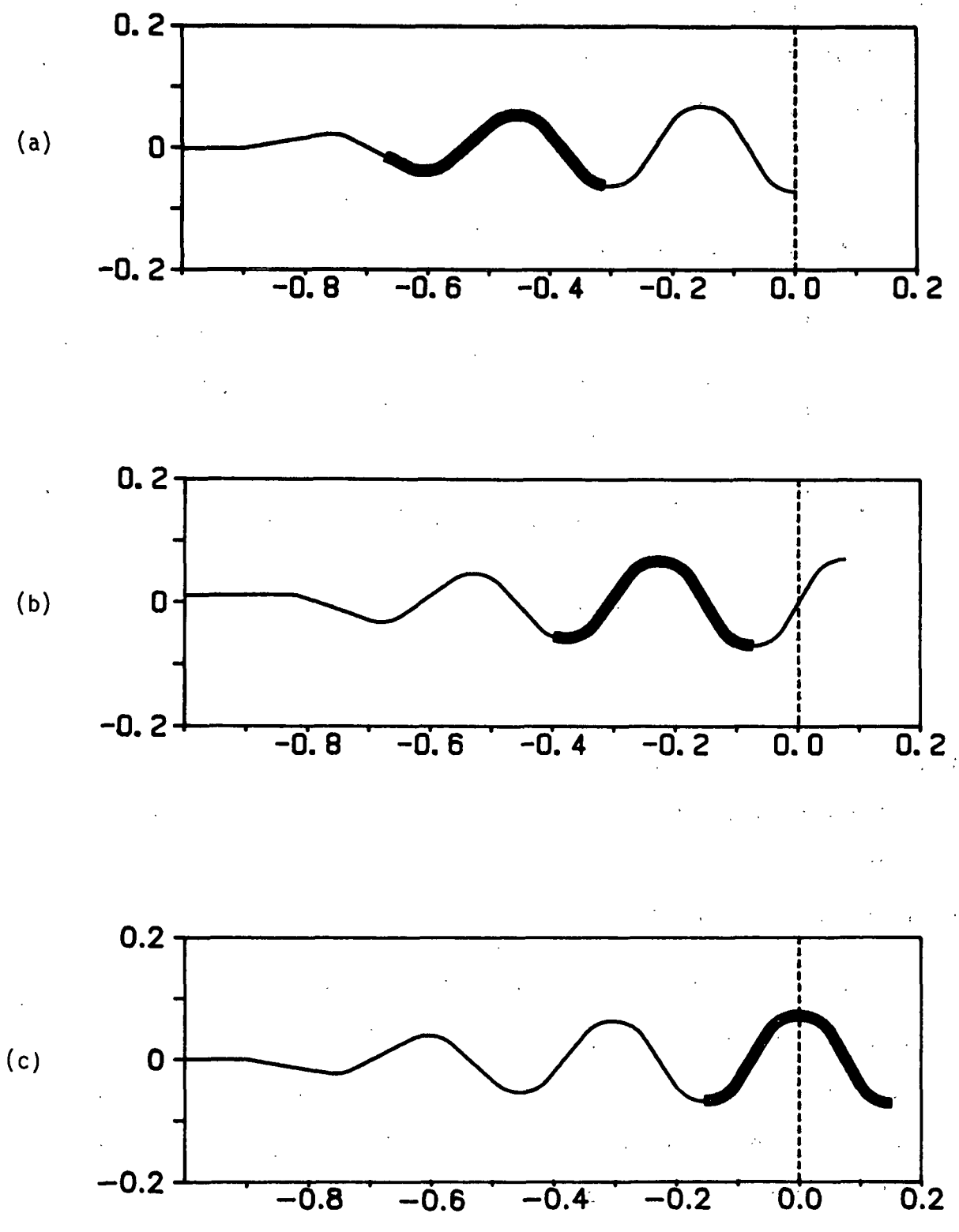

Figure 19. Simulation of the forming of a web segment into a completed flute shape.

Figure 20a shows the initial flat configuration of the flute formation model prior to entering the labyrinth. Figure 20b shows the final configuration of the model with a fully formed flute. The locations of the flute tips and flank midpoints are marked in Figure 20a and 20b with a "T" and "F" respectively. The addition of the one-half flute lengths ahead and behind the flute being studied modeled the effects of adjacent flute formation. The flute formation analysis was carried out with 16 approximately equal interations. The change in the 33 joint coordinate locations at each interation was determined in the flute formation program. This joint displacement information was used as a loading condition in the finite element analysis program. The finite element analysis program determined the bending stresses produced in the medium due to the displacements. The calculated stresses were then copied into a spreadsheet program where the appropriate stresses at each iteration were tabulated. Medium material properties used in this analysis were as follows:

1) Elastic modulus $E_x = 1 \times 10^6$ psi

2) Shear modulus $G_x = 1 \times 10^3$ psi

3) thickness t = 0.010 in.

Figure 21a shows the shape of the medium at interation 2 of the forming process. At this time, the leading flute has begun to form but the flute which is being studied has not yet started the formation process. Figure 21b plots the bending stress occurring along the top surface of the medium. Because this is an elastic analysis, the bottom surface of the medium would be experiencing an equal but opposite stress from that of the top surface. The bending stress at the leading edge of the flute (joint #9) was approximately 6,000 psi in tension on the top surface and the same stress in compression at the bottom surface. This demonstrates the effect of the medium displacement

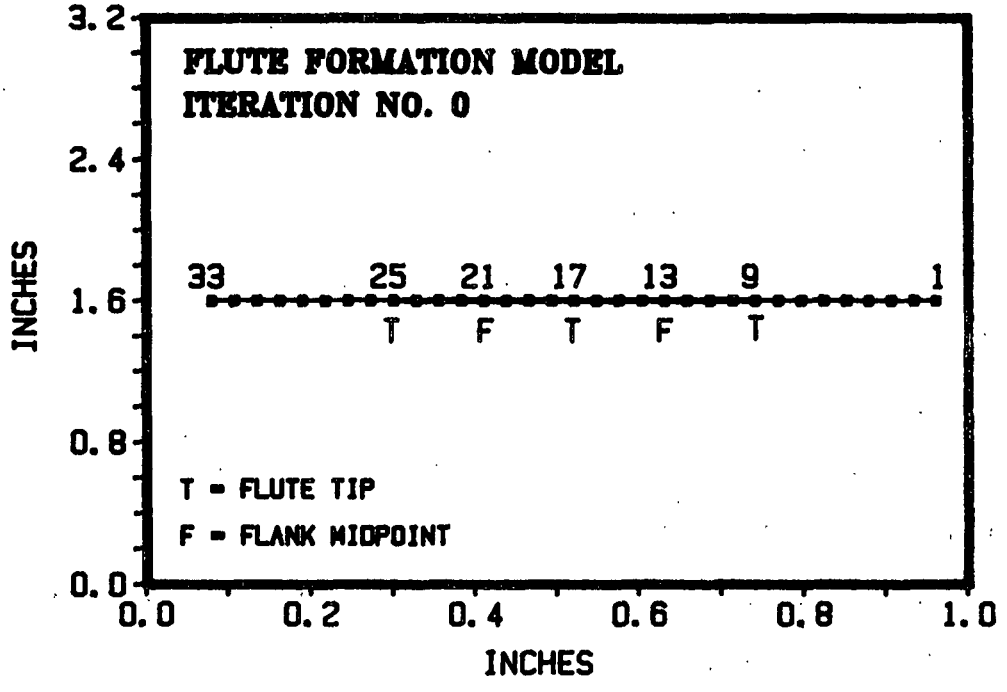

Figure 20a. The initial flat configuration of the flute formation model.

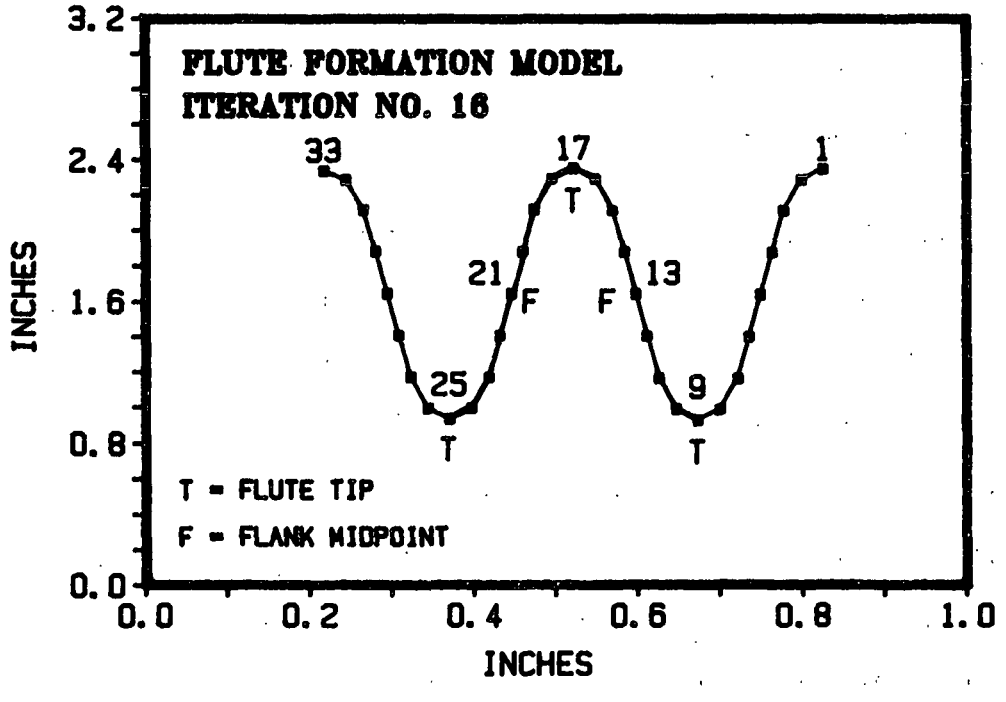

Figure 20b. The final configuration of the model with a formed flute.

ahead of the flute. Stresses at the leading edge of the flute are already above the ultimate limit in compression before the forming has begun. When completely formed, joint #9 will become a flute tip with the top surface of the medium on the concave side of the tip. Therefore, this portion of the medium will undergo a complete stress reversal during formation.

Figure 22a shows the shape of the forming process at iteration #5. At this time, joint #13 (which will become a midpoint on the leading flute flank) is experiencing a bending stress of approximately 50,000 psi in tension on the top surface as shown in Figure 22b. A compression stress equal to the tension stress occurs at the bottom surface (concave side) of the medium. This large bending stressing explains the significant loss in compression strength of the flank.

Figure 23a indicates the forming shape at iteration #7. At this stage of formation, the midpoint of the trailing flank is experiencing a maximum bending stress of 50,000 psi as shown in Figure 23b. The stress level is similar to that calculated for the midpoint of the leading flank.

While the formation stress history at the midpoints of the flanks was approximately the same, stresses in other sections of the flute were not symmetrical. In particular, the leading shoulder of the flute tip experienced bending stresses which were greater than that of the trailing shoulder. This suggests that the leading shoulder of the flute tip would experience more strength loss than the trailing shoulder. Due to increased frictional forces between the corrugator roll tooth and the medium, a greater amount of tension would be applied to the leading flank. This suggests that when fractures occur during corrugating on flute tips, they would more likely occur on the leading

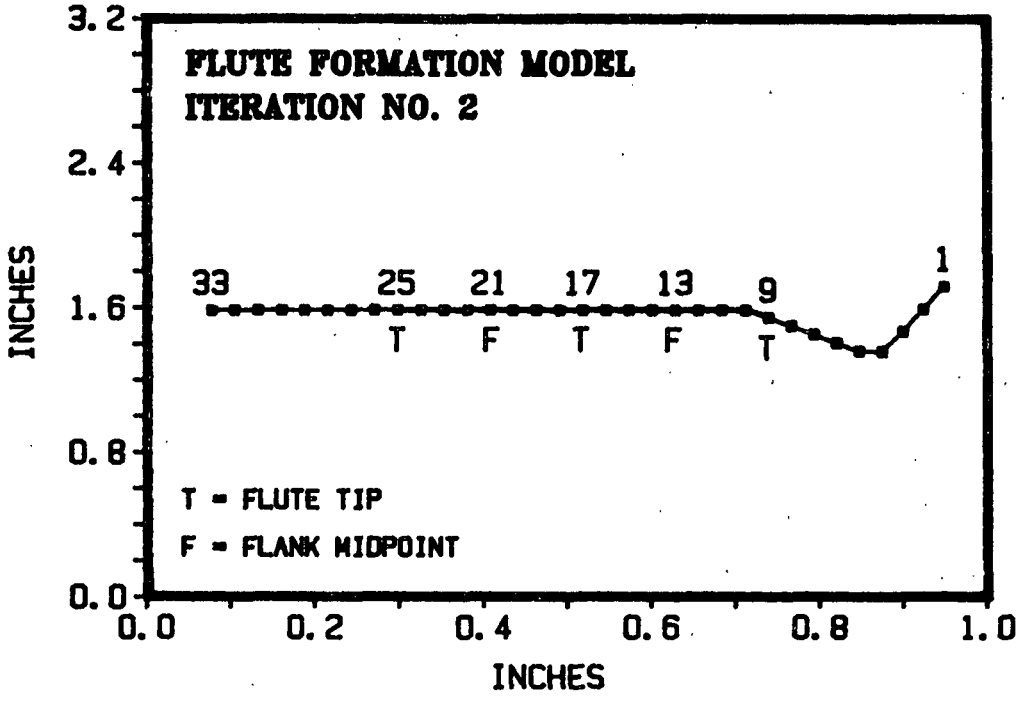

Figure 21a. Medium configuration prior to forming.

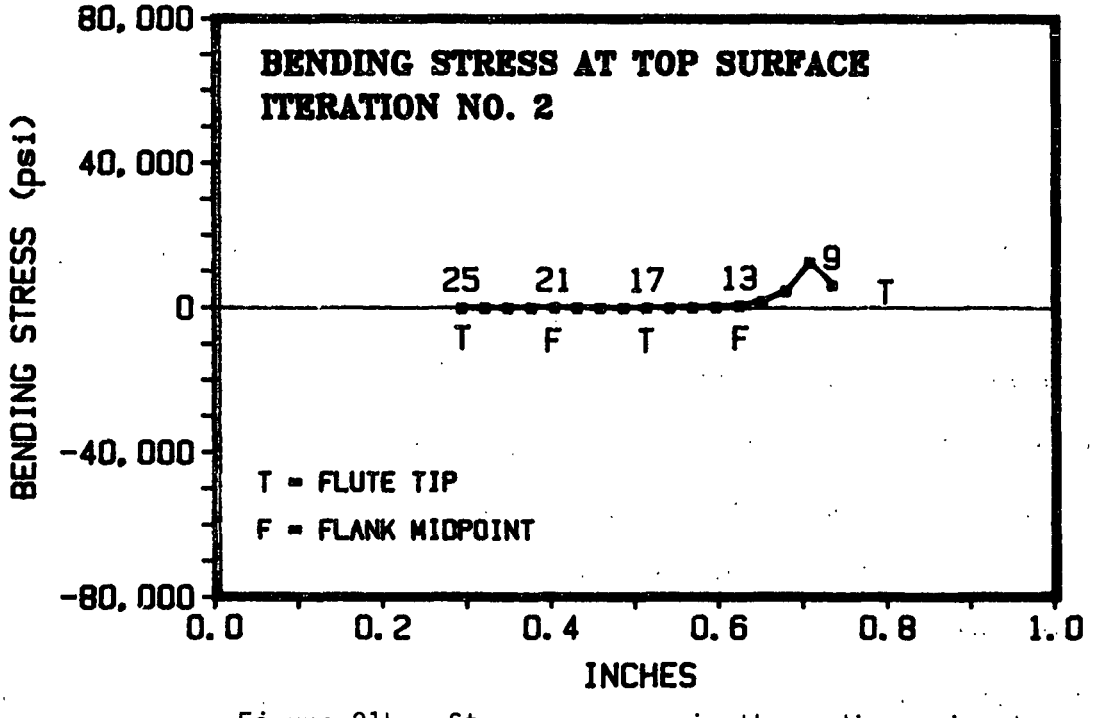

Figure 21b. Stresses occur in the medium prior to forming.

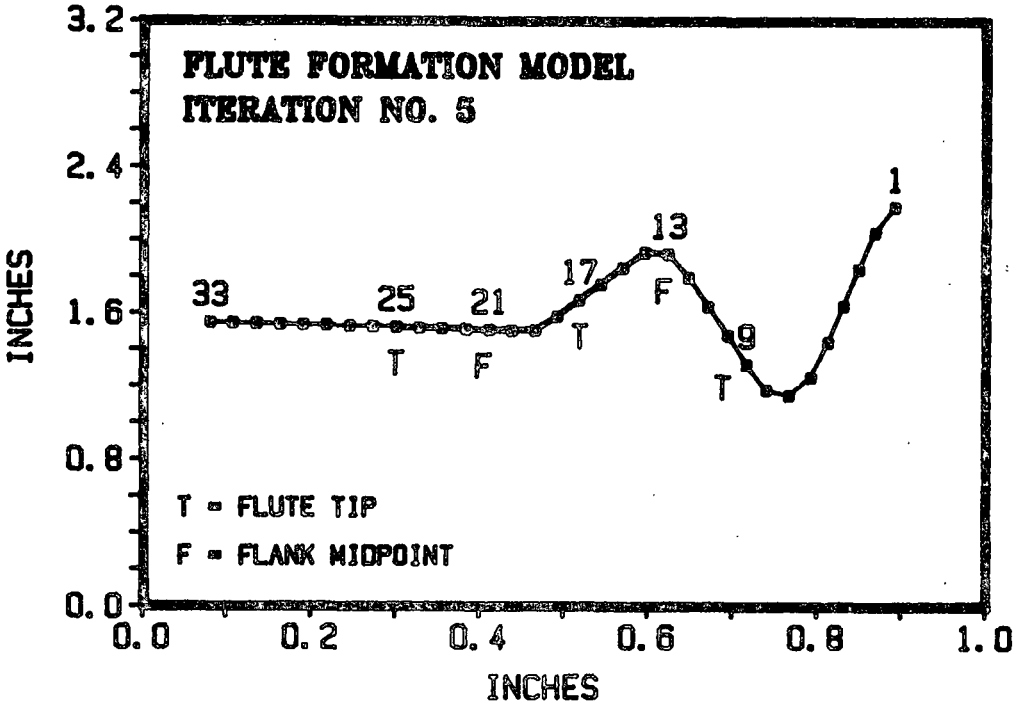

Figure 22a. Medium configuration at maximum bending of leading flank (joint #13).

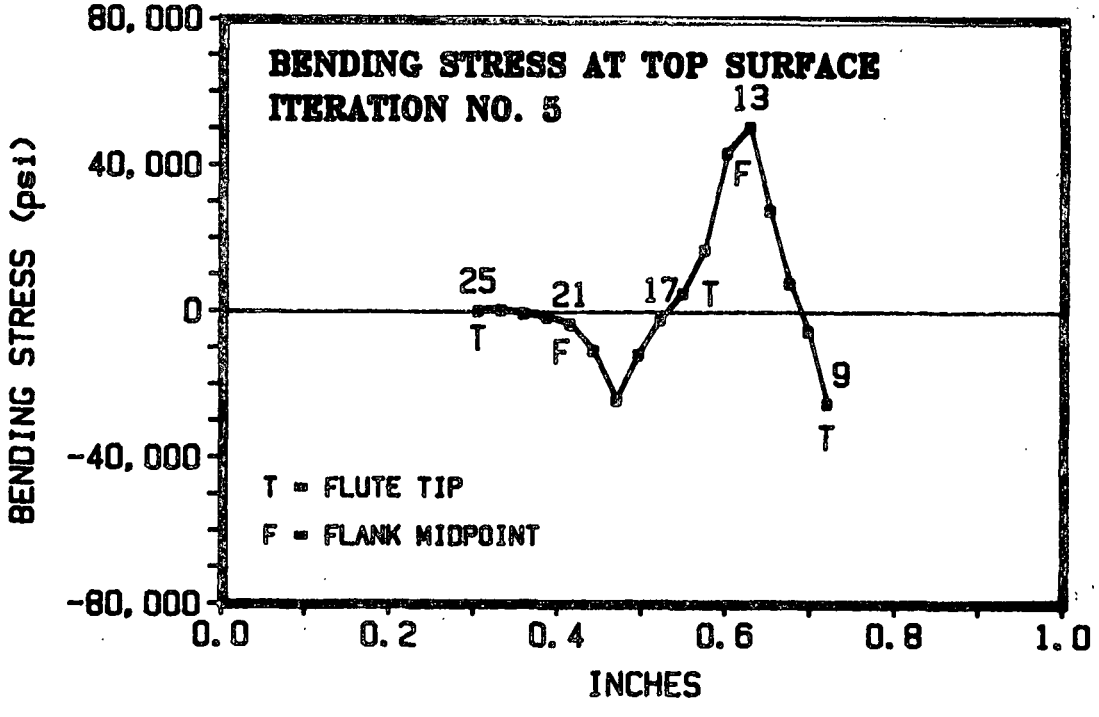

Figure 22b. Maximum bending stress in leading flank (joint #13).

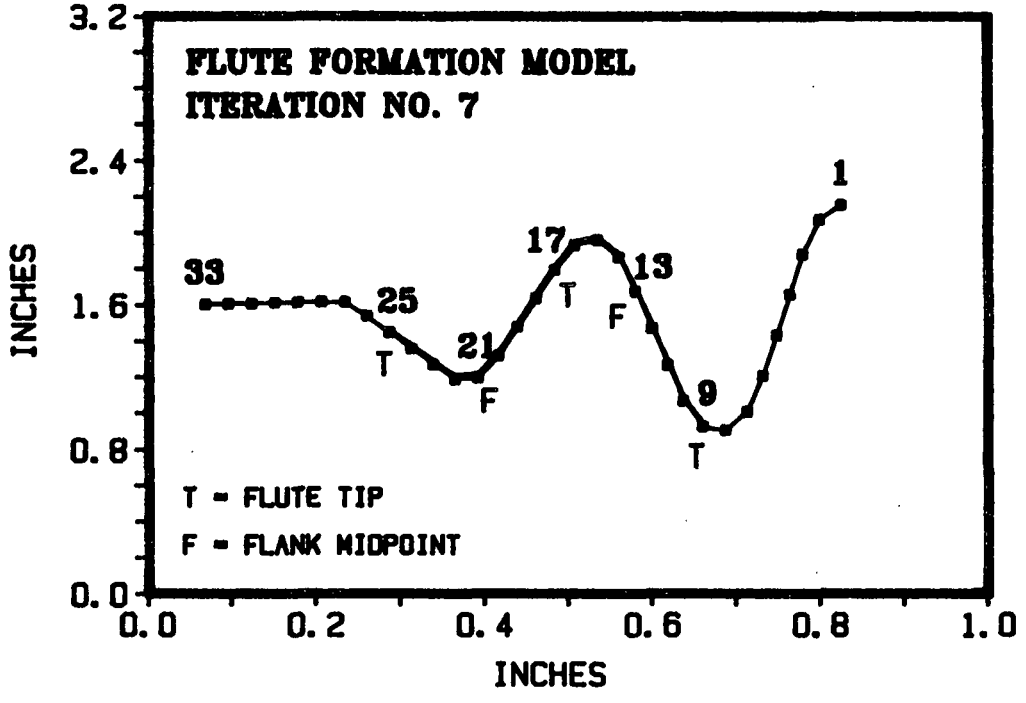

Figure 23a. Medium configuration at maximum bending of trailing flank (joint #21).

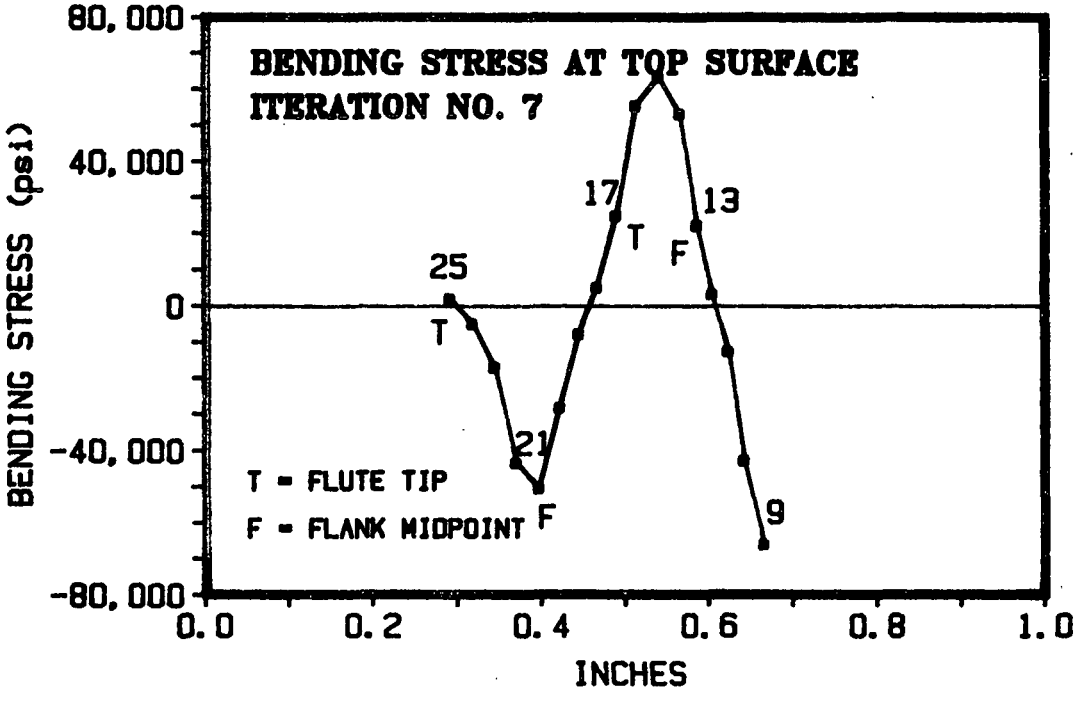

Figure 23b. Maximum bending stress in trailing flank (joint #21).

side than on the trailing side. There is some visual evidence to support this hypothesis.

Figure 24a shows the complete formation of the flute at iteration #16. Figure 24b indicates that the flute tips are at their maximum bending stress of approximately 75,000 psi. This is slightly less than but comparable to the stress predicted by the simple bending case which was previously illustrated. As expected, the flute tips (marked with a "T") are now at approximately the same bending stress. This level of stress is more than ten times greater than the failure stress for a typical 26-lb medium. Also, this stress is higher than the maximum stress that had occurred at the midpoint of the flank. This may explain the greater strength losses at the flute tip than at the flute flanks. The midpoint of the flanks have straightened in the final formation and the bending stress at this location is now nearly 0 psi.

To verify the stress analysis, a laboratory study has been started to determine the cause, extent and location of damage to the medium during flute formation. In this test series, a medium specimen would be bent around a radius which is similar in size to that of a flute tip (radius of 0.06 inches). After the medium has been flexed around the radius the following set of tests would be conducted:

1. A section of the specimen would be tested for its MD STFI compression strength.

2. Using a surface grinder, three other sections of the specimen would have portions of the compression side (concave side of the bend) removed to a depth of 2, 4 and 6 mils. Following the surface grinding, the MD STFI compression strength would be determined.

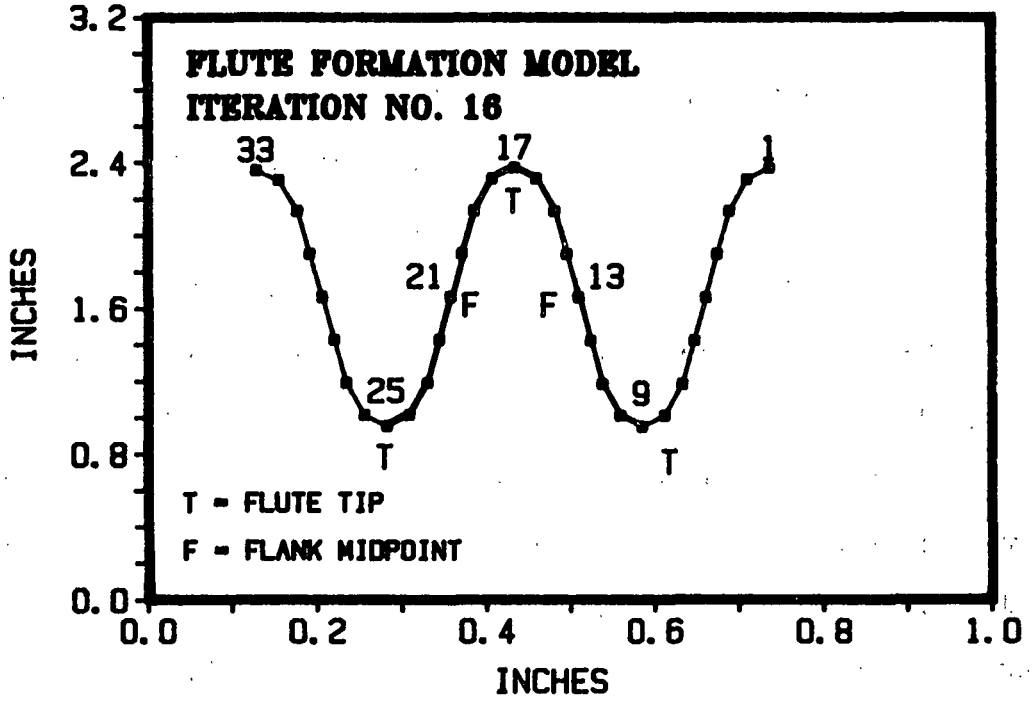

Figure 24a. Medium configuration at maximum bending of flute tips (joints #9, #17, #25).

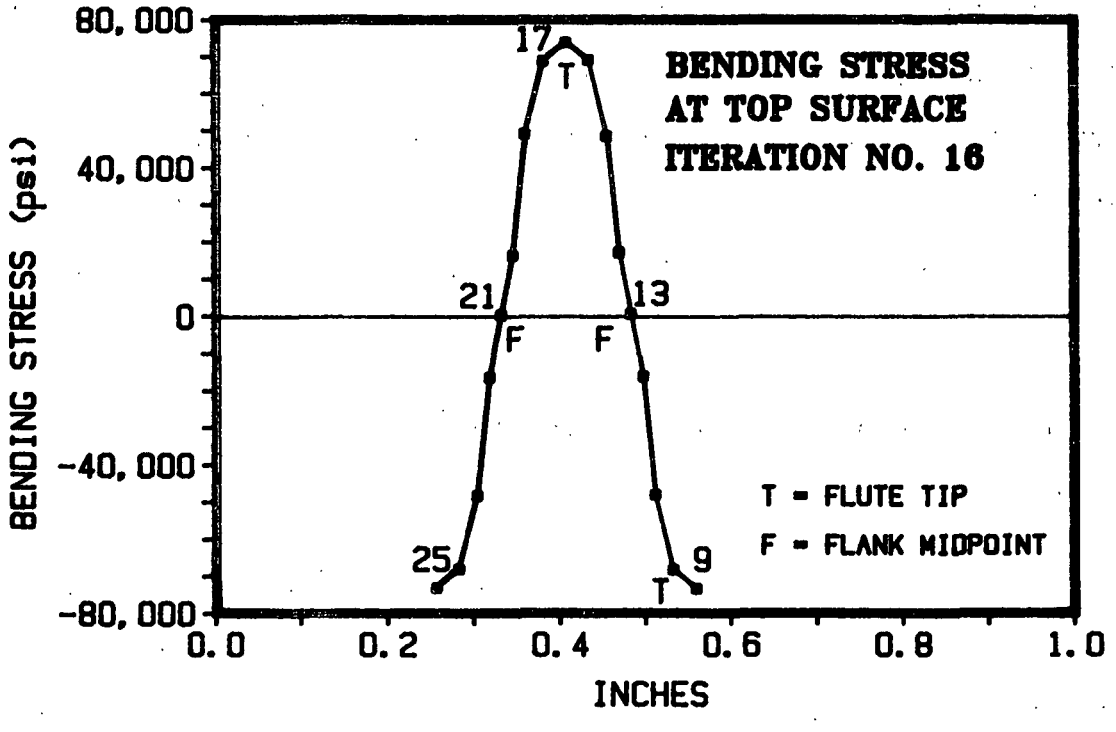

Figure 24b. Medium bending stress in flute tips (joints #9, #17, #25).

3. Three other sections of the specimen would be surface ground on the tension side of the bend and tested in the same way as described for the compression side.

4. A control specimen (unflexed) would be tested in the same way as described in parts 1, 2, and 3 above. The control specimen would account for any initial non-uniformity in the compression strength contribution and any damage which may due to the surface grinding.

The grinding process would provide a profile of the compression strength contribution to the medium through the thickness direction. This would expose the portion of the medium which has experienced damage in the flexed specimen. This portion of the laboratory study is in progress.

Although the bending stresses apparently play a large role in damaging the medium during formation, other factors may be present to reduce the strength. One important factor may be the level of Z direction compression stress on the flute tip. The compression stress on the medium occurs at the nip of the corrugator. A thickness loss of approximately 30% at the flute tips has been observed. The significant level of thickness direction compression may result in fiber-to-fiber bond failure and contribute to strength losses. A reduction in the strength retention at the flute tips would adversely affect the first yield point of the board in flat crush loading. Testing will be conducted to investigate the damage caused by Z-direction compression of a medium specimen. A test series similar to that for the flexed specimens would be carried out.

Further investigation of strength losses due to flute formation would involve combining the effects of flexing the medium and Z-direction compression.

A single flute forming apparatus may also be used to study the load deflection curve required to form a flute and investigate the strength losses at various positions around the flute.

Future work in this area will include the following:

1. Further analysis of the stresses produced in the medium during flute formation. The use of a finite element analysis program with non-linear material capabilities will be investigated.

2. Determining possible flute geometry changes which would reduce the strength losses during formation and thus increase the flat crush and board compression strength.

3. Continuation of the laboratory study which will attempt to determine the cause, extent and location of medium damage.

4. Using the information acquired from the flute formation analysis and laboratory study of medium damage, a more accurate estimate of medium properties after corrugating may be made. A non-linear finite element analysis program would allow an analysis of the entire flat crush load deflection curve.

5. Investigate the effect of medium damage and flat crush loads on other board properties such as bending stiffness and compression strength.

References

1. Baum, G. A., Habeger, C. C. and Fleischman, E. H. IPC Technical Paper Series No. 117, November 1981.

2. Mechanics of Fluting, Project 3396, Report No. 1 to the Members of the Institute of Paper Chemistry, June 15, 1981.

3. W. J. Whitsitt and G. A. Baum, Compressive Strength Retention During Fluting, Part 2. Improved medium strength, Tappi Journal, May, 1986.

Appendix

COMPRESSIVE STRENGTH RETENTION DURING FLUTING. PART 2: IMPROVED MEDIUM STRENGTH

W. J. Whitsitt
Research Associate
The Institute of
Paper Chemistry
Appleton, WI 54912

G. A. Baum
Division Director
The Institute of
Paper Chemistry
Appleton, WI 54912

ABSTRACT

Previous research has shown that the compressive strength of corrugating medium is degraded in the fluting operation. In this article, attention is focused on papermaking ways to alter the properties of the medium so it can be formed with less damage and thus give more strength to the combined board. At constant basis weight, compressive strength retention is favored by high density (if associated with better fiber bonding) and a high out-of-plane to in-plane stiffness ratio (E_z/E_x). These may be achieved by using higher wet pressing pressures. Higher pressing pressures densify the medium and tend to increase E_z at a faster rate than E_x. The higher out-of-plane stiffness helps the medium resist fiber-to-fiber bond damage during fluting, and hence the medium retains more compressive strength. Densification also reduces caliper, which lowers the bending strains during fluting. As a result of the above, flat crush and ECT increase due to a better retention of strength during fluting and the higher base strength of the medium. Succeeding articles in this series will discuss other aspects of the forming operation and high speed runnability.

INTRODUCTION

In a previous article we discussed the strength losses which occur during fluting (1). Our results indicated that about 40% of the MD and 20% of the CD short span compressive strength (STFI) of the medium is lost in the fluting process. These losses are a result of the high bending strains imposed on the medium as it is fluted and by the high web tensions in the fluting labyrinth. By reducing these losses in strength, it should be possible to improve ECT and flat crush.

There are two approaches to minimizing strength losses during fluting. One approach is to make more effective use of preconditioning heat and steam. From a forming standpoint, the function of preconditioning is to temporarily alter the properties of the medium so it can be formed with less damage. Thus there is potential for improved fluting (minimizing losses) by optimizing the preconditioning heat and steam. Use of this approach will be discussed in a future article.

The second approach is to alter the properties of the base medium during its manufacture so that it can be formed with less damage. This area is the subject of this article.

Other research at The Institute of Paper Chemistry has shown that edgewise compressive strength is highly related to the elastic moduli of the sheet (2). Baum, Habeger and coworkers (3,4) have developed ultrasonic techniques for measuring the in-plane and out-of-plane elastic moduli of paper. High compressive strengths are favored by high moduli in the MD and CD directions (E_x and E_y) and by high thickness direction moduli (E_z, G_{xz}, G_{yz}). Sheet densification to increase fiber bonding is an effective way to increase all of these moduli and hence, compressive strength.

Our past work indicates that the retention of compressive strength during fluting is approximately related to the elastic stiffnesses of the sheet, basis weight and density as follows.

$$RR = 1 - (K/R)(E_x/E_z)^{1/4}\, W/\rho \qquad (1)$$

where RR = retention ratio (ratio of compressive strengths of fluted to uncorrugated medium)
E_x = MD Young's modulus
E_z = out-of-plane Young's modulus
W = basis weight
ρ = density
R = radius of curvature of the fluting rolls
K = constant

Thus in the fluting operation the retention of compressive strength should be favored by high density and a high thickness direction modulus (E_z), and adversely affected by high caliper (W/ρ) and MD modulus (E_x). This is shown in Fig. 1. Our initial research discussed here focused on wet pressing as a means for improving compressive strength retention and improved end-use properties.

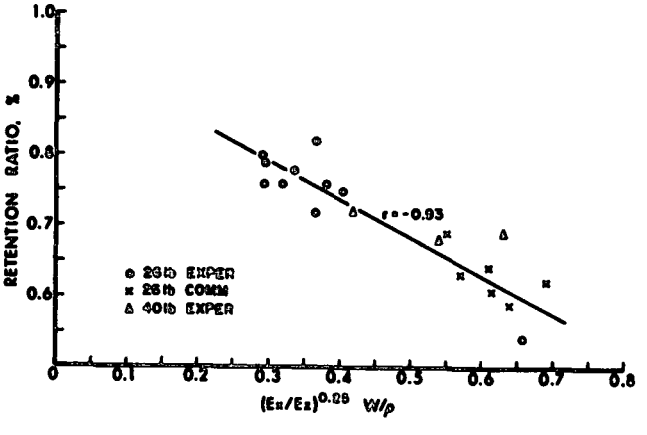

Fig. 1 Retention of compressive strength during fluting depends on elastic stiffnesses, (E_x/E_z), basis weight (W) and density (ρ).

Fluting Performance of Densified Mediums

We made oriented sheets on a Formette Dynamique from a 75% semichemical/25% softwood furnish over a range of densities from about 500 to 1100 kg/m^3, based on IPC soft platen caliper tests (5). To obtain an initial evaluation of corrugating performance, the 26 and 40 lb/1000 ft^2 experimental sheets were spliced into a commercial "carrier" medium, and made into single-faced boards at a speed of about 200 fpm.

All of the experimental and the commercial mediums used as controls corrugated with no difficulties at the low speed used. No bonding problems were encountered; the single face pin adhesion test values were satisfactory for all the mediums.

Figure 2 shows that increasing sheet density increases the retention ratio of compressive strength for both the 26 and 40 lb/1000 ft^2 experimental mediums, as compared to a commercial 26 lb/1000 ft^2 medium. The improvements in retention were less for the 40 lb/1000 ft^2 mediums than for the lighter material because of the greater thicknesses of the 40 lb/1000 ft^2 sheets.

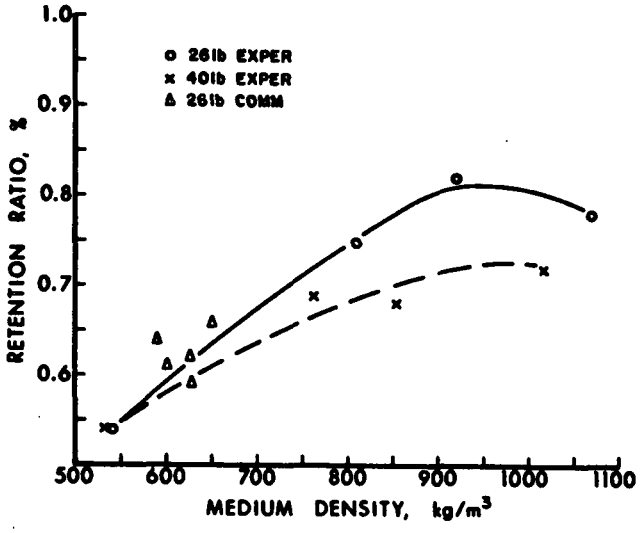

Fig. 2 Effect of density on retention of compressive strength during fluting.

Densification improves most strength properties, thus flat crush strength also increased substantially as density increased, as shown in Fig. 3. At the higher densities the flat crush strengths are greater than those obtained with most commercial mediums. These improvements in flat crush can be attributed to both better retention during fluting as well as the higher MD compressive strengths of the densified sheets.

Compression tests on the combined board show that increasing the medium density markedly increases CD ECT (Fig. 4) as a result of the higher CD compressive strength of the medium.

Increasing medium density monotonically increases CD STFI compressive strength; however, CD ring crush passes through a maximum at a density of 750-800 kg/m^3 (Fig. 5). Thus the shortspan compressive strength results were more indicative of combined board ECT performance. A similar situation prevails when MD STFI and MD ring crush results are compared with the combined board flat crush results (6). Seth (7) also has shown that ring crush passes thru a maximum as wet pressing is increased.

Higher wet pressing pressures also produce substantial increases in the tensile strength of the medium (Fig. 6). The higher tensile strengths should allow higher corrugating speeds before flute fracture occurs because the medium will be better able to tolerate the high tensile stresses imposed during fluting.

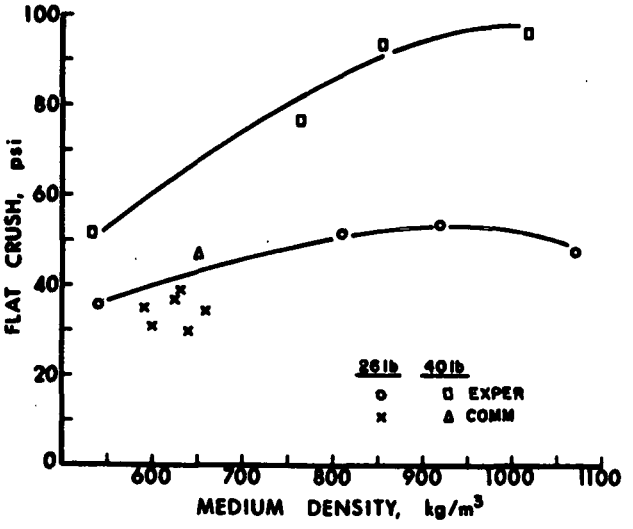

Fig. 3 Increasing medium density improves flat crush.

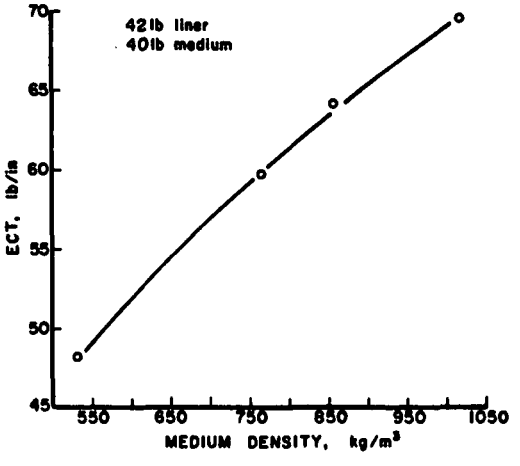

Fig. 4 Increasing medium density improves ECT strength.

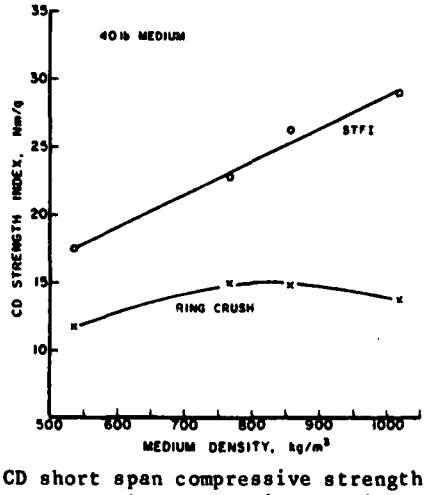

Fig. 5 CD short span compressive strength and ring crush results vs. medium density.

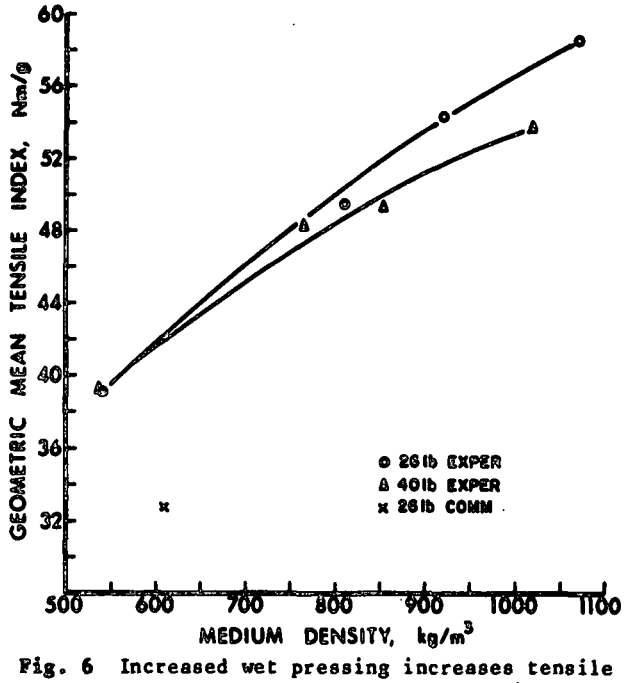

Fig. 6 Increased wet pressing increases tensile strength.

The specific in-plane and out-of-plane elastic stiffnesses also increased with increasing density as shown in Fig. 7. As noted earlier, compressive strength is dependent on the product of $E_x^{3/4}E_z^{1/4}$ or $E_y^{3/4}E_z^{1/4}$ for the MD or CD directions, respectively (2). Because densification increases all three stiffnesses, it would be expected that compressive strength would increase as illustrated in Fig. 5 for the short span STFI compressive strength results.

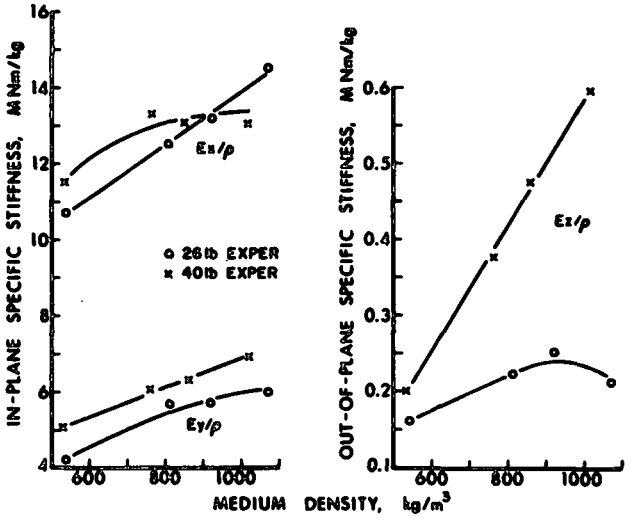

Fig. 7 Effect of density on elastic stiffnesses.

Runnability

Work was carried out to determine whether densification of the medium would adversely affect high speed runnability, including flute fracture, high-lows, and bonding. Because of their greater strength, densified mediums should be better able to resist fracture, but densification could reduce porosity and water receptivity, which would affect high speed bonding.

Oriented medium sheets were made at several densities achieved by wet pressing. The sheets were made with typical MD/CD orientation of about 2/1, using a 75% semichemical plus 25% softwood furnish. Two pressing/drying techniques were employed, namely:

(1) Blotter pressed and dried. One side of sheet was in contact with blotters, while the other side was in contact with a belted rotary press-dryer drum.

(2) Felt pressed and dried. One side of sheet was in contact with a linerboard press felt, with the other side in contact with the belted rotary press-dryer drum.

The blotter and felt-pressed sheets exhibit different compressive strengths at the same density as shown in Fig. 8. The same trend has been observed in other work in progress. This demonstrates that pressing conditions (such as the felt structure) also can affect compressive strength. The elastic stiffnesses of the sheets are affected in a similar way by these drying techniques, as shown in Fig. 9. While the felt-pressed sheets gave lower compressive strengths and stiffnesses, they exhibited higher tensile strengths at the same density, see Fig. 10.

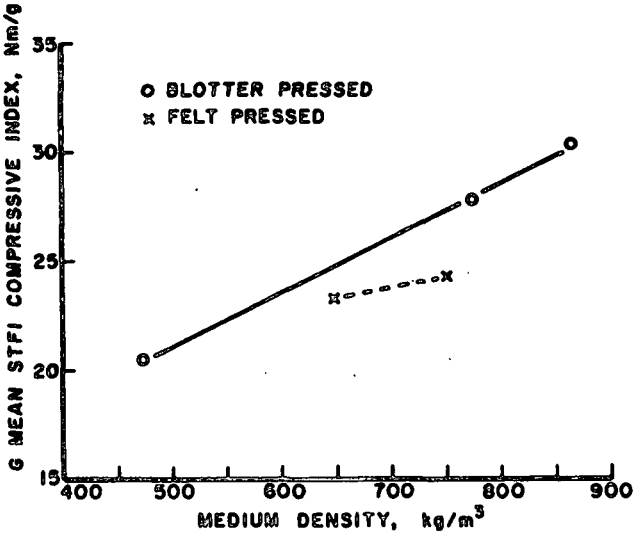

Fig. 8 Effect of densification on geometric mean compressive strength for different pressing/drying conditions.

The air porosity of the sheet decreases, as shown in Fig. 11, as pressing pressures are increased. Commercial mediums, however, exhibit a wide range of porosities. For example, the three commercial mediums used for controls in this study gave Bendtsen porosities ranging from about 350 to 1300 mL/min. Experience indicates that mediums having quite different porosities can be successfully bonded at normal corrugating speeds, although some adjustments in the adhesive or the preheaters and steam showers may be necessary.

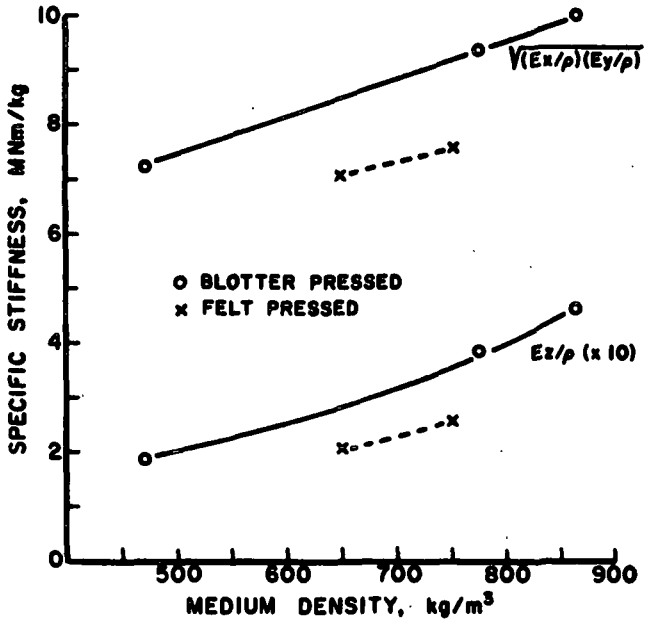

Fig. 9 Effect of densification on specific elastic stiffnesses for different pressing/drying conditions.

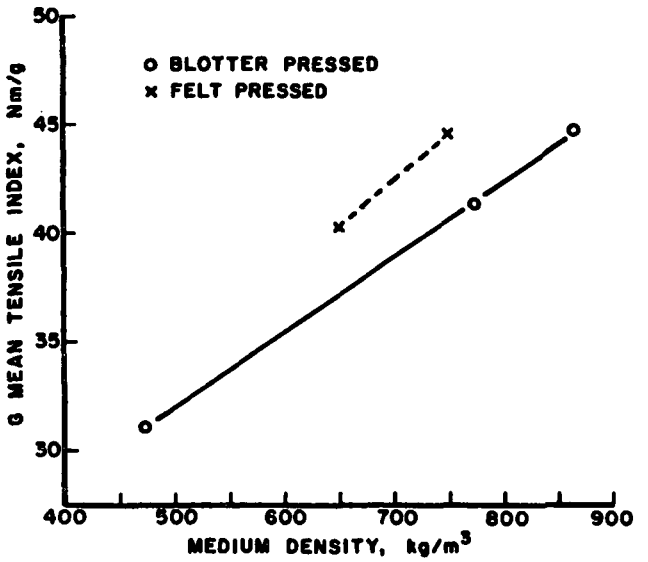

Fig. 10 Effect of densification on tensile strength for different pressing/drying conditions.

The water drop values for the blotter-pressed sheets increased with density, as expected. At the same density, however, the felt-pressed sheets gave lower water drop values, showing that pressing and drying conditions can affect the water receptivity of medium. In general, however, the experimental sheets had water receptivities in the same range as the commercial controls.

All of the mediums corrugated without fracture at speeds up to 650 fpm (Table 1), except that the lowest density sheets exhibited minor fractures in the 400 to 650 fpm range. This was probably due to their lower strength and relatively high caliper, which would increase the bending strain during fluting.

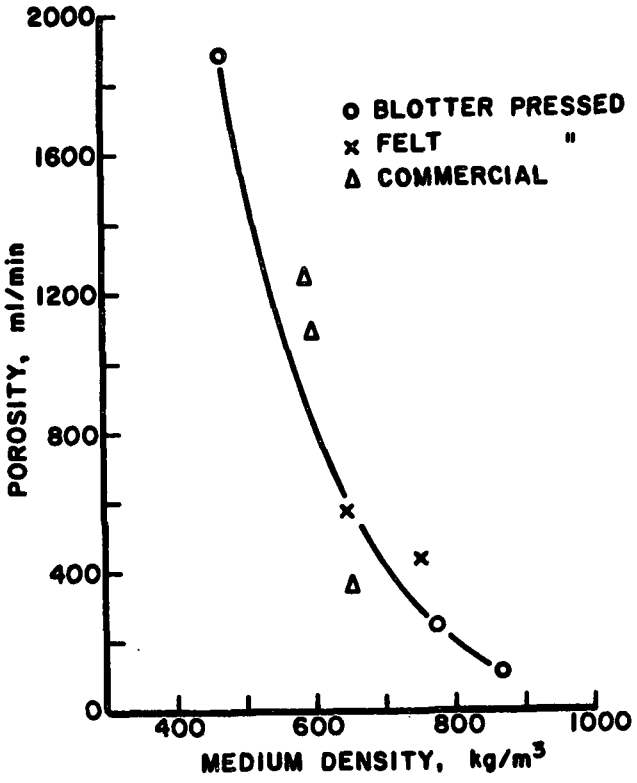

Fig. 11 Effect of densification on porosity.

Table 1. Corrugating results.

	Speed fpm	Low Dens. (185)	Med. Dens. (186)	High Dens. (102)	Felt Pressed[a] Med. Press.[a] (63)	Felt Pressed[a] High Press.[a] (77)	Commercial Controls 6171	6208	6209
Fracture[b]	400	SlF	No F	No F	No F	No F	No F	No F	No F
	550	SlF	No F	No F	No F	No F	No F	No F	No F
	650	SlF	No F	No F	No F	No F	No F	No F	No F
Pin adhesion lb/ft	400	26.2	37.0	36.5	--	--	38.5	36.0	36.5
	550	28.1	33.1	31.8	--	--	33.0	32.4	31.1
	650	20.1	22.8	--	--	--	18.5	24.8	23.5
High-low, % >4 mil	400	1.0	11.4	6.2	0	4.2	3.6	12.5	15.6
	550	0	7.8	17.2	0	6.2	15.6	--	20.8
	650	1.0	1.0	--	6.2	8.3	11.5	14.6	16.6
% >3 mil	400	6.2	20.8	15.6	2.1	14.6	12.2	27.1	35.4
	550	3.1	15.4	28.9	10.4	22.9	30.2	11.4	27.1
	650	4.2	4.2	--	10.4	27.1	34.0	27.1	35.5
ECT, lb/in.	400	33.1	40.1	41.7	--	--	39.2	36.6	36.2
	550	34.2	40.0	43.0	--	--	38.8	36.6	35.2
	650	33.1	41.6	--	--	--	36.8	34.7	33.6
	Av.	33.5	40.6	42.4	--	--	37.6	36.0	35.3
Flat crush, psi	400	38.1	56.1	59.2	36.5	40.6	34.5	34.8	30.5
	550	39.7	57.1	57.2	35.4	40.1	35.2	36.2	30.8
	650	37.7	57.3	--	38.2	40.2	34.1	35.4	30.9
	Av.	38.5	56.8	58.5	36.7	40.3	34.6	35.5	30.7

[a]Low and high felt pressed sheets, fabricated at a later time with new 42-lb liner roll.
[b]SlF = slight fracture; No F = no fracture.

Figure 12 indicates that the experimental blotter-pressed mediums exhibited high-low levels which were about the same or less than the commercial controls. High-lows were defined as the percentage of flute height differences exceeding 4 mils. They were measured using a SELCOM laser displacement gage. Thus, densification does not appear to increase the proclivity to form high-lows. It is believed this is due to the lower thickness and better fiber-to-fiber bonding achieved by wet pressing.

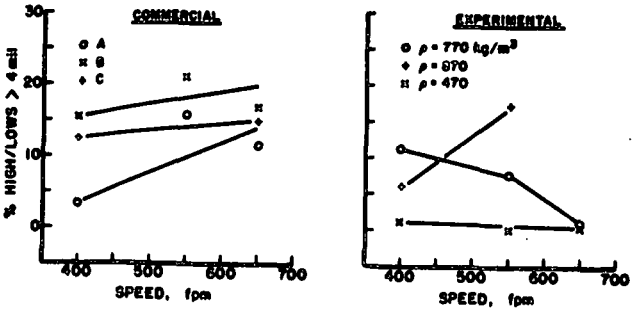

Fig. 12 High/low results on commercial and densified mediums. (A, B, and C are three 26-lb commercial mediums used as controls and corrugated at the same time as the experimental medium).

In Fig. 13 the single-face adhesion results for the densified blotter-pressed mediums are compared to the commercial controls. In general, the densified sheets exhibit about the same pin adhesion strengths as the commercial mediums at the same corrugator speeds. In both cases the adhesion strengths decrease with increasing speed, consistent with other results from our pilot corrugator.

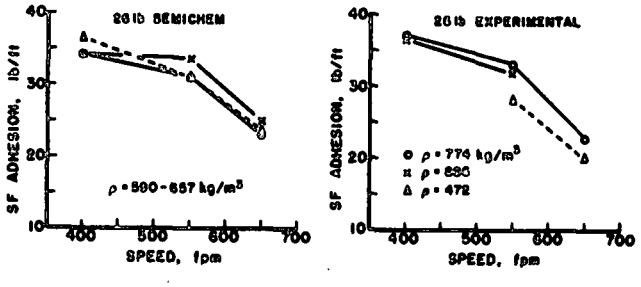

Fig. 13 Comparison of single-face adhesion results on commercial and experimental densified mediums.

Summarizing, these results indicate that densification of medium can be beneficial to high speed runnability. If necessary, adhesive formulations could be changed to optimize adhesion. It would still be possible to adjust the water receptivity of the medium with surfactants as is commonly done today.

CONCLUSIONS

This work explored ways to minimize the strength losses that occur during fluting (1). This would enhance ECT and flat crush strength in combined board. The results show

1. Densification of medium by increasing the wet pressing pressure makes substantial increases in flat crush and the ECT strength of combined board made from the medium. These improvements are due to the retention of compressive strength during fluting and the higher compressive strengths and elastic stiffnesses obtained from densification.

2. The retention of compressive strength during fluting is favored by lower weight to density ratios (caliper) and by a higher out-of-plane stiffness (E_z/ρ) relative to the in-plane stiffness (E_x/ρ).

3. The high density mediums gave single-face bonding levels in the corrugator which were comparable to those obtained with commercial mediums. High-low flute formation levels were also comparable for the experimental and commercial mediums. While these results are not necessarily conclusive because of the small sheet sizes and narrow width of the pilot corrugator, they do indicate that commercial corrugating should be feasible. If necessary, adjustments in surface receptivity or starch formulation could be made.

LITERATURE CITED

1. Whitsitt, W. J., and Sprague, C. H. Compressive Strength Retention During Fluting. Part I, Strength Losses. To be published.

2. Habeger, C. C., and Whitsitt, W. J., Fibre Science and Technol. 19:215-239 (1983).

3. Baum, G. A., Brennan, D. C., and Habeger, C. C., Tappi 64(8):97 (1981).

4. Mann, R. W., Baum, G. A., and Habeger, C. C., Tappi 63(2):163 (1980).

5. Wink, W. A., and Baum, G. A. A rubber platen caliper gage - a new concept in measuring paper thickness. Tappi 66(9):131-133 (1983).

6. Whitsitt, W. J. Compressive Strength Factors and Relationships. Forest Products Laboratory Compression Symposium, Madison, WI, Oct. 1-3, 1985.

7. Seth, R. S., Tappi 67(2):114 (1984).

THE INSTITUTE OF PAPER CHEMISTRY

Appleton, Wisconsin

Status Report

to the

PAPER PROPERTIES AND USES

PROJECT ADVISORY COMMITTEE

Project 3467

PROCESS, PROPERTIES, PRODUCT RELATIONSHIPS

September 11, 1987

PROJECT SUMMARY

PROJECT NO. 3467: PROCESS, PROPERTIES, PRODUCT RELATIONSHIPS

PROJECT STAFF: G. A. Baum, C. C. Habeger September 11, 1987

PROGRAM GOAL:

Develop relationships between the critical paper and board property parameters and how they are achieved in terms of raw material selection, principles of sheet design, and processing conditions.

PROJECT OBJECTIVE:

(1) To improve our capability of characterizing paper and board materials,
(2) to relate measured parameters to end-use performance (especially in the case of Z-direction measurements), and
(3) to relate measured parameters to machine and process variables.

PROJECT RATIONALE, PREVIOUS ACTIVITY, AND PLANNED ACTIVITY FOR FISCAL 1987-88 are on the attached 1987-88 Project Form.

SUMMARY OF RESULTS LAST PERIOD: (October 1986 - March 1987)

(1) Construction of the instrument for measuring scattering coefficients in heavy board materials is now underway.

(2) Work on the variables which affect polar diagrams is continuing with measurements on carton boards and a study of the z-direction distribution of properties.

(3) A new in-plane robotics system is under construction using commercially available robots and electronics. IPC will supply software to member companies upon request.

(4) Work to automate the out-of-plane shear measurements is nearly complete.

(5) Work with z-direction loss measurements suggests that they may be useful for establishing ply bond failures in multiply boards.

(6) A paper describing the effect of transverse slice flows on sheet properties was written for presentation at the TAPPI Process Control Conference in March, 1987.

(7) The paper concerning the use of microwave attenuation as a measure of fiber orientation anisotropy was published in TAPPI 70(2):109(1987).

(8) In student work, Brian Berger is making good progress on his thesis concerning the relationships between transverse fiber properties and z-direction sheet properties.

SUMMARY OF RESULTS THIS PERIOD: (April 1987 - September 1987)

(1) Polar diagrams being studied as a function of position in the z-direction.

(2) The size and shape of polar diagrams have been studied in terms of the interaction between fiber orientation and wet straining.

(3) The effects of machine adjustments on polar diagrams are currently being investigated on commercial linerboard samples.

(4) Construction of the instrument for measuring scattering coefficients on high basis weight grades is nearing completion.

(5) We have started construction on higher frequency laboratory out-of-plane transducers using a newly developed piezoelectric film, having better temperature performance and greater sensitivity.

(6) New in-plane bender transducer of better modal purity, greater sensitivity, smaller size, and more rugged construction have been built and tested.

(7) The end effector for the in-plane robot has been received and the initial design flaws have been corrected.

(8) The robot has been returned twice because of malfunctions, but it has been shown capable of performing its intended functions.

(9) Demonstrations on artificially contrived interfaces and on mill produced multilayer board continue to demonstrate the utility of out-of-plane acoustic loss coefficient as an indicator of z-direction mechanical inegrity in layered paper.

(10) A paper which summarizes much of our earlier work was published in Appita. Baum, G. A., "Elastic properties, paper quality, and process control", Appita 40(4):288(1987).

(11) A paper describing some of the polar diagram work was presented at the 1987 International Paper Physics Conference in Mont Gabriel in September, 1987. "Polar Diagrams of Elastic Stiffness: Effect of Machine Variables" is attached as Appendix 1.

(12) In student work, Brian Berger is nearing completion of his thesis concerning the relationships between transverse fiber properties and z-direction sheet properties.

PROJECT TITLE: Process, Properties, Product Relationships

PROJECT STAFF: G. Baum, C. Habeger

PRIMARY AREA OF INDUSTRY NEED: Properties related to end uses

PROGRAM AREA: Performance and Properties of Paper and Board

Date: 1/14/87

Budget: $200,000

Period Ends: 6/30/88

Project No: 3467

PROGRAM GOAL:

Develop relationships between the critical paper and board property parameters and how they are achieved in terms of raw material selection, principles of sheet design, and processing conditions.

PROJECT OBJECTIVE/GOAL:

(1) To improve our ability to characterize paper and board materials,
(2) to relate measured parameters to end-use performance,
(3) to relate measured parameters to machine and process variables.

PROJECT RATIONALE:

It is important to understand the relationships between process variables, end-use performance, and paper and board properties in order to improve these products or maintain performance within close tolerances while effectively utilizing available raw materials, minimizing energy requirements, and minimizing environmental impacts.

RESULTS TO DATE:

The major areas of activity and results can be separated into three areas: development of instrumentation; the impact of process variables on elastic properties; and the relationships between elastic properties and the end-use performance of paper. Ultrasonic techniques and instruments have been developed which enable us to measure all four of the in-plane elastic stiffnesses of paper and three of the five out-of-plane elastic stiffnesses. These instruments also are suitable for measurements on other planar materials. Some of the equipment has been automated, so that the measurements are carried out under computer control, appropriate calculations made, and the results printed out in a report format. A soft rubber platen caliper system was developed under this project to provide accurate caliper and density measurements. The ability to measure the three dimensional elastic behavior of paper has led to an extensive study of how process variables affect the elastic response. To date, process variables examined include wood species, pulping method, yield, refining, jet-to-wire speed ratios, wet pressing, wet stretching, drying restraints, and calendering. The effects of coatings, fillers, sheet composition, sheet structure, and environmental factors (temperature and relative humidity) have also been investigated. Several useful relationships between the elastic stiffnesses have been discovered. Finally, the elastic stiffnesses have been shown to be related to a number of the parameters now used to predict end-use performance and/or convertability. The elastic stiffnesses are fundamental properties of a material, and are good indicators of operating conditions on the paper machine and of final product quality. A microwave technique for determining fiber orientation has also been developed.

PLANNED ACTIVITY FOR FY 1987-88:

In recent years this project has been concerned with measuring the elastic properties of paper, and relating these to process variables and end use performance, where possible. These activities will continue in FY 1987-88.

The in-plane and out-of-plane elastic constants will be measured on a representative group of samples made from fibers differing in composition and structure (yield and refining) at different ambient environments. The data will be compared to individual fiber measurements and to use-oriented test results.

A device currently under construction that can measure specific scattering coefficients in heavy board materials will be used to test boards differing in composition and structure.

The use of polar diagrams to evaluate machine operating characteristics will continue.

With respect to instrumentation development, we plan to automate the Z-direction shear measurement apparatus and construct a second generation in-plane automatic system.

We will be working to develop out-of-plane loss measurement techniques. These may lead to non-destructive tests for determining poor ply bonding. We will also study the in-plane loss process using the strip resonance and attenuation techniques.

We will continue the study of the linear transient effect.

A study of formation will be undertaken in Project 3469, which will be complementary to the work in this project.

STUDENT RELATED RESEARCH:

B. F. Berger, Ph.D.-1987, B. J. Berger, Ph.D.-1987, R. R. Willhelm, MS-1988.

Status Report

PROCESS, PROPERTIES, PRODUCT RELATIONSHIPS

Project 3467

INTRODUCTION

Because Project 3467 is moving forward on several fronts, this status report is divided into different sections. Section 1 describes the continuing effort concerned with the interpretation of polar diagrams in terms of machine operating variables. Section 2 describes our new instrument for measuring transmitted light in heavy basis weight grades, enabling us to calculate scattering coefficients in these materials. Section 3 deals with new designs for ultrasonic transducers for out-of-plane and in-plane measurements and Section 4 outlines the activity concerning a new robotic in-plane ultrasonic testing instrument. Section 5 discusses some recent loss tangent results and explains how these may be applied.

Previous work on this project has been outlined in the Results to Date section. Much of the work, especially that of a fundamental or exploratory nature, has been carried out in student research.

SECTION 1. Polar Diagrams

The measurement of polar diagrams and their relationships with machine variables have been described in earlier Status reports (dated October 21-22, 1986, and March 25-26, 1987). The work relating transverse headbox flows to angle of lean was presented at the Tappi Process Control Conference in Nashville in March, 1987. A paper relating the shape and size of the diagrams to certain variables such as refining, jet-to-wire speed differentials, wet pressing, wet straining, and drying restraints was presented at the International Paper Physics Conference in Mont Gabriel in September, 1987. A copy of that paper is attached as Appendix 1.

The above work revealed that the "peanut shape", or necking down of the polar diagrams in the CD, was relatable to CD shrinkage effects. It is possible that a particular fiber orientation distribution might also give rise to a similar shape. The fact that the peanut shape is frequently observed near the edges of the web, however, lends credence to the notion of non-uniform CD shrinkage effects.

Current Activity

In addition to continual hardware and software (reporting) improvements, work relating to polar diagrams and their interpretation has been carried out in three areas.

(1) The measurement of polar diagrams and z-direction properties as a function of z-direction through the sheet. This activity was mentioned in the last report as items 2 and 3 on page 8. Figures 1 and 2 show the behavior of three in-plane and three out-of-plane specific elastic stiffnesses, respectively, as material is removed by grinding. The sheet is a single layer bleached kraft pulp prepared on a Formette Dynamique having a starting basis weight of 420 g/m^2. The in-plane properties, and density, are so far independent of basis weight, while the out-of-plane properties are decreasing. Thus far, a thorough analysis of the results has not been attempted, pending further data at still lower basis weights.

(2) We have explored the interaction between fiber orientation and wet straining on the shape and size of the polar diagrams, using special sheets prepared earlier for another project. Figure 3 shows the results obtained at three levels of wet straining and three levels of fiber orientation (actually three levels of jet-to-wire speed differentials). All of the nine sheets were wet pressed at the same pressure and all were dried under full

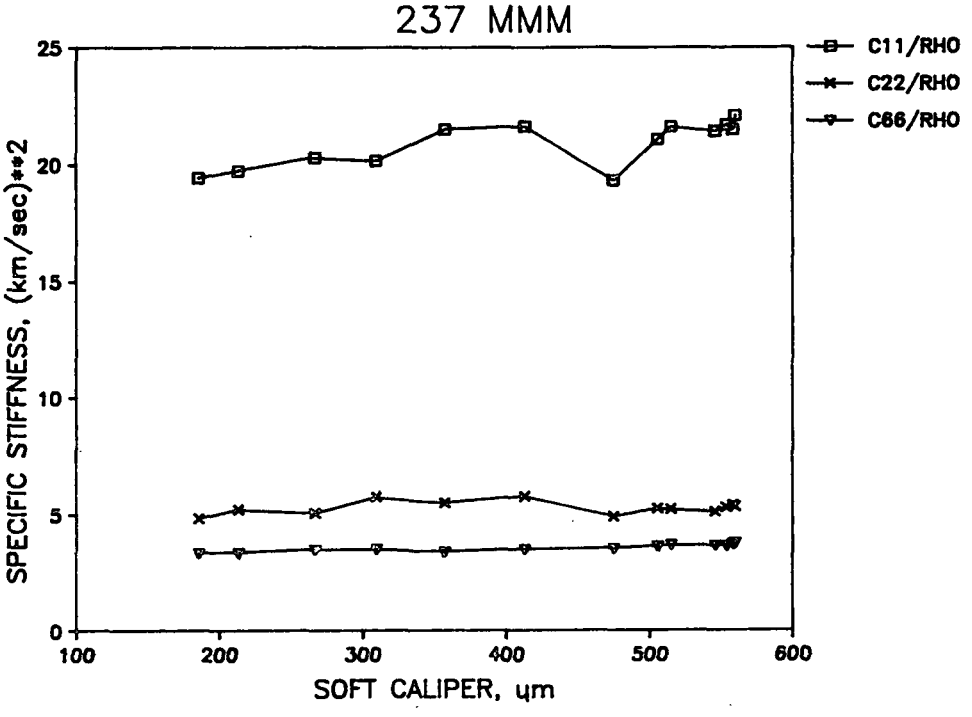

Figure 1. Specific stiffness vs. soft caliper.

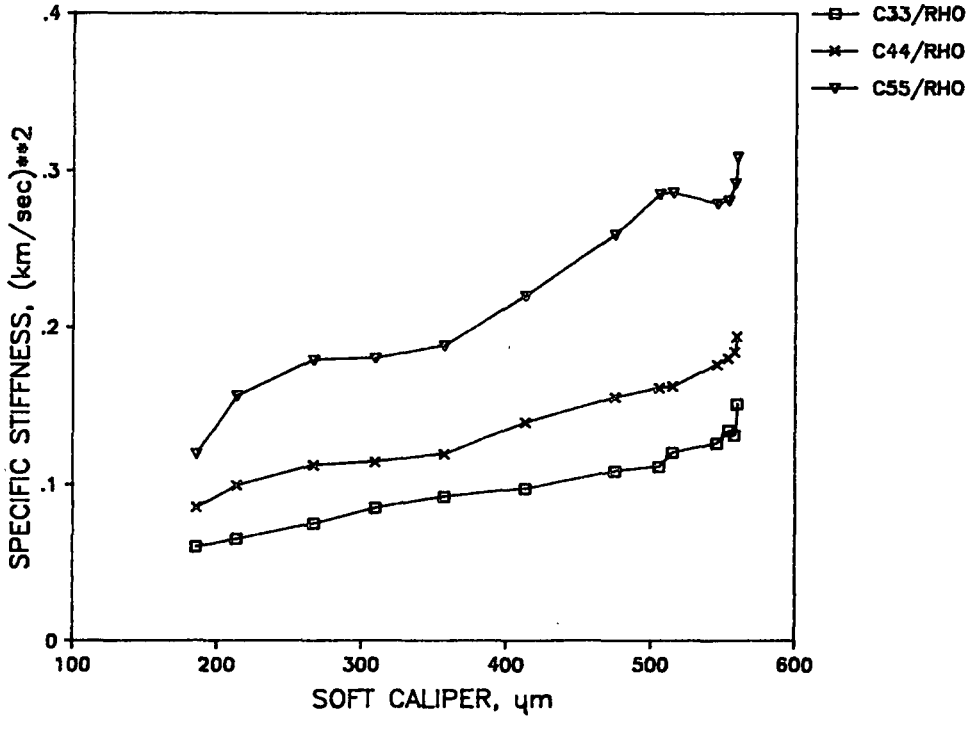

Figure 2. Specific stiffness vs. soft caliper.

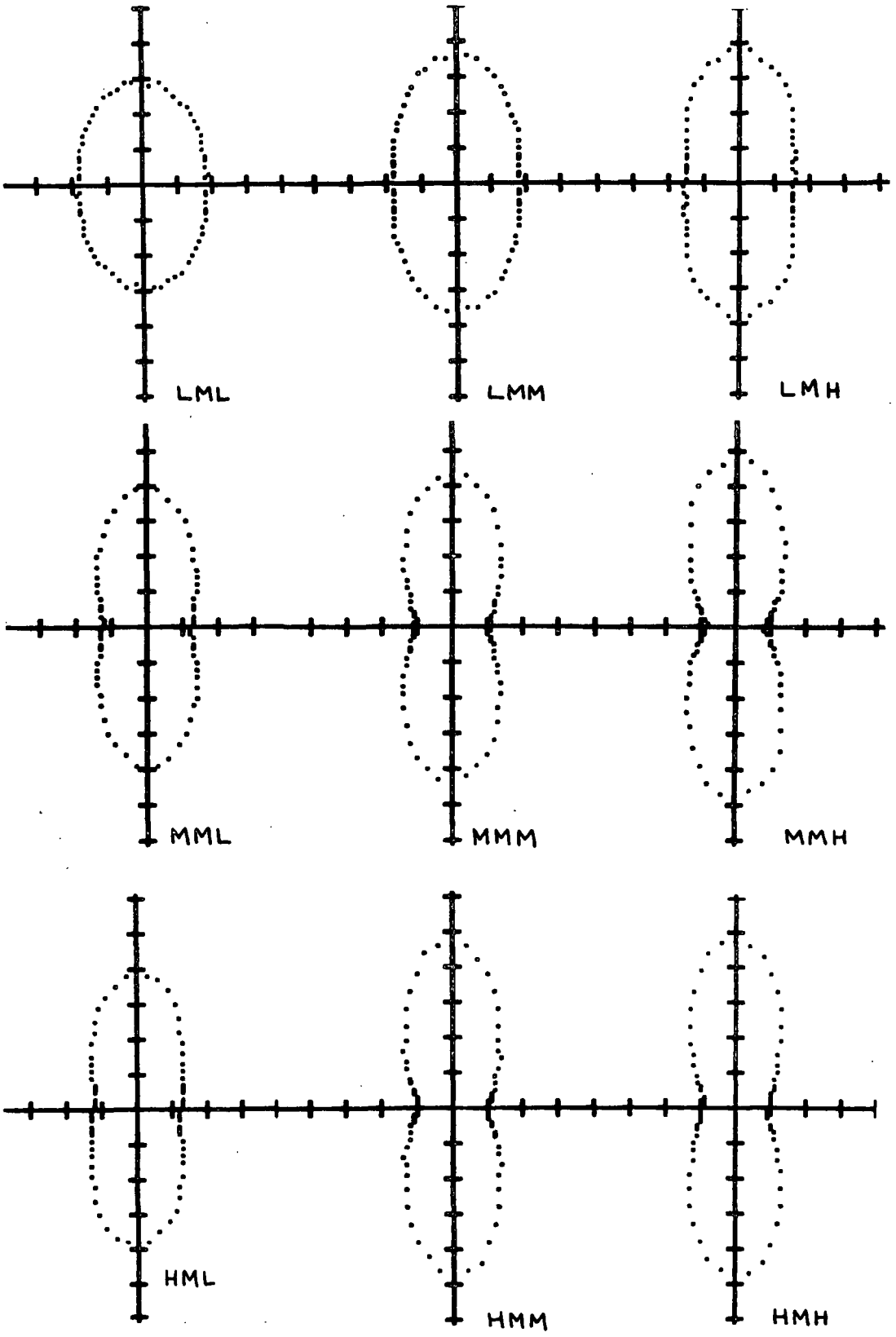

Figure 3. Change in shape of polar diagrams with fiber orientation (first letter, Low, Medium, High) and wet straining (last letter, Low (0%), Medium (1.2%), and High (2.4%). Middle letter denotes Medium wet pressing. All specimens were wet strained and then dried under full restraint.

restraint in both the MD and CD. The sheets were allowed to contract in the CD, however, during the wet straining step.

For the sheets examined, neither wet straining or fiber orientation alone seems to lead to the necked down shape, while the two together do. Other specific elastic stiffnesses have been measured on these sheets but time has not permitted a detailed analysis.

(3) In the last report (March 25-26, 1987) we asked for CD strips obtained before and after changes in one or more slice screws and also CD strips in which the machine speed had been changed in a series of steps. We have received several such samples and tests are currently underway. We hope to have some results available for discussion at the meeting on October 21-22, 1987.

SECTION 2. Scattering Coefficients of Board

INTRODUCTION

The degree of bonding of paper is commonly estimated from the light scattering coefficient determined from the reflectance of a single sheet on a black background (R_0) and the reflectance of a stack of sheets thick enough that addition of another sheet does not change the reflectance value (R_∞). For high basis weight papers, however, there is little difference between R_0 and R_∞; consequently, the calculation is imprecise.

A way around the dilemma is provided by the Kubelka-Monk theory, which shows that the scattering coefficient can also be determined from one reflection and one transmission (T) value. IPC student B. J. Conor was assigned the design and construction of an instrument based on reflection and transmission values as

a second-year research problem[1]. The instrument was later refined and evaluated by Knox and Wahren[2], who demonstrated that transmittance of heavy boards (to 699 g/m^3) could be measured, and that very good correlation was obtained for values of scattering coefficient of lighter weight papers calculated from measurements of R_0 and R_∞ and from measurement of R_0 and T.

In this instrument, the light source is a continuuosly-operated incandescent lamp. Photomultiplier tubes detect incident and transmitted light levels. The specimen is sandwiched between two Teflon diffusers, which become the top and bottom sheets of the "specimen stack." Specimen transmission is calculated from the measured light transmission of the stack and the previously determined reflectances of the top and bottom "sheets"[2]. The reflectance of the sample is determined on a separate instrument.

The results obtained with the instrument are quite satisfactory, but getting valid measurements is a rather demanding operation. In view of an anticipated routine use for the measurements, it was decided to construct a new instrument, much easier to operate, and which measures reflectance and transmittance directly.

NEW INSTRUMENT

As a basic concept for the new instrument, the specimen is placed between two integrating cavities. With the specimen to be viewed over a 15-mm diameter area, minimum integrating sphere size is about 20 mm diameter[3]. For easy, rigid attachment of source, detectors, and mounting means to the spheres, they have been made as spherical cavities inside cubic blocks. Figure 4 shows the arrangement.

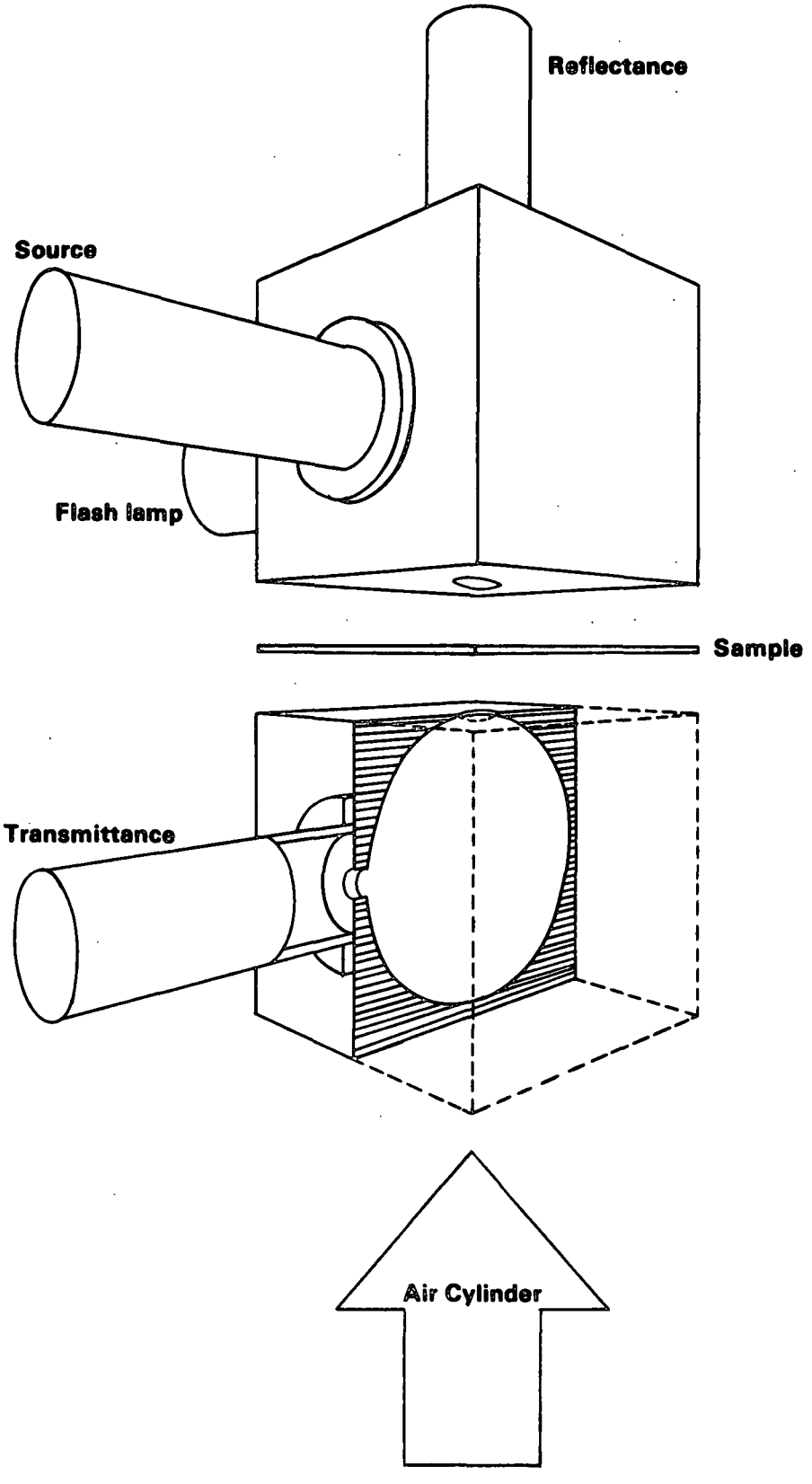

Figure 4. Schematic of the Optical Transmission Meter.

The upper cube is fixed in place and has attached to it the flash lamp source, the source intensity detector, and the reflected intensity detector. An air actuator moves the lower cube up and down on linear bearings. This cube supports the transmitted intensity detector. The sphere surfaces are lined with barium sulfate.

Illumination is provided by a flash lamp. This source gives the very high intensity level needed for sufficient light to pass through the specimen for detection. The very short duration will minimize heating effect on the specimen.

Three detector circuits are used. Each consists of a silicon photodetector, an amplifier, a peak-detection circuit, and a digital voltmeter. Optical filters are placed just ahead of the photodetectors to give spectral responses the same as the B&L Opacimeter. The arrangement is shown schematically in Fig. 5.

The source detector looks at the wall of the upper integrating sphere, registering a reference level for the illumination intensity. The reflectance detector sees only the top of the specimen, while the transmittance detector senses the light which passes through the specimen.

At present, the system is nearly assembled. It is anticipated that considerable work remains, however, in adjusting and calibrating the instrument.

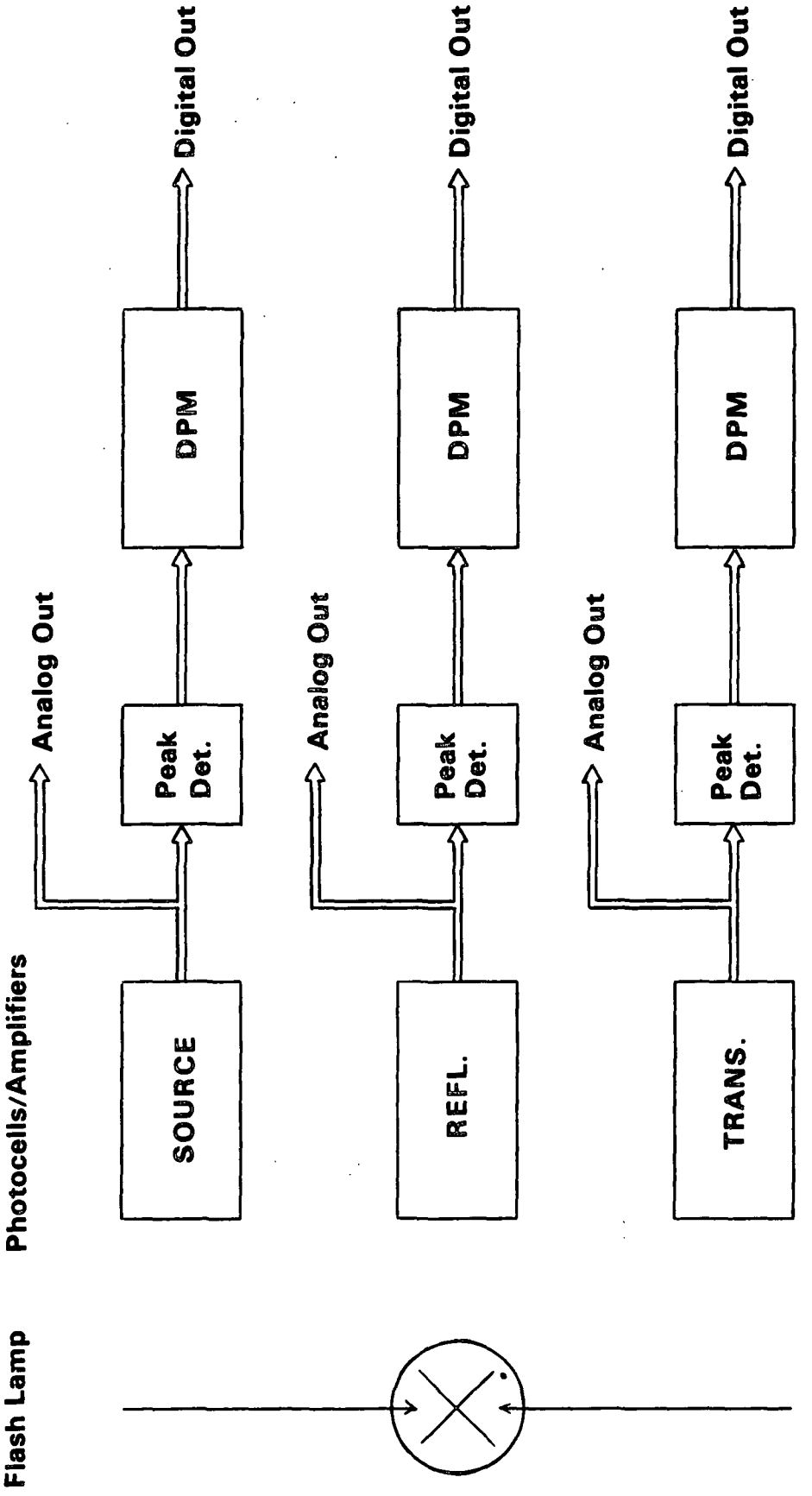

Figure 5. Block diagram of the detector circuits.

LITERATURE CITED

1. Conor, B. J. Development of a prototype instrument for measurement of diffuse light transmission properties of paper and board. A291 Research Problem. 30 p. The Institute of Paper Chemistry, Appleton, WI (June 21, 1982).

2. Knox, J. M., and Wahren, D. Determination of light scattering coefficient of light and heavy sheets. Tappi J. 67. no. 8:82-85 (Aug., 1984).

3. McNicholas, H. J. Absolute methods in reflectometry. J. Res. NBS 1, no. 1:29-74 (July 1928).

SECTION 3. New Ultrasonic Transducers

LABORATORY OUT-OF-PLANE TRANSDUCERS DEVELOPMENT

The piezoelectric film used in our longitudinal out-of-plane transducers is PVDF, a semi-crystalline high-molecular weight fluorocarbon which has a repeat unit of $(CH_2 - CF_2)$. We have been very successful in constructing broad-band low-impedance transducers for application to paper using PVDF film as the active element. However, there are some limitations. The piezoelectric coupling coefficient for PVDF is about one third that of the commonly used ceramic piezoelectrics. Also, at temperatures over 80°C, PVDF experiences a rapid irreversible loss in sensitivity.

Recently, Pennwalt, the leading US manufacturer of piezoelectric film, has developed a new film. This is a proprietary copolymer of PVDF, which they call VF2-VF3. It is not yet in high-volume production and detailed specifications are not available. Nonetheless, they claim that it has twice the piezoelectric coupling coefficient of PVDF and that it does not degrade below 100°C. The high temperature performance of the new film could be a godsend for our out-of-plane on-line work, in that our main concern in using PVDF on-line is its poor temperature stability. Increased piezoelectric sensitivity is, of course, always appreciated.

We have procured a small amount of the new film and are constructing transducers to be used in the out-of-plane laboratory apparatus. The construction is following our accepted procedure, with one important exception. Instead of a four-stack film assembly, only two layers of 110 micron film are being used. This could result in less sensitive transducers, but hopefully the increased activity of the new film will compensate. The reason for reducing the stack thickness is to increase the frequency response. The present transducers

are not effective above 2 MHz, limiting our ability to test thin samples. Higher frequency transducers could generate shorter pulses which could be transferred through thin samples without interference from multiple reflections. There are limitations in the use of higher frequencies, as the scattering of acoustic energy by the fibrous structure of paper increases rapidly with frequency. However, we hope that we can push the technology a little further and perhaps be capable of putting sub-microsecond pulses through thin sheets of paper with the new transducers.

AN ANALYSIS OF IN-PLANE BENDER TRANSDUCERS

(A) Limitations of the Present Design

The transducers, used in our in-plane ultrasonic velocity measuring equipment, are constructed from standard 0.5334 mm thick piezoelectric sheets of a lead zirconate-titanate ceramic (PZT-5H). These sheets are parallel bimorphs (or benders). That is, they are composed of two layers of ceramic which are polarized in the same direction. There are electrodes on the two outer surfaces of the sheet and in the middle. In our application, the outer surfaces are grounded, while the middle is used as the active electrode. In this way, the active electrode is electrically shielded. Mechanical motion can be generated by applying a voltage to the middle electrode, causing one layer to contract, the other layer expand, and the sheet to bend. Bending can be sensed electrically by monitoring the voltage at the center electrode. To construct a transducer, the PZT-5H sheet is cut into a rectangle 6.35 mm wide by 10.30 mm long. One end is rounded to a radius of 4.0 mm. The other end of the transducer is rigidly clamped; so that, the free length of the bender is 7.9 mm.

When two transducers, as described above, are applied to a piece of paper, acoustic energy can be effectively transferred between them. Relatively

pure longitudinal waves are generated if the transducers are facing each other, while transverse waves are detected when the transducers are rotated 90 degrees about their long axes. These transducers have operated satisfactorily. However, they do have limitations.

First of all, the modal purity could be improved. In order to separately determine transverse and longitudinal velocities, it is important that only motion perpendicular to the transducer face be generated and received. If this is not the case, the signals can be complex interferences between longitudinal and transverse motions. This is not generally a problem for the longitudinal motion, since the longitudinal wave is faster than the transverse and the analyzed portion of the signal is complete before any of the shear disturbance is received. However, the shear signal is invariably tainted by the longitudinal. In an anisotropic sheet of paper the shear wave has the same velocity in the MD and the CD, but the longitudinal velocities are different. Therefore, modal impurity can cause the calculated transverse velocities to have different values in the two principal directions. On very anisotropic samples (MD longitudinal velocity about twice as large as CD), we do often see a MD-CD transverse velocity difference of a few percent. In addition, we do observe a signal when the transducers are oriented at right angles. The amplitude is well below the normal transverse and longitudinal signals, but it is worrisome.

Another disturbing feature of the transducers is that the phase of the received signal is sensitive to the loading pressure of the transmitter and receiver on the sample. This means that, in order to make proper measurements with a two transducer technique, the movable transducer must be applied to the sheet in exactly the same manner at the "near" and "far" displacements. In a three transducer application the limitation is more severe as the loading of separate transducers must be identical.

The transducers are not broad-banded. They have a strong resonance at 55 kHz that causes an excited transducer to ring for many cycles. This precludes any possibility for achieving temporal separation of signals of different origin and doing group velocity measurements on discrete pulses. The transverse signal cannot be time separated from the longitudinal; thereby, avoiding the modal purity problem.

(B) Modal Analysis of Present Transducers

Before attempting to improve the transducer design, it is necessary to analyze the present configuration. One step is to calculate the resonant frequencies of the benders. This will tell us which motions are expected in the frequency range of interest. The transmitter is excited in a bending mode, and the receiver is most sensitive to bending motion. However, other modes with natural frequencies near 60 kHz could be excited, and the motion may not be pure bending.

The natural frequencies of bending modes can be calculated from a simple analytical relation, if it is assumed that the bender is a thin beam oscillating so that planer cross-sections remain planer. The relationship for the fundamental bending mode is:

$$f_0 = 0.560\ (EI/pA)^{1/2}/l^2\ . \qquad (1)$$

Using the value of 2800 m/s for $(E/p)^{1/2}$ of PZT-5H and expressing E/A in terms of the thickness, T, gives:

$$f_0 = 454\ T/l^2\ . \qquad (2)$$

Here, as elsewhere, mks units are used.

A finite element analysis program (MSCPAL) was used to determine the natural frequencies of the benders. The bender was modeled as a series of twenty beams of specified area, torsional moment of inertia, moments of inertia, and shear areas. The PZT-5H was treated as an isotropic material with a modulus of 6.0E-10 Nt/m^2, a density of 7600 kg/m^3, and a Poisson ratio of 0.395. The beam parameters for each section were calculated assuming a rectangular cross-section. A clamped boundary condition was imposed on the back end of the first beam in the series, and the front end of the last beam was free.

The results are presented in Fig. 7. Two cases are shown: (1) a rectangular bender; and (2) a rectangular bender tapered to the approximate curvature of the actual benders. The results are plotted as functions of length; so that, the effects of beam size variations can be demonstrated. The modes predicted by MSCPAL are classified into three groups. Those, that are predominantly width direction rotations with thickness direction translations at the end, are called bending modes. The twisting modes are length direction rotations with little middle beam end translation, and the wobble modes are thickness direction rotations with width direction translations at the end. The curve generated by equation (1) for the fundamental bending resonance of a long thin beam is represented by dotted lines in both graphs. Notice that it matches the finite element results of the rectangular beam well until the length to thickness ratio gets below three. A comparison of Fig. 7 and 8 shows the results of end rounding. The natural frequencies of the bends and twists go up about 10 percent, while the increase is somewhat less in the wobbles. Length reduction increases the natural frequencies of the bending modes more rapidly than the twists and wobbles. The effect of width reduction (not shown in the figure) is to raise the frequency of the twists; however, since they become more of a bending deformation and less of a shear deformation, the wobble frequencies decrease.

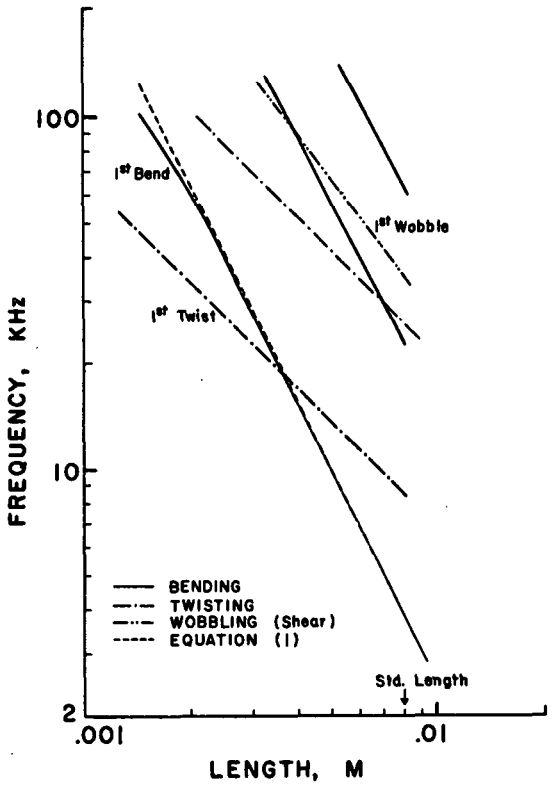

Figure 7. Normal modes of rectangular bender 0.021 inches thick, 0.25 inches wide.

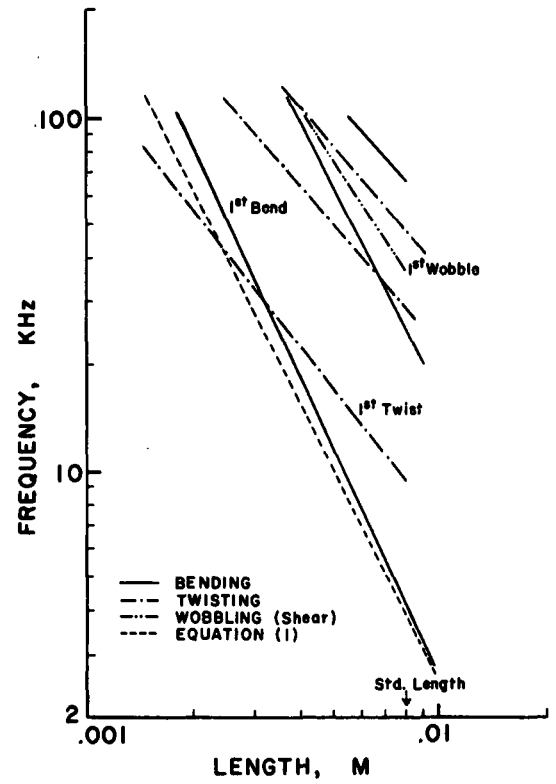

Figure 8. Normal modes of same rectangular bender with standard rounded tip (5/16 diameter).

The next step is to compare the finite element results with experiment. To do this the transducers were placed 30 mm apart on a linerboard sample. A continuous wave from a frequency synthesizer was applied to the transmitter, and the received signal was input to a lock-in amplifier. The source frequency was swept slowly from 5.0 to 100 kHz. The frequency from the synthesizer and the output of the lock-in amplifier were applied to an X-Y recorder, which plotted the response spectrum. The frequencies of the resonant peaks and their relative voltage amplitudes are listed in Table 1. Figure 9 is the full spectrum.

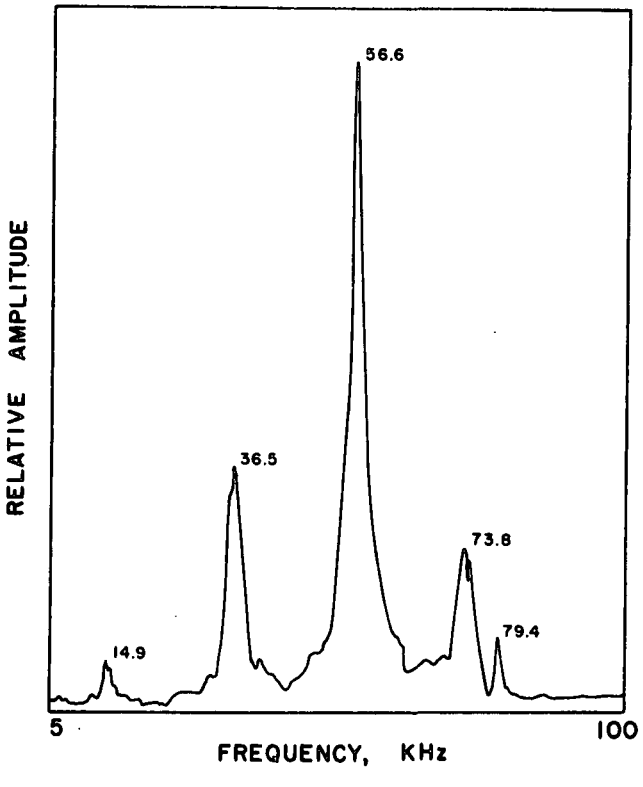

Figure 9. Experimental spectrum of "long" transducers.

Table 1. "Long" transducer resonances

Peak Frequency kHz	Relative Voltage
3.7	by ear
14.9	0.11
36.5	0.39
56.6	1.0
73.8	0.25
79.4	0.14

The resonance at 3.7 kHz was not detected in the received signal. However, when the transmitter was lifted from the sample, a sound, which is loudest at 3.7 kHz, is heard. When the transmitter is returned to the sample all is quiet, and (for reasons explained later) no peak signal is detected.

An identification of the experimental with the theoretical frequencies is speculative; however, I think it goes like this. The 3.7 kHz resonance is clearly the fundamental bending mode; it is below the predicted value probably because the end clamping is less than perfect. The first and second harmonic bends are at 15 and 56 kHz respectively. These are below the predicted values because, as before, the clamping is not perfect. The peak at 36 kHz is the fundamental wobble; it is only slightly below the theory as hard clamping is not as important in establishing its boundary conditions. The twists from these rounded transducers couple little energy into the sheet, and they are not represented in the experimental spectrum. The peaks at 74 and 79 kHz are anybody's guess. If this is all correct, the major motion detected in the time of flight measurements comes from the second bending harmonic at 55 kHz. The culprit in the modal impurity problem is the fundamental wobble near a subharmonic of the 60 kHz excitation signal. Even though the bender construction tends to down play its action, the wobble generates shear when the transducer are aligned for longitudinal and vice versa.

From this analysis, it is clear that the transducer is being operated in a region where there is a large number of resonances. This is unwise if broadband transducer is required and if the effects of secondary motions must be eliminated. An obvious solution is to shorten the transducers and rely on a lower order bending harmonic. The wobble could be jacked out of the operating frequency range, and operation could be maintained below the bending harmonics, thereby increasing the bandwidth. Although the twists may not represent a problem, a concern with this strategy is that the fundamental twist could be excited. However, this is avoided by decreasing the width (but not so much that the fundamental wobble comes into play). Another solution is to reinforce the benders with structural elements. This was explored, but it tended to raise the bend frequencies faster than the wobbles and to make it more difficult to get the wobbles out of operation. It is possible that reducing the bender length and width would reduce sensitivity since less volume of active piezoelectric material is employed; however, in the long benders the piezoelectric coupling is canceled out over much of the bender when the higher order bends are excited. The shorter transducer may be just as sensitive. A major concern (to be addressed later) is the efficiency of coupling to the paper sample.

(C) A Lumped Parameter Analysis

When bimorph transducers are operated below their fundamental bending resonance, the piezoelectric action can approximated by a lumped parameter model supplied by the manufacturer (Vernitron). Since it seems wise to consider below resonance operation, applying the lumped parameter model is the next step in the bender analysis.

First we investigate the mechanical motion in a sample produced by a rectangular bender clamped at one end and driven electrically. One of the

models for PZT-5H operated below resonance in this manner is diagramed below. The left side of the circuit represents the electrical input. The right side is the mechanical circuit. Here, currents become velocities and voltages become forces. An ideal transformer models the piezoelectric interaction. The transformation ratio 1:N' is the ratio of the force out to the supplied voltage, V_I.

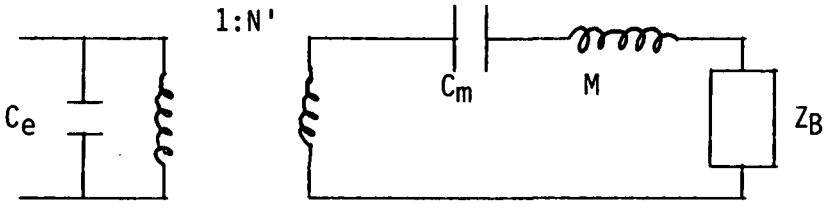

For a parallel PZT-5H bimorph the parameters are N' = 7.48 WT/1 Nt/Vm, C_m = 6.35E-11 $1^3/WT^3$ m^2/Nt, M = 2013 W1T kg/m^3, and C_e = 102E-9 1W/T f/m. Assuming that the function generator is capable of driving the circuit, the voltage at the transformer equals the input voltage and the value of C_e does not effect this outcome.

The symbol Z_B represents the acoustic impedance of the paper plus the impedance due to tension in the paper and in the rubber backing material (i.e. $Z_B = Z_p + Z_t$). These impedances are zero if the transducer is lifted from the sample or infinity if the live end of the bender is fixed, but in normal operation they are finite. The value of Z_p will increase with loading pressure only until the transducer is sufficiently coupled to the sample to create full production of the acoustic waves. The magnitude of the force necessary for full acoustic coupling will increase with basis weight. The impedance from local tension near the tip should continue to increase with loading, since the tip motion is more restrained at high pressure. The paper impedance is real since force and velocity are in phase in traveling acoustic waves; however, Z_t should be primarily elastic and thereby have a large imaginary component.

Before proceeding, a value for Z_p must be approximated. It is difficult to supply an exact figure, since the effective impedance depends on the transducer loading. However, if loading is sufficient for complete acoustic coupling, it is possible to estimate Z_p. To do this, it is assumed that: (1) a continuously oscillating transmitter generates longitudinal acoustic waves that are equivalent to a wave in a strip of width W traveling in both directions perpendicular to the face of the transducer; (2) shear waves with the same effective width are produced parallel to the face; and (3) the velocities in the sample are uniform in the thickness direction and equal to the velocity at the bender tip. The second assumption is admittedly contrived, but I feel a need to include some impedance originating from the shear stiffness of the sample, and I don't have a better proposal. Under these assumptions, the effective impedance of the paper is equal to the intrinsic longitudinal impedance of two strips of width W and caliper t plus the shear impedance of two strips of the same dimensions. That is,

$$Z_p = 2Wtp_p(V_{long.} + V_{shear}). \quad (3)$$

This can be written simply in terms of the sheet basis weight, B, as:

$$Z_p = 2WB(V_{long.} + V_{shear}). \quad (4)$$

Now we can make an estimate of the mechanical impedance of different grades of paper. We do it for three cases: tissue, paper, and paperboard. The basis weights are taken as $B_T = 0.01$ kg/m^2, $B_P = 0.06$ kg/m^2, and $B_{PB} = 0.25$ kg/m^2. The sum of the longitudinal and shear velocities is estimated as 2000 m/s for the tissue and as 4500 m/s for the paper and paper board. The resulting impedances per unit transducer width are $Z_T/W = 40$ kg/ms, $Z_P/W = 540$ kg/ms, and $Z_{PB}/W = 2250$ kg/ms.

Experiments were performed to estimate the value of Z_t. Assuming that this part of the interaction is elastic, it is modeled as $Z_t = 1/iwC_t$, where C_t is an effective compliance. Including the elastic restraint from tension, the fundamental resonance condition is $Mw^2 = (1/C_m + 1/C_t)$. That is, the elastic restraint is a sum of a contribution from the bender stiffness and the loading pressure. Using this relationship, the magnitude of C_t can be determined relative to C_m by measuring the resonant frequency of the benders as a function of loading pressure. The resonant frequency of the standard bender peak near 55 kHz was measured by placing the transducers a small distance apart on a sample. A peak in the received signal was noted as the frequency of a sinusoidal voltage applied to the transmitter was varied. A zero load value was taken as the resonant frequency when the minimal load necessary to detect a significant signal was applied. Using the resonant condition, the relation between the stiffnesses is $(1/C_t)/(1/C_m) = (f^2 - f_o^2)/f_o^2$, where f_o is the resonant frequency with no load. The results are listed in Table 2.

Table 2. Effect of loading on the major resonance of "long" transducers.

Loading Mass gms	Frequency kHz	Std. Dev. kHz	$(1/C_t)/(1/C_m)$
0	54.46	0.11	
100	55.86	0.03	0.052
300	56.00	0.03	0.057
500	56.08	0.04	0.060

From the table it appears that elastic stiffness coming from loading is small compared to the bender stiffness and that it is safe to ignore it. This conclusion is confirmed by the observation that the amplitude of the time of flight signal is decreased only slightly as loading is increased, once there is sufficient pressure for acoustic coupling to the sample. It must be pointed out

that the 55 kHz peak is a second harmonic, while the resonant condition is for the fundamental. However, the effective stiffness for this mode is near that for a shorter bender with fundamental near 60 kHz. Therefore, this is considered a proper demonstration that the elastic restraint from loading is small compared to the bender stiffness in a transducer operating below a 60 kHz fundamental resonance.

Taking all this into consideration, the current in the mechanical part of the circuit (i.e. the velocity) can now be written:

$$I_m = iwC_mVN'/(1 - w^2C_mM + iwC_mZ_p), \quad (5)$$

where w is the angular frequency, V is the applied voltage, and i is the square root of -1. The force per unit width radiated in the sample, in terms of the intrinsic impedance, Z, and velocity, V, of the mode in question, is $F/W = ZtI_m = BVI_m$. The magnitude of the velocity is:

$$MI_m = wC_mN'V/((1-w^2MC_m)^2 + w^2C_m^2Z_p^2)^{1/2}, \quad (6)$$

and the tangent of the phase shift relative to the input voltage is

$$Tan = (1 - w^2MC_m)/wC_mZ_p. \quad (7)$$

Now an attempt is made to model the action at the receiver. The lumped parameter circuit is used. This time the impedance of the preamplifier is assumed large compared to $1/wC_e$; so that the preamplifier impedance can be ignored.

The critical problem is to model the interaction between the acoustic wave and the receiver bender. In the longitudinal case, we address the problem by likening it to an acoustic wave in a strip of width W incident on the sample-

receiver interface. There would result a motion in the receiver, a reflected wave in the strip, and a transmitted wave in the strip. The velocity at the interface is equal in the strip and the receiver. The force and velocity equations at the interface are:

$$F + F_{RF} = F_T + F_{RCR}, \quad \text{and} \tag{10}$$

$$F/ZWt - F_{RF}/ZWt = F_T/ZWt = F_{RCR}/Z_{RCR}, \tag{11}$$

where the subscript RF signifies the reflected wave, T the transmitted wave, and RCR the bender. Solving for F_{RCR} as a function of F gives

$$F_{RCR} = 2F/(1+2ZWt/Z_{RCR}) \quad . \tag{12}$$

The equivalent lumped parameter model is below.

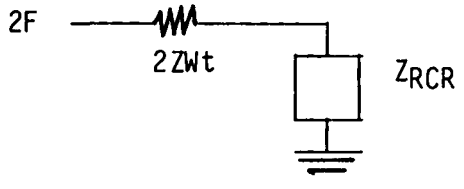

If we incorporate the manufacturer's lumped parameters into, Z_{RCR} we have the next circuit.

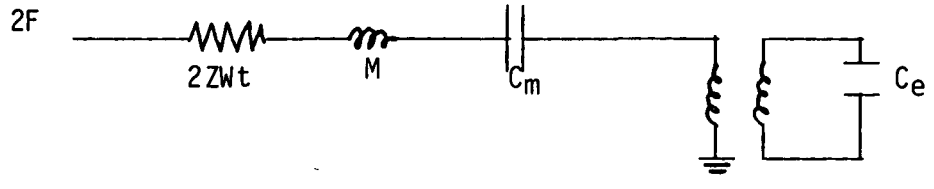

Finally, for calculating the mechanical current, we use the circuit below:

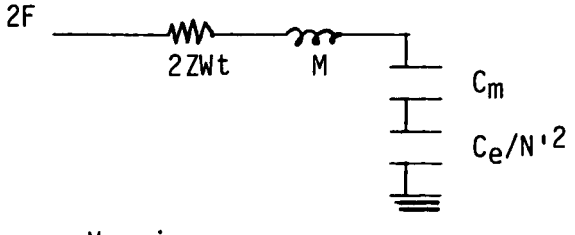

The receiver voltage, V_o, is:

$$V_o = (1/N')I_m/iw(C_e/N'^2) = N'I_m/iwC_e \tag{13}$$

The dimensions used in calculating C_e should be the total dimensions of the bender, including the clamped area. Therefore, to maximize V_o, the clamped area in the receiver will be small and the area for C_e will approximately equal to that of the other parameters. In this case, the ratio of C_m to C_e/N'^2 is 0.035, and little is lost in excluding C_e from the I_m calculation. (This approximation is actually better if there is extra clamped area; however, we stay with this assumption as it will be important later.) From Equations (5) and (13), the last lumped parameter circuit, and the impedance relationship between force and velocity in the sample, we get the following voltage transfer equation.

$$V_o/V_I = \frac{2iZWtN'^2wC_m^2}{C_e(1-w^2C_mM+iwC_mZ_p)(1-w^2C_mM+2iwC_mZWt)} \qquad (14)$$

In order to reach Eq. 14, it was effectively assumed that transmitter and receiver are connected by a paper strip, which had a width equal to the transducer width. This ignores any wave spreading that could occur in the extended samples actually used, and overestimates the transfer coefficient.

Since we will stay well below resonance keeping w^2C_mM small and since Z_p and $2WtZ$ are close to the same value for longitudinal waves, there are effectively only two terms in the denominator of Eq. 14. If one term dominates, equation (14) is simplified. When wC_mZ_p is much less than one (the "low impedance" case) Equation (14) is:

$$(V_o/V_I)_{LZ} = 2iZWtN'^2wC_m^2/C_e = 2.21E\text{-}12(ms^2/kg)w(Z_p/W)(l^3/T^3)i \qquad (15)$$

Conversely in the "high impedance" case (wC_mZ_p much greater than one) Eq. (14) is:

$$(V_o/V_I)_{HZ} = -iN'^2/C_ewZ_p = 5.48E8(kg/ms^2)(W/Z_p)(T^3/l^3w)i \qquad (16)$$

In the second parts of Eq. 15 and 16 the clamped area was ignored in C_e.

The voltage transfer coefficient is maximum when wC_mZ_p is about one. However this is not an ideal operating range. In going from the high impedance to the low impedance regime there is a change in phase of 180 degrees; therefore, in the high response range, phase is sensitive to frequency and loading. Considerable wave form dispersion and time of flight sensitivity to unequal loading pressures are expected here. For rectangular PZT-5H bender operated at 60 kHz the $wC_mZ_p = 1$ condition is

$$Z_p/W = 4.17E4(kg/ms)(T^3/l^3). \quad (17)$$

From equation (2), the value of l/T is fixed once the resonant frequency of the fundamental bending mode and T are given. For the standard PZT-5H thickness and 120 kHz resonant frequency, l/T is 2.66. This predicts that the 60 kHz transistion for Z_p/W is about 2000 kg/ms. This is near the predicted value for paperboard; therefore, it appears that low basis weight paper would safely be in the low impedance regime, but there might be a problem with board.

Recalling the case of the easily damped out fundamental harmonic in the long transducers, it is clear that, since l/T is about 14, this is a high impedance regime for paper and board samples. Therefore, wC_mM is greater than one, and from Eq. (5) the motion of the bender tip is significantly decreased when the transmitter is applied to the sample.

(D) New Transducer Design Considerations

If it is possible to get sufficient sensitivity, there are advantages to building much shorter transducers. The transducers could be driven well below resonance making them much more broad-banded. Operating below resonance could also avoid the excitation of a spurious wobble resonance and the loss of modal purity. The response could be studied with the relatively simple lumped parameter model just discussed.

Operation would have to be maintained in the low or high impedance regime; so that, the receiver phase is not load dependent and receiver amplitude and phase are not frequency dependent. That is, the dimensions of the transducer and the impedance of the sample must be such that $w_o = 1/Z_p C_m$ is not in the range of the operating frequency. Remember, this portends trouble for paper board; however, the estimations of effective sample impedance are not very rigorous, and judgement is withheld until transducers are built and tested.

The sensitivity at low 1/T can be estimated from Eq. (15). Using an 1/t of 2, a frequency of 60 kHz, and a Z_p/W of 400 kg/ms, produces a transfer coefficient of 0.0027. This is likely an overestimate, but it encourages an attempt to build short transducers. At the 56 kHz resonance, the long transducers have a measured transfer coefficient of about 0.01. However, the nonresonant signal is much lower, (see Fig. 9) and a very resonant response is not helpful at the front end of a pulse used in time of flight measurements.

The new transducers will be built of unequal lengths: the transmitter will be 1.5 mm long and the receiver 1.3 mm. This assures that the two benders do not have exactly the same resonance characteristics and helps to make the system more broad-banded. The receiver was selected to be shorter since the C_e in the denominator of the transfer coefficient comes from the receiver, and reducing its area increases sensitivity.

The finite element computer program (MSCPAL), discussed earlier, was used to calculate the normal modes of the new design. The parameters for a beam 3.0 mm wide, 0.5334 mm thick, and 1.4 mm long were input to the program. Since the 1.4 mm length is intermediate between the actual receiver and transmitter dimensions, it should provide a suitable average response. The three lowest

frequency resonances were: a fundamental twist at 127 kHz; a fundamental bend at 133 kHz; and a fundamental wobble at 306 kHz. Notice all resonances are well above the intended operating frequency of about 80 kHz, and the wobble is blown so far out that it should not be a problem.

(E) New Transducer Construction and Performance

In an effort to hold the end of the cantilevered transducer more uniformly, to avoid damaging the piezoelectric element, and to more closely approximate the fixed end boundary conditions, a "cartridge" type transducer design was used. The housing for a transducer is a short delrin rod with a slot cut across one face. The slot is slightly wider than the PZT bender element. The depth of the slot in the receiver cartridge is minimized to reduce C_e. A parallel bender element, with leads soldered to the middle electrode and the two surface electrodes, is placed in the slot. The leads are passed through a hole in the bottom of the slot. Epoxy is poured into the slot; so that, the element is held rigidly, except for a rounded beam of PZT bender material extending out from the rod. The transmitter beam is 1.5 mm long and 3.0 mm wide, while the receiver is 1.3 mm long and 3.0 mm wide. The completed cartridge is mounted in an aluminum housing, and the leads are soldered to a miniature coaxial connector at the base of the housing. See Fig. 10 for details and dimensions.

The first evaluation of the short transducers is a comparison of their voltage transfer coefficients (R) with those of the long transducers. Table 3 is a listing of results when a transducer pair is separated by about 30 mm apart on a paper sample, and aligned so that the MD longitudinal mode couples the two transducers. In order to demonstrate their highly resonant response, results for the long transducers are taken at 56 kHz and 80 kHz. For both pairs, a continuous wave coefficient and a "pulsed" coefficient are presented. The con-

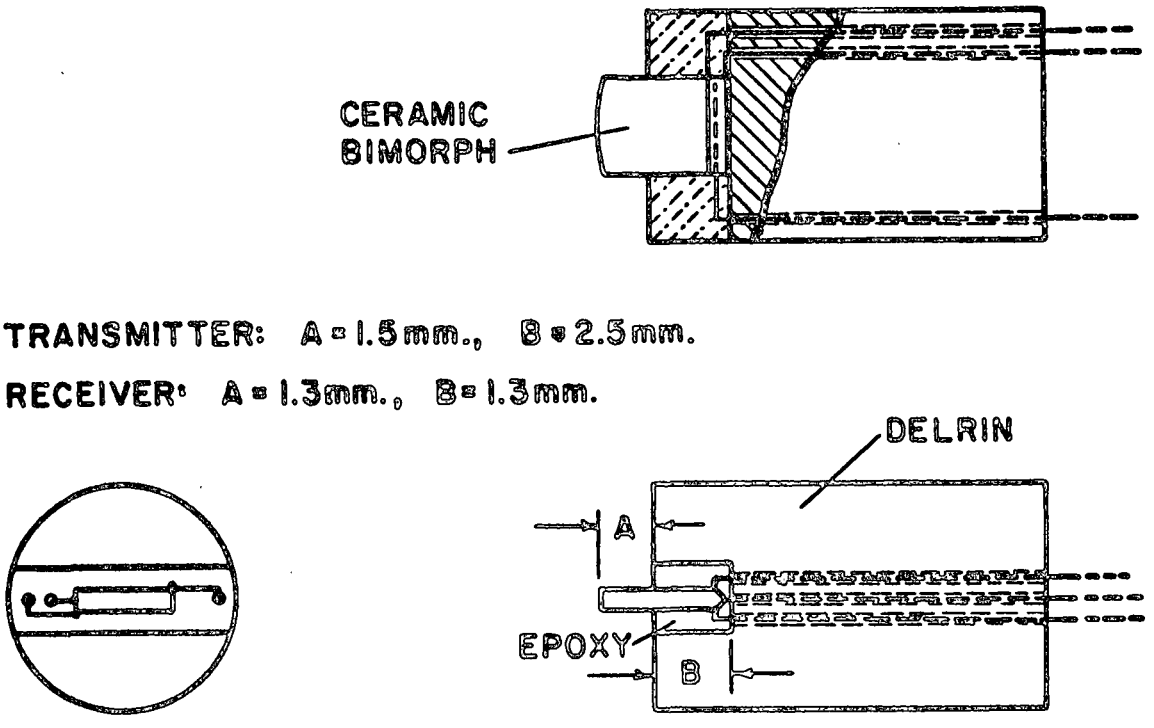

Figure 10. In-plane bender transducer (cartridge type).

tinuous coefficient should correspond to the mathematical models, while the pulsed coefficient is more indicative of the sensitivity realized in time-of-flight velocity measurements. The pulse is generated by exciting the transmitter with a single-cycle sine wave; the recorded output is the height of the first half-cycle at the receiver.

Table 3 demonstrates a number of interesting points. First, notice that the large difference in the long transducer continuous response at resonance and off resonance is not reflected in the pulsed coefficient. The large resonant response of the long transducer is not very helpful in time-of-flight work, where, because of interference from reflections, only the initial part of the pulsed signal is useful. The continuous coefficient for the short trans-

ducers is relatively frequency independent and at a considerably lower level than the long transducer coefficient. However, the more important pulse ratio is about three times greater in the new transducers. That is, for time-of-flight measurements the new design yields a significant improvement in sensitivity.

Table 3. Transducer performance.

Freq. kHz.	style	mode	R
80	long	pulse	5.04E-5
80	long	cont.	2.83E-3
80	short	pulse	1.57E-4
80	short	cont	5.67E-4
56	long	pulse	4.11E-5
56	long	cont.	1.04E-1

The broadband construction of the new transducers results in a much different appearance of pulse train generated by a single sine wave disturbance of the transmitter. The long transducer signal requires about six cycles to build to a maximum, which is a order of magnitude higher than the first pulse. The signal continues to oscillate for about 100 cycles. The nonresonant, short transducer signal reaches full amplitude after one cycle and dies out in less than two cycles. Signals coming from distinguishable reflections off the sample boundaries are observed further on. The total pulse width is about ten percent of that from the long transducers. This presents an opportunity for the computer to perform delay time measurements more rapidly, since signal averaging can be repeated at shorter intervals.

A spectrum of the short transducer response through paper can be made as described earlier for the long transducers. The results are in Fig. 11. Three runs were made using different basis weight samples. Individual traces show a great deal of low frequency structure. This is due to the constructive

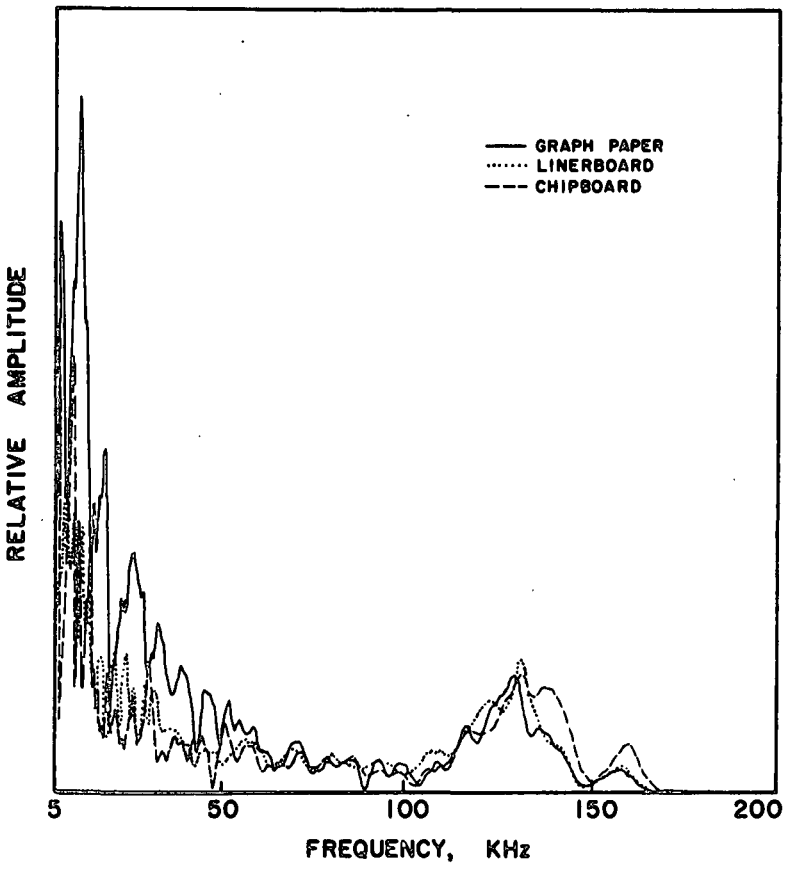

Figure 11. Relative amplitude vs. frequency.

and destructive interference of reflected waves from the boundaries. The frequency of the response peaks depend on the sample acoustic properties and on the location of the transducers relative to sample boundaries. Notice there is no systematic relation between low frequency peaks and valleys in the three spectra, and it must be inferred that they are the result of sample characteristics. If the sample generated structure is taken out, these transducers provide a remarkably flat response between 50 and 110 kHz (the frequency of interest for time-of-flight measurements). All three spectra have common peaks at about 130 kHz and 160 kHz. The 130 kHz peak is taken to correspond to the fundamental bending mode predicted by mathematical analysis. Fortunately, it is much broader than the long transducer resonances, presumably because of the different transmitter and receiver lengths. The 160 kHz peak is not so easily identified.

The low frequency response is partially consistent with the lumped parameter model, if the transition from low impedance to high impedance can be rationalized to occur at a lower frequency. Mentally smoothing the responses reveals an approximately inverse dependence of response on frequency above about 25 kHz. As predicted, the transition frequency does appear to decrease with basis weight; however, the dependence is clearly not as strong as expected for the high impedance regime. The $w_o = 1/C_m Z_p$ condition clearly over estimates the transition frequency, and the sensitivity to sample type is over stressed. A straight forward way to make the model consistent with these results is to argue that a large real impedance should be attributed to the transducer backing. This would put the spectra safely in the high impedance regime and account for the small drop in signal with basis weight. All the modeling aside, bear in mind that the proof is in the pudding, and that sensitive transducers with a very broadbanded response between 50 and 110 kHz, when coupled to a wide range of papers, have been produced.

A major motivation for constructing new transducers was to resolve the modal purity problems with the long transducers. It is very important that transducers communicate through a pure longitudinal mode when their faces are oriented perpendicular to their separation and a pure transverse mode when parallel to the separation. If modal purity is not achieved, shear and longitudinal measurements can be tainted. This is less of a problem in longitudinal time-of-flight measurements, as the longitudinal wave arrives before the shear, and the first peak is complete before significant shear energy is present. Shear velocities, especially MD shear, are another story. Longitudinal impurities do effect the first shear pulse. A good way to investigate this phenomenon

is to look at the difference between the calculated shear velocities when measured along the MD and CD in highly anisotropic samples. Shear waves have the same velocity in the MD and CD; however, the interfering longitudinal impurities show directional dependence. The MD longitudinal wave arrives early and has a large amplitude, while the CD longitudinal is weaker and comes later. The measurement in the CD is a better determination of shear modulus. If modal impurity causes a meaningful problem, significant differences should be observed between MD and CD shear velocities measurements on anisotropic sheets. Figures 12 and 13 show typical results for the long transducers. They are, respectively, longitudinal and shear velocity squared polar plots for a Formette Dynamic made linear board sample. Notice MD and CD shear are significantly different.

There are two features of the long transducers that exacerbate the modal purity problem. First, they have a "wobble" resonance (discussed earlier) near the operating frequency that could lead to undesirable transducer motions. Second, they are very resonant, and any early arriving longitudinal impurity can ramp up by the time the shear disturbance comes in. In a non-resonant system the longitudinal signal could be fading out as the shear arrives. The short transducers were designed to reduce both of these faults. Figure 14 is the shear polar plot for the same liner board sample with short transducers. Notice the MD and CD shear velocity squared values are nearly equal. This is an important improvement, which is realized in even more anisotropic samples. The improvement of modal purity in the short transducer velocities can be demonstrated by comparing the ratio of MD to CD shear velocity squared values for the same sample, using different transducers. A 42-lb linerboard with a 3.6 MD-CD modulus ratio was subjected to shear polar testing for five different combinations of long transducer and one set of short transducers. The shear

THE INSTITUTE OF PAPER CHEMISTRY
LONGITUDINAL SPECIFIC STIFFNESS (VEL SQR) VS ANGLE TO MD

OPERATOR: D BRENNAN
PROJECT : CARTRIDGE T-117 R-118
DATE :5 14 87
SAMPLE : LB2 8INCH LONGIT

ANGLE DEGREES	VEL SQR KM2 / SEC2	STD DEV	ANGLE DEGREES	VEL SQR KM2 / SEC2	STD DEV
0	14.73	.47	90	4.14	.24
5	14.60	.85	95	4.13	.28
10	13.78	.68	100	4.13	.21
15	12.64	.47	105	4.22	.23
20	11.77	.53	110	4.37	.25
25	10.53	.30	115	4.59	.25
30	9.45	.47	120	4.92	.24
35	8.34	.37	125	5.51	.40
40	7.19	.33	130	6.03	.39
45	6.49	.27	135	6.66	.41
50	6.03	.41	140	7.57	.46
55	5.27	.24	145	8.55	.47
60	4.85	.15	150	9.88	.56
65	4.54	.20	155	10.92	.57
70	4.41	.24	160	11.82	.41
75	4.28	.27	165	13.15	.58
80	4.19	.20	170	13.87	.42
85	4.11	.15	175	14.39	.67

TEST PER 5 DEGREE INCREMENT = 8
THE ANGLE TO MAJOR PRINCIPAL AXIS = -.6
AREA (KM^4/SEC^4) = 240.3
SIGNALS AVERAGED = 8
STIFFNESS RATIO = 3.56

ENLARGMENT FACTOR: 4/1
SCALE: 1 KM2/SEC2/DIV

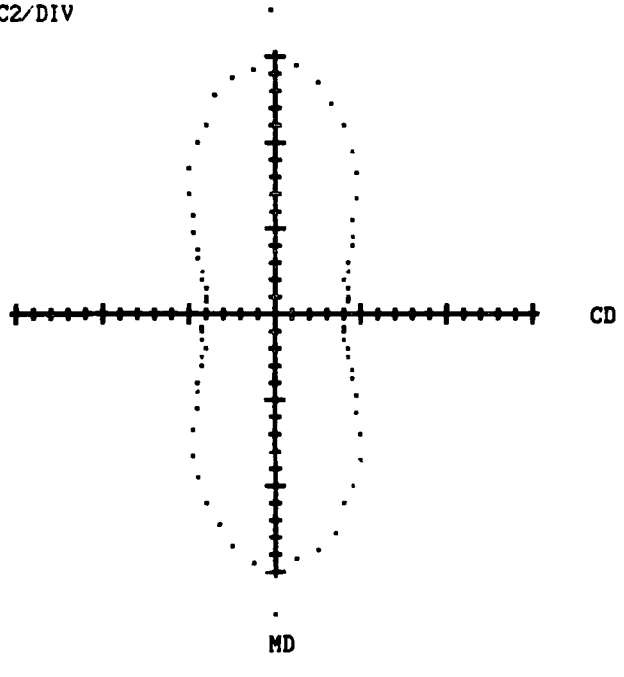

PLOT OF VEL SQR VS ANGLE AS SEEN FROM FELT SIDE

Figure 12.

THE INSTITUTE OF PAPER CHEMISTRY
SHEAR SPECIFIC STIFFNESS (VEL SQR) VS ANGLE TO MD

OPERATOR: D BRENNAN
PROJECT : 3467
DATE :5 6 87
SAMPLE : LB2 CUT TO 8 INCH SQUARE

ANGLE DEGREES	VEL SQR KM2 / SEC2	STD DEV	ANGLE DEGREES	VEL SQR KM2 / SEC2	STD DEV
0	2.63	.09	90	2.82	.08
5	2.64	.09	95	2.83	.09
10	2.62	.09	100	2.90	.11
15	2.61	.10	105	2.95	.11
20	2.63	.12	110	3.03	.12
25	2.70	.20	115	3.11	.12
30	2.71	.16	120	3.11	.12
35	2.73	.17	125	2.86	.20
40	2.68	.19	130	2.71	.20
45	2.57	.20	135	2.65	.15
50	2.63	.30	140	2.64	.14
55	3.00	.37	145	2.60	.14
60	3.16	.20	150	2.60	.14
65	3.10	.12	155	2.60	.11
70	3.03	.10	160	2.62	.10
75	2.93	.10	165	2.63	.09
80	2.86	.09	170	2.61	.08
85	2.82	.09	175	2.63	.08

TEST PER 5 DEGREE INCREMENT = 16
SIGNALS AVERAGED = 6
THE ANGLE TO MAJOR PRINCIPAL AXIS = 87.4
STIFFNESS RATIO = .93
AREA (KM^4/SEC^4) = 24.3

ENLARGMENT FACTOR: 12/1
SCALE: 1 KM2/SEC2/DIV

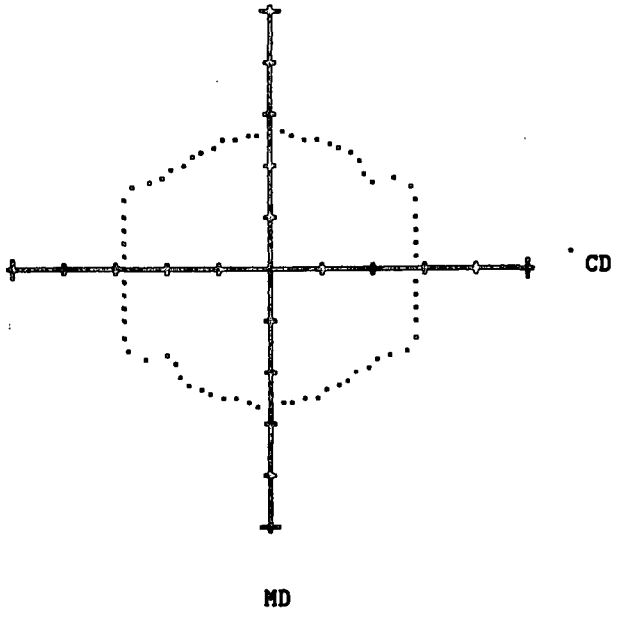

PLOT OF VEL SQR VS ANGLE AS SEEN FROM FELT SIDE

Figure 13.

anisotropy for the long transducers was 1.08 with a standard deviation of 0.04 for the long transducers and 1.045 for the short transducer. Also, in a grinding study on a bleached board (longitudinal anisotropy = 4) ten shear polar plots were made with long transducer and three with short transducers; the shear anisotropy was 1.087 (standard deviation = 0.017) for the short transducers and 1.043 (standard deviation = 0.015) for the long transducer. The new transducers do appear to improve the modal purity problem.

Figure 15 is the shear polar plot for a highly oriented sample (MD-CD ratio of 6.7) and MD and CD shear are still equal. Please take particular notice of crazy things happening in Fig. 15 midway between the MD and CD directions. When the receiver signal for these off axis tests are examined, a complex, irregular interference between shear and longitudinal waves can be witnessed. The reason for this is that in anisotropic samples the off axis normal modes are "quasi-shear" and "quasi-longitudinal". They are neither perpendicular to or parallel with the direction of propagation. If the anisotropy ratio is low, the off axis modes are nearly shear and longitudinal, but for highly anisotropic samples the off axis normal modes can vary as much as 20 degrees from their expected values. Therefore, since the transducer is aligned for neither off axis quasi-shear or quasi-longitudinal, a mixture of the two modes is observed regardless of the modal purity of the transducers. A solution to this, of course, is to align the transducers for pure mode off axis operation. However, our present system and the in-plane robot, now under development, only allow parallel and perpendicular orientations.

(F) Special Transducers for In-Plane Robot

We have also constructed a version of the short transducers to be used with the in-plane robot. These transducers must be mounted on the end of a

THE INSTITUTE OF PAPER CHEMISTRY
SHEAR SPECIFIC STIFFNESS (VEL SQR) VS ANGLE TO MD

OPERATOR: D BRENNAN
PROJECT : 3467 TRANSD 204 209

DATE :7 3 87
SAMPLE : LB2 SHEAR POLAR

ANGLE DEGREES	VEL SQR KM2 / SEC2	STD DEV	ANGLE DEGREES	VEL SQR KM2 / SEC2	STD DEV
0	2.66	.10	90	2.64	.09
5	2.67	.11	95	2.65	.09
10	2.64	.07	100	2.66	.08
15	2.62	.13	105	2.69	.11
20	2.62	.09	110	2.75	.16
25	2.64	.12	115	2.62	.25
30	2.63	.14	120	2.31	.18
35	2.52	.13	125	2.23	.12
40	2.42	.13	130	2.29	.09
45	2.35	.12	135	2.34	.06
50	2.30	.12	140	2.41	.09
55	2.36	.16	145	2.45	.14
60	2.54	.24	150	2.50	.11
65	2.87	.21	155	2.57	.12
70	2.87	.17	160	2.61	.08
75	2.78	.13	165	2.61	.10
80	2.71	.14	170	2.65	.09
85	2.64	.08	175	2.63	.08

TEST PER 5 DEGREE INCREMENT = 8
THE ANGLE TO MAJOR PRINCIPAL AXIS = 58.5
AREA (KM^4/SEC^4) = 20.7

SIGNALS AVERAGED = 6
STIFFNESS RATIO = 1.00

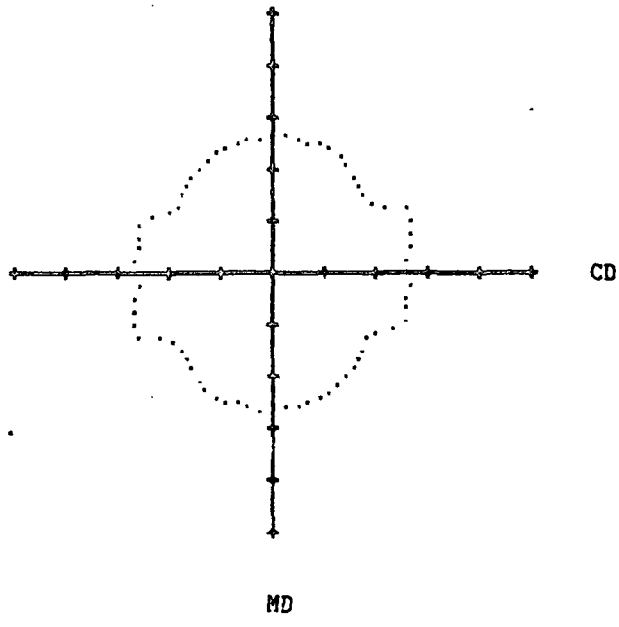

PLOT OF VEL SQR VS ANGLE AS SEEN FROM FELT SIDE

Figure 14.

THE INSTITUTE OF PAPER CHEMISTRY
SHEAR SPECIFIC STIFFNESS (VEL SQR) VS ANGLE TO MD

OPERATOR: D BRENNAN
PROJECT : SHEAR HIGH ANISOTROPY
DATE :8 5 87
SAMPLE : NO 6

ANGLE DEGREES	VEL SQR KM2 / SEC2	STD DEV	ANGLE DEGREES	VEL SQR KM2 / SEC2	STD DEV
0	1.98	.07	90	1.91	.08
5	1.94	.09	95	1.91	.08
10	1.94	.08	100	1.92	.08
15	1.96	.08	105	1.97	.08
20	1.97	.09	110	2.04	.10
25	1.97	.15	115	2.16	.16
30	1.96	.18	120	2.40	.31
35	1.96	.34	125	2.09	.72
40	1.92	.32	130	1.58	.14
45	1.74	.40	135	1.63	.15
50	3.01	1.88	140	1.74	.14
55	2.65	1.43	145	1.78	.26
60	2.15	.84	150	1.16	.73
65	2.37	.31	155	1.61	.60
70	2.17	.15	160	1.96	.15
75	2.05	.09	165	1.99	.12
80	1.97	.07	170	2.00	.10
85	1.93	.08	175	1.99	.07

TEST PER 5 DEGREE INCREMENT = 16
THE ANGLE TO MAJOR PRINCIPAL AXIS = 58.3
AREA (KM^4/SEC^4) = 12.5

SIGNALS AVERAGED = 6
STIFFNESS RATIO = 1.04

ENLARGMENT FACTOR: 12/1
SCALE: 1 KM2/SEC2/DIV

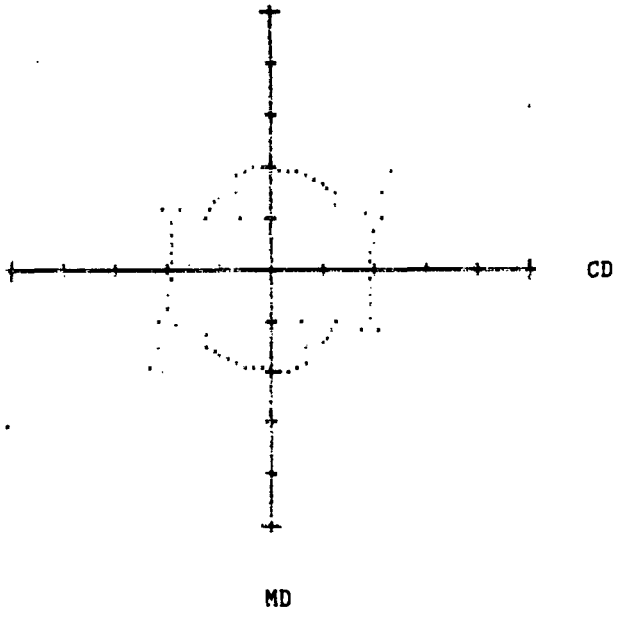

PLOT OF VEL SQR VS ANGLE AS SEEN FROM FELT SIDE

Figure 15.

shaft that passes through ball bushings. In order to reduce movements in the transducers due to play in the bushings and to minimize overall sensor head dimensions, it is advantageous to make these transducers as small as possible. Figure 16 is a schematic of the robot transducers. They have the same general features as the regular short transducers, but are designed to attach to a sensor head shaft.

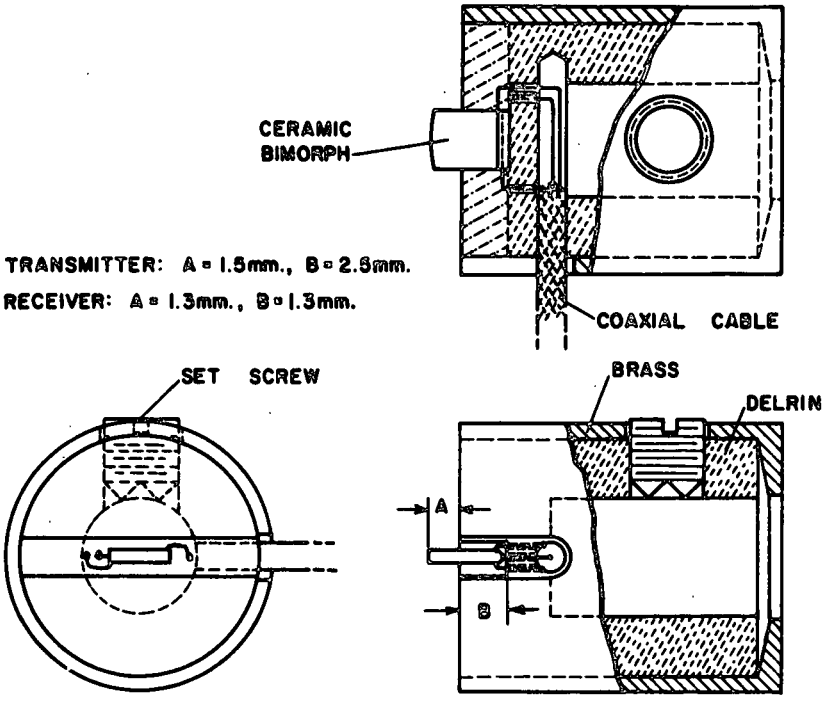

Figure 16. Miniature in-plane transducer.

DEVELOPMENTS ON THE IN-PLANE ROBOT PROJECT

As stated in the last PAC report, we plan to develop an in-plane ultrasonic velocity measuring apparatus using a standard robot. The robot, a Mitsubishi RM 501, will be used to translate the probes across the sample and orient the probes for measurements at any angle relative to the machine direction. Mountings for the probes, probe separation movement, and probe rotation

is accomplished through a specially designed "end effector". The robot and end effector are both provided by Johnson Scale, who will enthusiastically supply units to other interested parties. The electronics (an IBM PC AT or equivalent, an H.P. 54200A Digitizing Oscilloscope, a Wavetek Model 143 Function Generator, and a Panametrics 5050AE Preamplifier) are standard off-the-shelf instruments. The necessary software will be provided free-of-charge to IPC member companies. The foreseen advantages of this instrument are that it will simplify technology transfer to member companies and it will allow multiple sample testing without operator interference.

The robot and end effector have been delivered; however, problems have been encounter with both systems. The robot's electronic "drive unit" was damaged by U.P.S. in shipment. This led to subsequent damage to the robot and drive unit, and both had to be replaced at U.P.S. expense. The second robot developed shoulder problems after less than a week and has been returned to Mitsubishi for warranty repair. We are assured that there are many satisfied RM 501's customers experiencing long-time flawless operation and that we can soon expect to join their ranks.

The end effector is the first implementation of a new design, and we anticipated some initial difficulties. The only significant problems arose in connection with the splined ball bushings used to dead-weight load the probes on the sample. The play at the probe tips was unacceptably large, and there was far too much friction in the bushings. The probe play was reduced by changing the part of the design which accommodated rotation of the ball bushing for shear and longitudinal testing and by reducing the probe length as described in the transducer discussion. The original design achieved probe rotation by mounting

the ball bushings in split delrin bushings. Set screws were to be used to adjust the split bushings for minimal probe play without overly restricting probe rotation. This proved to be impossible. In order to realize satisfactory performance, we replaced the delrin bushings with teflon bushings which had not been split and got rid of the set screws. The teflon bushings were machined to press fit into the end effector mount and were custom reamed for a snug fit to the ball bushings. This requires a little more effort in the manufacturr, but it produces far superior performance. The problem of excessive friction in the ball bushings was first addressed by procuring new ball bushings to improved specifications; however, this did not result in significant improvement. Finally, we discovered that almost all the friction was coming from rubber dust seals in the ends of the ball bushings. We replaced these seals with brass end plates, which nearly touched the splined shaft, and reduced the ball bushing friction to an insignificant amount. Since in our apparatus the ends of the ball bushings are well protected, we are not concerned with dust fouling the ball bushings. At any rate, the ball bushing can now be opened up and easily cleaned. We are at last very pleased with the end effector, and we anticipate no further problems.

We have designed and partially constructed a frame for mounting the robot and holding the samples. It is a piece of half-inch thick plexiglass with five locations for sample holders. Paper samples were merely laid in position and held down with a metal or plastic frame.

Serious work on the robot software is waiting completion of the mechanical apparatus; however, the fundamental computer manipulations of robot and end effector motions have been verified and a technique for simplified computer control of the robot has been devised.

USING ACOUSTIC LOSS AS AN INDICATOR OF WEAK PLY BONDING

This report updates the ongoing work on out-of-plane acoustic loss in paper. The last PAC report defines the procedure and gives some results. Since that time, other experiments have been conducted which further document the fact that loss measurements are more sensitive to ply bonding in multilayer sheets than are velocity measurements. Before discussing the latest results, a brief review of the testing rationale and the early results will be given.

We now have the ability to compare the Fourier components of acoustic signals through paper with those through a standard sheet of thin aluminum foil. Knowing the velocity of sound and density of aluminum, the paper sample, and the rubber front-face of the transducers, this allows us to calculate the frequency dependent loss coefficients in paper samples. However, if the acoustic coupling between the sample and the rubber front-face is less than perfect, the calculation is invalid. We demonstrated that the perfect coupling assumption is grossly in error at 50 kPa, the TAPPI standard pressure for caliper measurement, but the assumption is fine at pressures above about 1000 kPa. Although this sensitivity to poor interface bonding is a nuisance in trying to make accurate loss determinations in paper, it can be used to advantage in detecting poor ply bonding in paper samples. At least this is our hope. In the last PAC report, we showed that damaging multilayer board by bending caused larger relative changes in loss parameters than in velocity. As expected, the effect of bending on both parameters decreased at high loading pressures. This is taken to demonstrate that at low loading pressure loss measurements are sensitive to poor internal interface bonding as well as transducer-sample coupling.

Work done at IPC has shown that in single ply samples out-of-plane ultrasonic velocity correlates well with z-direction tensile tests. This should

not be expected to occur in multilayer sheets which fail at an interface, since the time of flight through the critical interface is a small portion of the total transit time. However, poor ply bonding could lead to signal reflections and an apparent increase in loss. This could make loss a sensitive indicator of poor interface bonding. To test this hypothesis, unbleached kraft multilayer board samples (made on a single commercial machine but having different out-of-plane strength properties) were tested for ZDT, out-of-plane longitudinal velocity, and out-of-plane loss. The results, at 50 kPa loading pressure, are presented in Figs. 17 and 18. Notice that the loss coefficient (alpha) and velocity both correlate with ZDT in the expected manner. However, alpha has a much higher correlation coefficient, and it appears to be a better indicator of ZDT in multilayer board. The ZDT tests were also compared with velocity and loss measurements made at 2107 kPa. This time both r-squared values were lower (the loss number went to -0.67 and the velocity to 0.38). Presumably the higher pressure improved the bonding between plies and reduced interface effects.

We performed another small experiment that has some interesting implications. From past experience, we feel that the velocity and loss measurements at high loading pressure are largely sensitive to only properties in the cell wall. Therefore, we expect changes in the cell wall to be reflected in high pressure acoustic measurements. We obtained a series of paper samples (from Rajai Atalla's group) that had various amounts of a special heat treatment designed to increase crystallinity. The increase in crystallinity should lead to an increase in velocity and a decrease in loss tangent. Therefore, measurements on these samples could test the sensitivity of sheet loss tangent values to crystallinity. The heat treatments did lead to about 20 percent decreases in loss tangent. However, the out-of-plane velocity decreased. Since this modulus

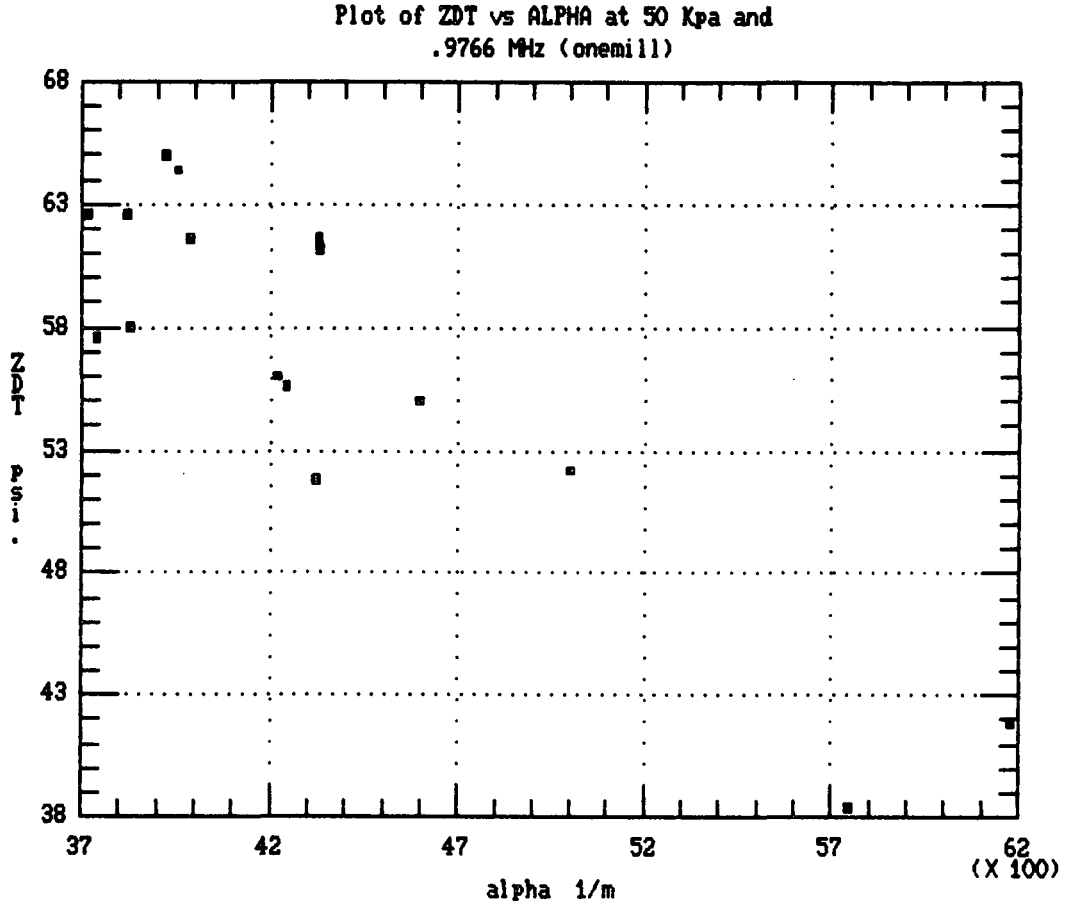

Regression Analysis - Linear model: Y = a+bX

Dependent variable: C:ONEMILL.ZDT Independent variable: C:ONEMILL.ALPHA50

Parameter	Estimate	Standard Error	T Value	Prob. Level
Intercept	98.2788	5.82431	16.8739	1.06214E-10
Slope	-9.53817E-3	1.31626E-3	-7.24643	4.24728E-6

Analysis of Variance

Source	Sum of Squares	Df	Mean Square	F-Ratio	Prob. Level
Model	690.12256	1	690.12256	52.51077	.00000
Error	183.99494	14	13.14250		
Total (Corr.)	874.11750	15			

Correlation Coefficient = -0.888542 R-squared = 78.95 percent
Stnd. Error of Est. = 3.62526

Figure 17.

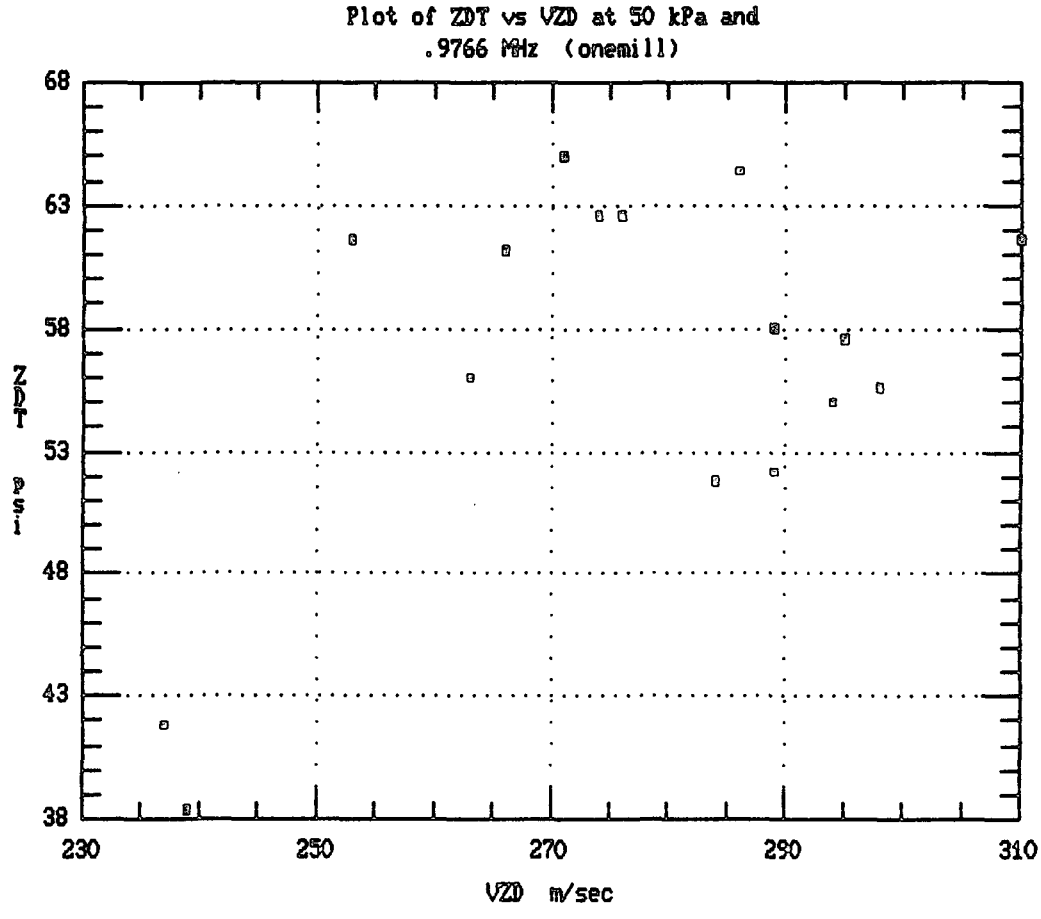

Regression Analysis - Linear model: Y = a+bX

Dependent variable: C:ONEMILL.ZDT Independent variable: C:ONEMILL.VZD50

Parameter	Estimate	Standard Error	T Value	Prob. Level
Intercept	6.60188	23.5449	0.280395	0.783275
Slope	0.18078	0.0849268	2.12866	0.0515224

Analysis of Variance

Source	Sum of Squares	Df	Mean Square	F-Ratio	Prob. Level
Model	213.73598	1	213.73598	4.53117	.05152
Error	660.38152	14	47.17011		
Total (Corr.)	874.11750	15			

Correlation Coefficient = 0.494486 R-squared = 24.45 percent
Stnd. Error of Est. = 6.86805

Figure 18.

loss was also found in in-plane measurements, we assume that the heat treatment lead to some degradation along with the crystalization. Most processes that decrease velocity tend to also increase loss; therefore, it seems that the effects of increasing crystallinity must have overcome effects of heat degradation on the loss.

We are at present planning two further experiments. Betty John is making multilayer sheets with and without a thin middle layer of very lightly refined pulp. This will produce an artificial weak zone, and we will be able to compare its influence on out-of-plane velocity and loss measurements. Also, we will take a closer look at the correlation of ZDT to velocity and loss on single ply sheets. This will confirm or deny our suspicions that for homogeneous sheets loss is not superior to velocity as an indicator of ZDT.

Appendix 1

POLAR DIAGRAMS OF ELASTIC STIFFNESS: EFFECT OF MACHINE VARIABLES

GARY A. BAUM

The Institute of Paper Chemistry
P.O. 1039
Appleton, WI 54912

ABSTRACT

Polar diagrams of specific elastic stiffness have been measured on CD strips of commercial papers and on special laboratory sheets. The results provide information about operating conditions on the paper machine including fiber orientation, wet straining, and MD and CD drying restraints. This paper discusses how the shape, size, and angle of lean of the resultant polar diagrams are affected by the process variables. A new parameter, the "effective" stiffness, is defined. This provides a description of the collective effect of the operating variables which appears to be superior to the arithmetic average or geometric average of the MD and CD stiffnesses. The results, which reveal the complex nature of the interactions between headbox conditions, draws, and CD drying effects, should be beneficial in improving headbox design and in understanding CD variations in paper mechanical properties.

INTRODUCTION

Equipment has been developed at The Institute of Paper Chemistry which can measure the orthotropic elastic stiffnesses of paper in the laboratory and on the paper machine [1-4]. The elastic stiffnesses are sensitive to paper machine operating conditions and often can be related to the end-use tests normally used to characterize paper [5]. A recent development is the ability to automatically measure specific elastic stiffnesses as a function of angle from the machine direction. This instrument has been described in detail elsewhere [6]. It measures the longitudinal specific stiffness (related to C_{11} and C_{22} or Young's moduli E_{MD} and E_{CD}) or the shear specific stiffness (related to C_{66} or G_{MD-CD}). When the elastic stiffnesses are plotted *vs.* angle from the MD, as a polar graph, the results typically look like those shown in Fig. 1. The area and major axis of the generally elliptical shape can be computed and the angle the latter makes with the MD determined.

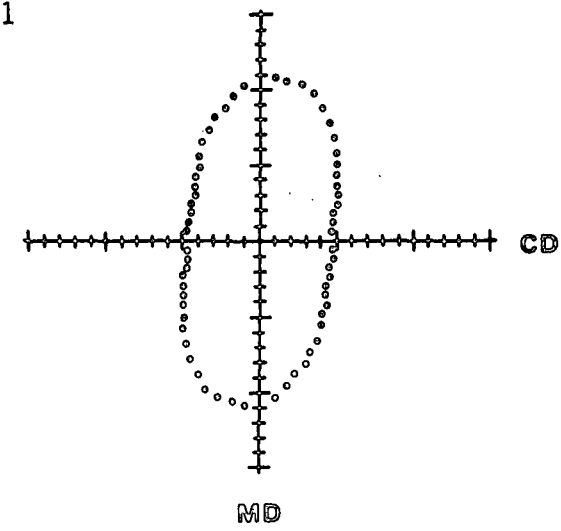

Fig. 1. Typical in-plane polar plot.

The shape, area, and angle of lean of the polar "diagrams" typically vary across the width of the paper machine. Figure 2 shows five such diagrams taken at regular intervals across the web for a fine paper, starting from the front side of the machine. The variations in shape, size, and angle of lean are related to changes in the level and direction of fiber orientation, refining, wet pressing, stretching of the wet paper web in open draws, and nonuniform drying conditions in the web. The variations in the inclination of the major axis of the ellipse with the machine direction (MD) of the paper (e.g., Fig. 1 or Part E of Fig. 2), are traceable to transverse stock flows from the headbox and have been discussed in detail elsewhere [7]. This paper primarily deals with the effects of machine variables on the shape and size of the diagrams. Such information can be useful in interpreting the nature of the interactions between variables across the width of the paper web.

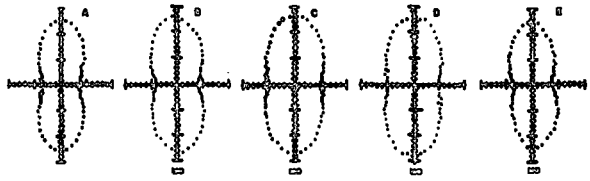

Fig. 2. Five polar diagrams taken across the web. A is near the front side, E the drive side.

RESULTS AND DISCUSSION

Lean Angle

Figure 3 shows two laboratory sheets made from the same furnish and having the same nominal basis weights. The circular shape is the

result obtained for a handsheet made on a Noble and Wood machine, for which the fiber orientation would be expected to be random (no preferred fiber orientation). The elliptical shape was obtained for a sheet made in a Formette Dynamique anisotropic sheet former, in which there is some fiber orientation along the machine direction. The ratio of the stiffnesses along the MD compared to the CD for this latter case is about 1.4. The elliptical shape clearly is related to the extent of fiber orientation in the paper. Later we will see that it is also related to the extent of wet straining.

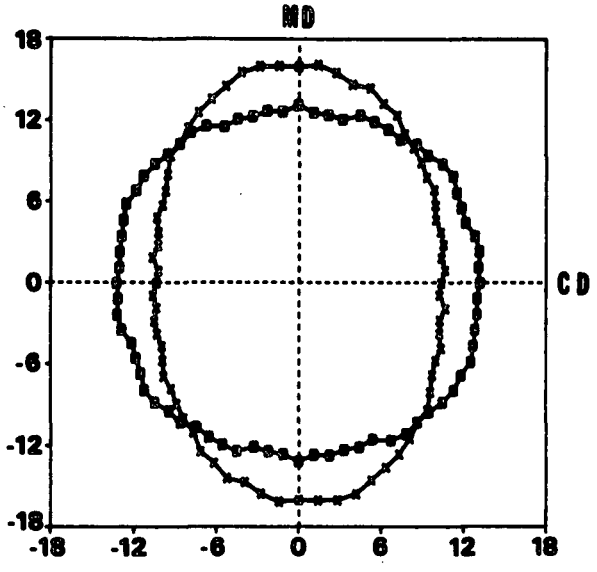

Fig. 3. C_{11} measured at various angles to the MD for a handsheet (squares) and oriented paper (X's).

In Fig. 3 the major axis of the ellipse for the Formette sheet is exactly along the MD. Figure 1 is a polar diagram for a commercial sheet in which the major axis is about 8 degrees clockwise from the MD. This angle of inclination is caused by stock flows from the headbox which have a component that is at right angles to the MD. Such transverse flows apparently deposit fibers onto the paper machine wire that have a preferred orientation at some angle to the MD. It has been shown that the angle of lean does not depend on wet stretching or drying conditions. Commercial samples displaying various angles of lean were immersed in water for extended periods of time, dried, and remeasured. In all instances there was no change in the lean angle, even though the area of the polar diagrams decreased [7]. Figure 4 illustrates this for two commercial samples.

The observance of a lean angle is quite common. To date we have made measurements on numerous CD strips from many paper machines manufacturing a variety of grades. In most cases there is some angular offset of a few degrees, which typically varies from point to point across the paper machine. The angular displacement may be as large as plus or minus 15 degrees. In such cases, it is not unusual to experience difficulty during a subsequent converting operation or end-use application. Figure 5 shows lean angle vs. position for four CD strips taken from the same machine. In our experience the profile or pattern for a given machine seems to make a fairly reliable "fingerprint" of that machine. There does not seem to be any common pattern, however, in the measured CD profiles of angular displacement from machine to machine.

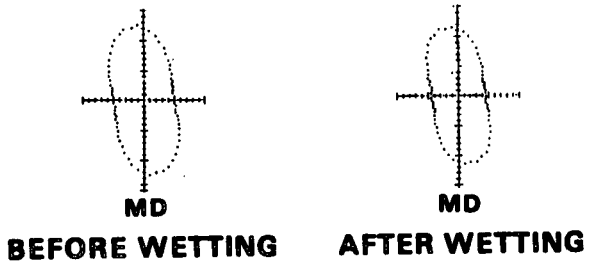

Fig. 4. Polar diagrams for a fine paper, before and after wetting and redrying. The wetting does not affect the angle of lean.

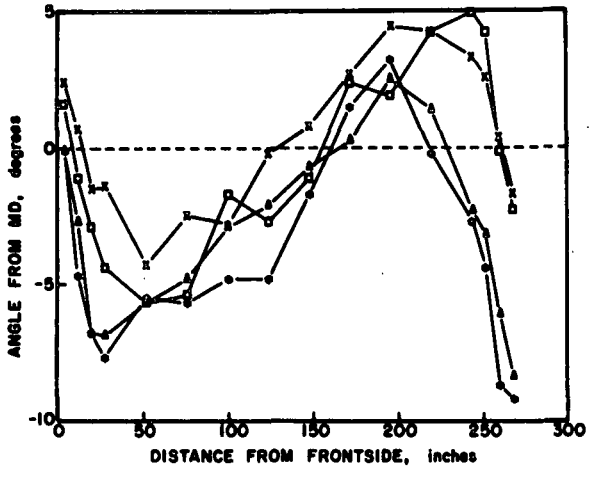

Fig. 5. Angle of lean vs. position across the machine for four separate reel turnups. Diagrams like these seem to be a "fingerprint" of the headbox and slice conditions.

Fiber Orientation, Wet Straining, and Drying Restraints

In an attempt to elucidate the effects of fiber orientation, wet straining, and drying restraints on the shape and size of the polar diagrams, southern pine unbleached kraft sheets

were prepared under various conditions and constructions. Two layer composite papers were made by wet pressing together Formette Dynamique sheets having a nominal basis weight of about 100 g/m^2 and an anisotropy of 1.62 due only to the orientation of fibers in the sheets. The resultant 200 g/m^2 sheets were wet strained or dried under various conditions. In each case duplicate sheets were made. Values reported below are the average of the two sheets.

The results are shown in Fig. 6 for the four constructions and drying conditions. In sample A the two plies were aligned with their MD directions parallel, and the composite was wet pressed and then dried under full MD and CD restraint. No shrinkage was allowed. Sample B had the same construction with parallel MD directions and was wet pressed to the same pressure but dried under only MD restraint. There was about 6.5% shrinkage in the CD direction during drying. Sample C also had the machine directions of the two plies aligned, but after wet pressing was stretched in the MD about 2% while still wet. It was then dried under MD and CD restraint. After drying, a 2% shrinkage was measured in the cross machine direction, presumably a consequence of the MD wet straining. In sample D the two plies were oriented so that their MD's were perpendicular and the composite was then wet pressed and dried under MD and CD restraint.

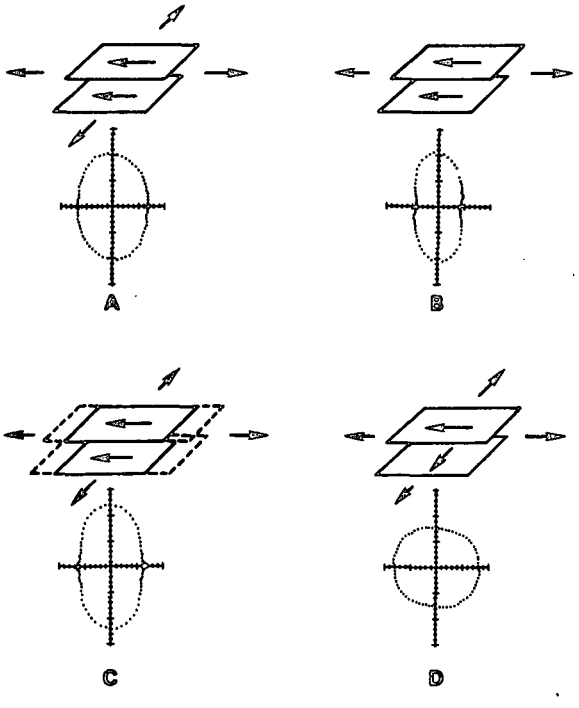

Figure 6. Four different paper constructions and drying conditions, and the resultant polar diagrams.

The polar diagrams measured for the different constructions and drying conditions are also shown in Fig. 6. In A the elliptical shape is due only to the orientation of the fibers in the two layers. The anisotropy ratio (C_{11}/C_{22}) for the composite is 1.54. Sample B differs from A in that it was allowed to shrink in the CD. The resultant polar diagram is quite different from that found for A. It no longer has the elliptical shape but appears "necked down" in the cross machine direction, similar to the results obtained for Samples A and E in Fig. 2, near the edges of the paper web. The area of the polar diagram for 6B is much less than that found for 6A, about 152 (km/s)^2 vs. 225 (km/s)^2, again a result of the CD shrinkage during drying. (It may be possible to obtain a necked down diagram similar to that observed here which is due entirely to some particular distribution of fibers in the paper. That is clearly not the case here. Most likely the changes in shape found for commercial grades are not caused by differences in the distribution of fibers from point to point, but rather are caused by the shrinkage effects described here.)

Sample C differs from A only in that it was wet strained 2.3% before drying. The polar diagram for C has an elliptical shape similar to that for A except that the anisotropy ratio has increased to 2.05. There is a very slight increase in the area of the diagram to 239 (km/s)^2. In D, where the two plies were oriented at right angles, the resultant polar diagram is a circle, as expected, having an anisotropy of 0.98 and an area of 227 (km/s)^2.

The experiments described in Fig. 6 illustrate that the size and shape of the polar diagrams can vary with changes in fiber orientation, wet straining, and drying restraints. Comparison of samples A and D suggests that the area of the polar diagrams is independent of fiber orientation and possibly wet straining (Sample C). CD shrinkage, however, resulted in a decrease of about 30% in the area (Sample B).

Increasing the level of refining or wet pressing increases the area of polar diagrams as shown in Fig. 7, which shows an unbleached hardwood kraft pulp beaten to five levels. The wet pressing pressure was varied over three levels at each refining level. Other sheet preparation parameters remained constant, except at the CSF level of 350 mL, where two levels of fiber orientation are shown. The size of the polar diagrams is clearly sensitive to the level of refining and wet pressing, as expected.

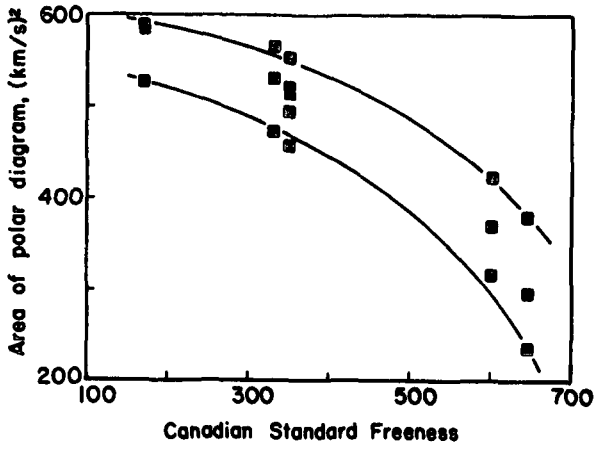

Fig. 7. The areas of the polar diagrams increase with increasing refining and wet pressing. There are three wet pressing levels at each refining level. The six points at 350 CSF represent two different fiber orientation levels.

Since refining and wet pressing effects would be expected to be uniform over the width of the web, changes in the shape and area of the polar diagrams taken across the web, such as those shown in Fig. 2, would best be explained in terms of a nonuniform CD shrinkage between the center and edges of the web. An increase in the CD shrinkage as one goes outward toward the sides would account for both changes. This, of course, also would explain the often observed lower values for mechanical properties near the edges of the web.

Effective Stiffness

It is common for the papermaker to use a single number to characterize production when possible. For example, the squareness or anisotropy ratio or arithmetic or geometric mean of MD and CD properties is often used. Polar diagrams such as those shown in Fig. 1, 6B, or 2A, however, suggest that such ratios or averages will be misleading because of a lean angle or a necked down shape. The area enclosed by the polar diagram appears to be a useful quantity in this respect, but there is a more meaningful way to express the results. The "effective stiffness" is taken as the radius of a circle having the same area as the measured polar diagram, as shown in Fig. 8. Figure 9 compares specific effective stiffness *vs.* the geometric specific stiffness for the eight specimens (four constructions) described in Fig. 6. Note that in all cases the effective stiffness value is greater than the geometric mean value. This turns out to be true in the case of commercial papers as well, as we will see next.

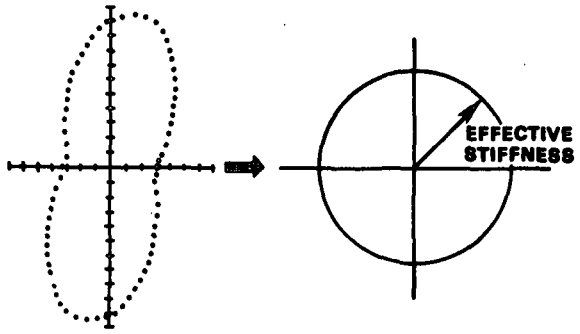

Fig. 8. The "effective stiffness" is defined as the radius of a circle having the same area as the polar diagram.

Commercial Paper Samples

Polar diagrams have been obtained for a large number of commercial papers. Most testing has been done on CD strips in which information was sought concerning the nature of the flows from the headbox. Figure 10 shows a fine paper sample in which polar data were obtained every eight inches across the width of the web. In this case the angular displacement is a maximum on the front side of the machine (about six degrees) and decreases gradually until it approaches zero near the back side. Figure 11 shows polar diagrams taken near the front side (A), middle of the web (B), and back side (C). In addition to the changing lean angle, the area of the polar diagram from the center of the web is noticeably larger than those taken from the edges, similar to the behavior noted in Fig. 2. Figure 12 shows that the polar diagram areas have a maximum at the center of the web. Again, based on the experiments described in Fig. 6, the behavior seen in Fig. 12 could be explained in terms of a nonuniform CD shrinkage between the center and edges of the web.

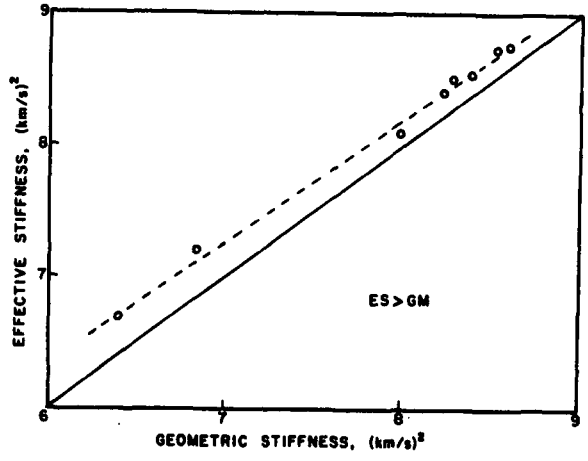

Fig. 9. Effective stiffness *vs.* geometric stiffness for the experimental sheets.

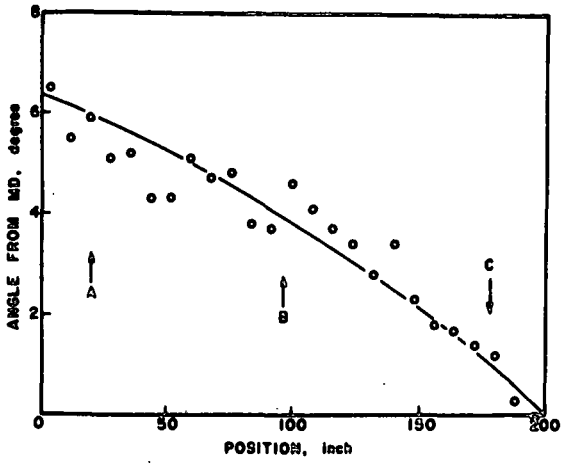

Fig. 10. Angle from MD vs. position. The letters show where the profiles in Fig. 11 were obtained.

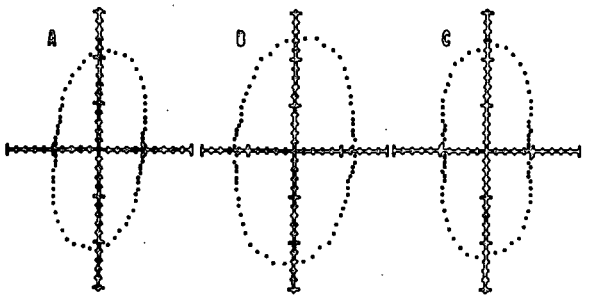

Fig. 11. Polar diagrams taken from three different CD web positions as shown in Fig. 10.

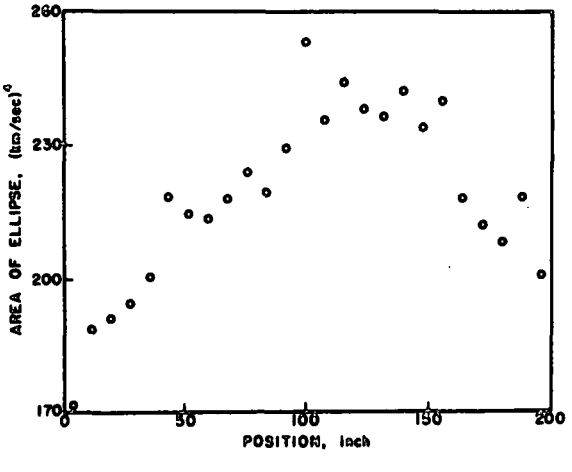

Fig. 12. Area of ellipse vs. position for same specimens as in Fig. 10.

The same argument explains why other mechanical properties show the same convex curvature in CD profiles. The MD or CD specific elastic stiffnesses vs. position, as shown in Fig. 13, for example, both show this behavior. Figure 13 also shows the geometric mean value of the specific stiffnesses. Figure 14 compares the specific effective stiffness, defined above, and the geometric stiffness. The difference between the two quantities increases as we go toward lower stiffness levels. The lowest stiffness levels are from specimens taken near the edges of the web (Fig. 13) and which tend to have the necked down shape. Thus the calculated geometric mean values would not appear to be very reliable indicators of product quality, especially near the edges of the web. For the same reasons, the MD/CD ratios would vary across the web with higher values at the edges. A plot of anisotropy ratio vs. position for the specimens depicted in Fig. 10-14 shows such a concave upward behavior.

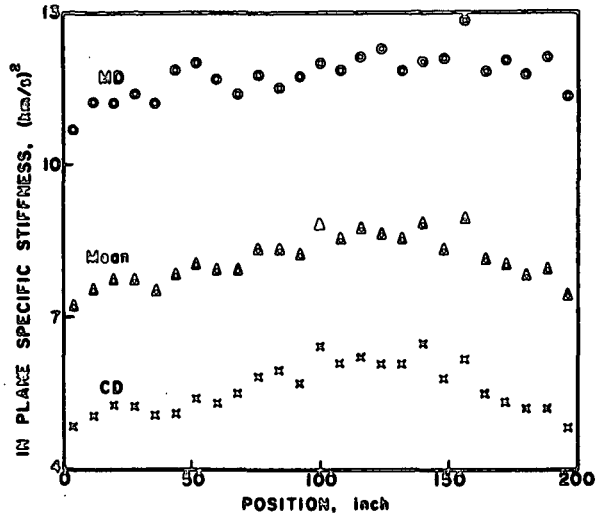

Fig. 13. In-plane specific stiffnesses vs. position for fine paper specimens of Fig. 10.

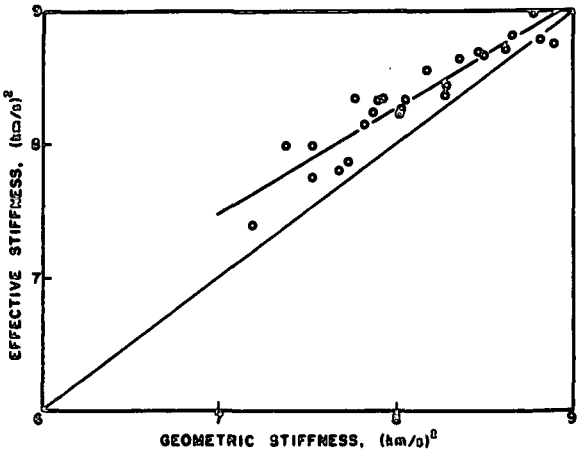

Fig. 14. Effective stiffness vs. geometric stiffness for the fine paper specimens in Fig. 10.

Because nonuniform drying restraints in the CD affect the local values of the measured mechanical properties (especially those measured in the CD), geometric mean values or anisotropy

ratios may give misleading information concerning paper quality. The specific effective stiffness may be a more meaningful parameter.

CONCLUSIONS

For a given furnish, sheet mechanical properties are determined by conditions at the slice (jet-to-wire speed differentials), the level and uniformity of wet pressing pressure, the extent of stretching of the web in any open draws, the MD restraint applied as the web passes through the dryer section, and the CD restraint (or lack thereof) offered by the dryer felts and contact with the cans during drying. Variations in sheet mechanical properties in the cross machine direction are a consequence of differences in how these variables interact locally. The nature of the interactions is often difficult to ascertain using traditional testing methods.

The study of polar diagrams, however, seems to offer considerable insight as to how process variables interact and suggests the possibility of separating their effects. Transverse stock flows at the slice are traceable to the angle of lean of the polar diagrams. An increase in the pressing pressure (or refining) increases the area of the polar diagrams but does not change shape. An increase in wet stretching (draws) increases the ellipticity (or anisotropy ratio) of diagrams, but not the area. A change in CD (or MD) restraint in the dryer section during drying changes both the area and shape (anisotropy ratio) of the polar diagrams. The effective stiffness parameter may be a more meaningful number in describing the quality of the product than those quantities more commonly used.

The study of polar diagrams and their concomitant application to problems will help us to better understand paper machine operations and how to develop more uniform product quality. There is more information that can be obtained, however, which promises to be as important or even more important. A simultaneous measurement of a thickness direction (ZD) elastic stiffness provides additional information concerning the state of wet pressing (or refining) and wet stretching. For example, for the experimental sheets discussed in Fig. 6 the ZD specific stiffness changes by about 100% as a consequence of the changes in wet straining and drying restraints. The ZD stiffness decreases as wet straining or restraint during drying incRefining or wet pressing would offer equally large effects in the opposite direction. An increase in wet pressing pressure, for example, would cause ZD stiffness to increase substantially [8]. We are working to develop equipment that will quickly enable us to obtain polar diagrams and measure ZD elastic stiffness.

REFERENCES

1. MANN, R. W., BAUM, G. A. and HABEGER, C. C. Tappi 63(2):163 (1980).
2. BAUM, G. A., BRENNAN, D. G. and HABEGER, C. C. Tappi 64(8):97 (1981).
3. BAUM, G. A., HABEGER, C. C. and FLEISHMAN, E. H. Measurement of the Orthotropic Elastic Constants of Paper. In: The Role of Fundamental Research in Papermaking, Transactions of the Cambridge Symposium: September 1981. Mechanical Engineering Publications Ltd., London, 1983.
4. HABEGER, C. C. and BAUM, G. A. Tappi 69(6):106 (1986).
5. BAUM, G. A. Elastic Properties, Paper Quality, and Process Control. Presented at 1986 Tappi International Process & Materials Quality Evaluation Conference, Atlanta, GA, September 21-24, 1986.
6. VAN ZUMMEREN, M. L., YOUNG, D. J., HABEGER, C. C., BAUM, G. A. and TRELEVEN, R. Automatic Determination of Ultrasound Velocities in Planar Materials. Accepted for publication in Ultrasonics, 1987.
7. BAUM, G. A. and BRENNAN, D. G. Transverse Jet Flows Affect Paper Properties. Presented at the 1987 TAPPI Process Control Conference, Nashville, TN, March 23, 1987.
8. BERGER, B. G. and BAUM, G. A. Z-direction Properties: The Effects of Yield and Refining. In: Papermaking Raw Materials Transactions of the the 8th Fundamental Research Symposium, Oxford (1985). Mechanical Engineering Publications, Ltd., London, 1985.

THE INSTITUTE OF PAPER CHEMISTRY

Appleton, Wisconsin

Status Report

to the

PAPER PROPERTIES AND USES

PROJECT ADVISORY COMMITTEE

Project 3526

INTERNAL STRENGTH ENHANCEMENT

September 11, 1987

PROJECT SUMMARY

PROJECT NO. 3526: INTERNAL STRENGTH ENHANCEMENT

PROJECT STAFF: R. Stratton, K. Hardacker September 11, 1987

PROGRAM GOAL: Bring new attributes to fiber based products

PROJECT OBJECTIVE:

To improve internal strength and moisture tolerance in paper and paperboard. The short term goals are to establish those parameters fundamental to inter-fiber and intra-fiber bonding in conventional and ultra high yield pulps and to control these parameters, if possible, by chemical or mechanical treatments.

PROJECT RATIONALE, PREVIOUS ACTIVITY, AND PLANNED ACTIVITY FOR FISCAL 1987-88 are on the attached 1987-88 Project Form.

SUMMARY OF RESULTS LAST PERIOD: (September 1986 - March 1987)

(1) Strength aids added to the pulp prior to refining influence the rate of beating. The strength properties of handsheets made from such a pulp are inferior to those of handsheets for which the bonding agents are added after refining.

(2) Addition of a polymeric retention aid to a whole pulp to attach the fines to the long fibers prior to introducing the strength aids gave less strength enhancement than if the retention aid was not present.

(3) Comparison of sheets made with bonding agents at pH 7 and pH 4.5 shows that greater strength is produced at the higher pH.

(4) Further evidence was adduced that tensile strength and STFI compression strength are each affected to different extents by the various bonding agent combinations.

(5) A suitable hot melt adhesive has been found for cementing single fiber to the mounting fixtures of the FLER II.

(6) Latewood fiber/fiber bonds produce both higher average breaking load and specific bond strength than earlywood from the same unbleached loblolly pine kraft pulps.

(7) For fibers both untreated and treated with PAE/CMC refining did not change the bond breaking load, decreased the bond area, and increased the specific bond strength.

(8) Untreated TMP fibers produced rather weak bonds from the viewpoint of breaking load. The specific bond strength, however, was very high.

(9) Treatment of the several pulp fibers with the strength additive PAE/CMC enhanced breaking load, bonded area, and specific bond strength.

SUMMARY OF RESULTS THIS PERIOD (March 1987 - September 1987)

(1) Improving fines retention prior to strength aid addition was not an effective method to increase the strength of whole pulps.

(2) Increasing the strength aid dosage above that found to be optimum for classified pulps resulted in little additional strength improvement in a whole pulp. This suggests that adequate coverage of all surfaces (fiber and fines) with the strength additive is not the limiting factor in strength enhancement.

(3) Preliminary experiments suggest that strength aid located outside the main bonded area of the fibers may contribute to sheet strength.

(4) External treatment with a rigid SBR latex produced good dry and moist strength properties. Use of a polymer coupling agent did not increase the strength thus suggesting that only mechanical interlocking between the latex and the refined fibers and not chemical interaction was occurring.

(5) Preliminary experiments using external addition of some duopolymer strength aids suggest this may be a viable application method.

(6) Comparison of single fiber/fiber bonds prepared from either lightly or heavily refined pulps revealed no difference in specific bond strength. This suggests that the main effect of prolonged refining is the creation of fines which contribute to sheet strength but not specific bond strength.

(7) Chemical treatment with additives producing either covalent or ionic bonding gave substantial increases in specific bond strength. Covalent bonding is not necessary for strength enhancement.

(8) Specific bond strength was found to decrease with increasing relative humidity in a like manner to sheet strength and individual fiber strength.

PROJECT TITLE: Internal Strength Enhancement

PROJECT STAFF: R. Stratton/K. Hardacker

PRIMARY AREA OF INDUSTRY NEED: Properties related to end use

PROGRAM AREA: Moisture tolerant, superior strength paper and board

Date: 1/14/87

Budget: $230,000

Period Ends: 6/30/88

Project No.: 3526

PROGRAM GOAL: Bring new attributes to fiber based products

PROJECT OBJECTIVE/GOAL:

To improve internal strength and moisture tolerance in paper and paperboard. The short term goals are to establish those fundamental parameters affecting inter-fiber and intra-fiber bonding in conventional and ultra high yield pulps and to control these parameters, if possible, by chemical or mechanical treatments.

PROJECT RATIONALE:

Major limitations of paper and board for many uses are low internal bond strength and poor moisture tolerance. Improved internal strength and enhanced moisture resistance would allow a number of present grades to be produced using less fiber and would also allow new end uses to be developed.

At present, commercial papers do not attain strength levels that realize the full potential of the wood fibers. Most paper mechanical properties are markedly degraded with increasing moisture content. We need to better understand the nature of fiber properties and fiber-to-fiber bonding and changes in them with increasing moisture content, if we are eventually to improve the moisture tolerance of paper.

RESULTS TO DATE:

1) The duopolymer systems comprised of CMC/PAE and PAA/PAE were found to be effective bonding agents for a variety of bleached and unbleached, conventional kraft and high yield pulps.

2) The greatest increases in strength at a given polymer dosage were obtained when the polymer was applied to the long fiber fraction only. Apparently polymer adsorbed on fines is less effective.

3) Greater percentage increases upon treatment with polymers were found when using classified pulps compared with whole pulps. Attempts to obtain better enhancement of properties by polymer addition before refining produced negative results.

4) Diffuse reflectance FTIR analysis revealed that rather substantial strength improvements can be achieved in the absence of covalent bonding between the additives and the fiber surface. In these cases electrostatic (ionic) bonds apparently are capable of providing the necessary interactions.

5) Two Progress Reports detailing the results have been issued.

6) Single fiber/fiber bond measurements of bond strength, bonded area, and locus of failure for an unrefined, loblolly pine springwood, kraft pulp revealed a broad distribution of the quantitative results. Poor correlation between bond failure load and bonded area, in agreement with previous workers, may suggest that Page's technique is not a valid measure of bonded area. SEM micrographs showed permanent deformation in the bonded area but little fiber wall tearing or disruption.

7) The measurements were repeated on the same pulp which had been treated with the PAE/CMC additive combination found effective for conventional kraft pulps in the earlier handsheet studies. Increases in average load at failure, bonded area, and specific bond strength (load/area) of 150, 20, and 80% respectively were found. In contrast to the untreated fibers, examination of the formerly bonded areas by SEM now showed extensive tearing and picking of the fiber walls.

8) Measurements of bond strength, bond area, and locus of failure for a well-refined, classified southern pine provide a contrast to the unrefined sample. Frequent tearing of the fiber wall was now found for both untreated and chemically-treated fibers. However, extensive external fibrillation of the fibers make an unambiguous assessment of the damage due to bond failure difficult. Both breaking load and bond strength are considerably higher for the refined compared with the unrefined fibers.

9) A more sensitive, more versatile fiber load elongation recorder (FLER II) has been designed and constructed. Techniques are being developed for measuring the axial and transverse mechanical properties of single fibers and of Z-direction deformation of single fiber/fiber bonds using the FLER II.

PLANNED ACTIVITY FOR FY 1987-88:

Studies will continue in both the single fiber bond and handsheet programs. The objectives remain to a) gain a better understanding of bonding in paper and b) develop a material that will maintain its rigidity at high relative humidity.

To ascertain the relative contribution of decreased bond strength to moisture sensitivity, we will study the dependence of single fiber bond strength on relative humidity.

To clarify the mode of fiber wall failure, we will develop a method to determine the fibril angle on selected portions of the single fibers.

We will extend our current work on high yield fibers to examine the effects of elevated drying temperatures at both single fiber and handsheet levels. This will include sheets made under impulse drying conditions.

In other handsheet studies we plan to:

1) examine several alternatives for stiffening individual fibers,

2) extend our work on external treatments to a variety of aqueous additive systems, and

3) continue to seek polymer systems which have a potential for improving compressive strength. We also plan additional studies to better understand how to efficiently use these expensive additives in whole pulps.

New Research Area

As discussed at the RAC meeting of November 6, the Paper Properties and Uses PAC suggested the initiation of a new research project concerned with the wettability of paper. Specifically it was proposed that such a project should consider the surface properties of paper, how they are developed on the paper machine and their spatial distribution, as well as absorption and/or penetration issues.

This is an area of interest to IPC, but one in which we have little expertise. We do have an opportunity to replace one person in the Surface and Colloid Science Section, however, and are hopeful that we can locate a person having experience and interest in the surface wettability area. If so, we intend to pursue this area, by diverting funds from other projects, if necessary.

STUDENT RELATED RESEARCH:

Biasca, J. E., Ph.D.-1987; McCarthy, W. R., Ph.D.-1987; Proxmire, P. R., Ph.D.-1987; Goulet, M. T., Ph.D.-1988, Molinarolo, S. L., Ph.D.-1988, McCarthy, J. M., MS-1987; Luettgen, C. O., MS-1987; Stoffler, C. L., MS-1987; Breining, J. H., MS-1988; Friese, M. A., MS-1988.

Status Report

INTERNAL STRENGTH ENHANCEMENT

Project 3526

PART ONE: Improved Bonding Via Chemical Additives

Effect of Fines Retention

In previous work on this project we have shown that the relative improvement in strength of a pulp was much greater when the pulp fines were first removed from the pulp. For example the results for a typical unbleached softwood kraft pulp are given in Table 1.

Table 1. Influence of fines on strength aid effectiveness.

	Breaking Length, km		
	No Strength Aid	With Strength Aid	Enhancement, %
Whole Pulp	6.1	8.3	36
Classified Pulp	3.9	7.8	100

The strength of the sheets from treated or untreated whole pulp is, of course, higher than that from the corresponding classified pulp. Part of the observed difference in behavior of the two pulps may be a result of the added surface area of the fines. The same amount of strength aid (% based on o.d. pulp) was used for both. The larger surface area available for polymer adsorption in the case of the whole pulp would lead to a sparser coverage of the surface by the strength aid. The result could be a lesser strength enhancement.

In the last status report (March 25-26, 1987) we discussed attempts to minimize the effect of the fines by attaching them to the fibers with a retention aid prior to the introduction of the strength aid. For the retention aid we used a high molecular weight, low charge density cationic polymer of the type usually found effective for this purpose. The effects on strength improvement

were disappointing. If anything, preaddition of the retention aid slightly reduced the strength compared to the case where it was not used. These results were unexpected and we have since further investigated the interactions.

We used the Britt dynamic drainage jar to test the effectiveness of the retention aid in our furnish. The results showed that this polymer was, in fact, a very poor fines retention aid. We then tested other possible retention aids and settled on a combination of a high charge density cationic polymer followed by a high molecular weight, low charge density anionic polymer. Such two-step combinations are known to be quite effective retention aids and gave good results with our furnish. Retention was reduced somewhat, however, when the PAE/CMC strength aid combination was also added to the stock before the retention measurement. This is because the zeta potential of the furnish after treatment with the retention aids is positive and the addition of the strength aids drives the system even more positive. In spite of this, there is a net reduction in white water fines of 25% when both the retention aid combination and the strength aid combination are used. This should be a sufficient improvement in retention to produce a significant increase in strength, if the hypothesis that the increased surface area due to the fines is responsible for the smaller strength enhancement seen with the whole pulp.

The results shown in Table 2 do not support this hypothesis. When the strength values for the pulp treated only with the retention aid combination (set no. 8) are compared with those of the untreated pulp (set no. 1) significant increases can be noted. Whether these are due to the increased level of fines in the sheet or to improved bonding caused by the retention aids cannot be determined at this point. Additional experiments using the retention aid combination with a classified pulp could resolve this uncertainty, but are not

Table 2. Effect of dosage of PAE/CMC on whole pulp (softwood unbleached kraft - whole pulp)

Set No.	Additives, % Based on Fiber	Basis Weight, g/m^2	Apparent Density, g/cc	Dry Strength Properties: Breaking Length, km Av.	SD	TEA kgm/m^2 Av.	SD	Et, kg/cm Av.	SD	Stretch, % Av.	SD	Moisture Content, %	Moist Strength Properties: Breaking Length, km Av.	SD	TEA kgm/m^2 Av.	SD	Et, kg/cm Av.	SD	Stretch, % Av.	SD	Moist Tensile Factor
1	Blank Control	66.3	0.472	5.46	0.097	7.53	0.499	414	5.8	3.01	0.149	15.2	3.23	0.143	5.71	0.712	181	3.9	3.92	0.296	1.00
2	1% PAE	61.4	0.468	7.67	0.375	11.50	1.000	412	14.9	3.72	0.178	15.2	5.26	0.141	9.31	0.503	171	9.6	4.94	0.188	1.63
3	0.5% PAE,0.2% CMC	62.6	0.472	7.45	0.281	10.73	0.972	431	16.7	3.50	0.206	14.8	5.26	0.148	9.69	0.569	184	7.1	4.98	0.182	1.63
4	1% PAE,0.4% CMC	63.9	0.482	8.09	0.083	11.39	0.501	472	15.5	3.38	0.133	15.1	5.98	0.189	13.2	0.76	188	12.4	5.67	0.181	1.85
5	1.5% PAE,0.6% CMC	65.0	0.492	8.23	0.285	11.72	1.335	482	16.5	3.34	0.301	14.7	6.16	0.311	12.5	0.68	196	3.8	5.25	0.128	1.91
6	2% PAE,0.8% CMC	61.5	0.496	8.45	0.419	10.75	1.332	482	7.1	3.19	0.241	14.5	6.10	0.356	10.5	1.30	191	7.7	5.06	0.282	1.89
7	2.5% PAE,1% CMC	63.6	0.506	8.24	0.789	10.31	2.637	482	30.5	3.02	0.573	14.8	6.57	0.249	12.5	0.70	188	6.6	5.48	0.187	2.03
8	0.2% cationic, 0.3% anionic	65.2	0.482	6.23	0.389	7.62	1.446	463	9.6	2.74	0.348	15.3	3.74	0.355	6.40	1.236	182	1.6	4.17	0.499	1.16
9	0.2% cationic, 0.3% anionic, 1% PAE, 0.4% CMC	63.5	0.506	7.57	0.287	10.15	1.251	462	11.6	3.16	0.291	14.9	6.15	0.168	12.6	0.75	183	7.9	5.75	0.226	1.90
10	1% PAE, dried, dipped in CMC (0.4%)	62.5	0.479	8.18	0.182	11.92	0.516	441	13.1	3.61	0.140	14.8	5.65	0.204	10.0	0.55	169	9.8	5.00	0.093	1.75

Table 2 continued. Effect of dosage of PAE/CMC on whole pulp (softwood unbleached kraft - whole pulp).

Set No.	Additives, % Based on Fiber	Wet Breaking Length, km		Wet Tensile Factor	Dry STFI Compressive Strength, lbF/in.		Moist Compressive Strength, lbF/in.		Moist Compressive Strength Factor
		Av.	SD		Av.	SD	Av.	SD	
1	Blank Control	0.221	0.029	1.00	9.26	0.759	4.43	0.333	1.00
2	1.0% PAE	2.06	0.107	9.32	9.81	0.502	4.18	0.333	0.944
3	0.5% PAE, 0.2% CMC	1.74	0.053	7.87	9.87	0.838	4.14	0.274	0.935
4	1.0% PAE, 0.4% CMC	2.26	0.075	10.2	10.57	0.715	4.44	0.279	1.00
5	1.5% PAE, 0.6% CMC	2.62	0.134	11.9	11.07	0.800	4.79	0.384	1.08
6	2.0% PAE, 0.8% CMC	2.71	0.167	12.3	10.57	0.923	4.77	0.503	1.08
7	2.5% PAE, 1.0% CMC	3.09	0.165	14.0	11.22	0.818	4.73	0.405	1.07
8	0.2% cationic, 0.3% anionic	0.670	0.072	3.03	10.63	0.730	4.66	0.445	1.05
9	0.2% cationic, 0.3% anionic, 1.0% PAE, 0.4% CMC	2.40	0.114	10.9	10.82	0.707	4.65	0.435	1.05
10	1.0% PAE, dried, dipped in CMC (0.4%)	2.26	0.111	10.2	10.11	0.610	4.67	0.389	1.05

planned. The influence of the retention aid combination on the effectiveness of the strength aid can be judged by comparing set no. 4 (no retention aid) with set no. 9 (retention aid added first). No clear advantage in using the retention aids can be found.

Effect of Strength Aid Dosage

A more direct method to overcome the increased surface area when fines are present would be to increase the dosage of the strength aid. Levels used heretofore were based on dosages found to be optimum for classified pulps. A similar optimization study was carried out on the whole pulp using the PAE/CMC combination found to be most effective for this pulp. The ratio of CMC to PAE was kept constant at 0.4, since this had earlier been shown to be the optimum. The results for zero dosage (set no. 1) to 2.5% PAE (set nos. 3-7) are given in Table 2. There is a rapid increase in strength properties from zero to 0.5% PAE followed by a more gradual increase through 1.5% PAE. Little, if any, additional increase occurs at yet higher dosages. (An exception to this statement is found for the variation of wet strength with dosage. As is usually found for this property, wet strength continues to increase with increasing dosage, though at a lower rate than the initial increment.) Hence the dosage defined as optimum for the classified pulp (1% PAE, 0.4% CMC) gives dry and moist strength values only about 3-4% less than the plateau values achieved at higher dosages. Obviously, insufficient dosage does not account for the smaller enhancement of strength properties found for the whole pulp compared with the classified pulp. It may be that the plateau value of strength reached at the higher dosages represents the maximum strength achievable with this furnish. That is, the individual fiber strength or the distribution of bonds rather than the bond strength may be the limiting factor. Additional work will be necessary to clarify the situation.

Effect of Location of Additives

In most of the work to date we have added the strength aid(s) to the pulp slurry before sheet formation so that the fibers become uniformly coated over their entire surface. Bonding during web consolidation then occurs between treated fiber surfaces. It has been suggested that the bond strength around the perimeter of the bonded area is an important factor due to stress concentrations in those regions. To evaluate this factor, we prepared sheets with enhanced bonding just outside the normally bonded areas as follows. We have shown that the sequence cationic PAE followed by anionic CMC leads to stronger sheets than if only PAE is used. (Compare set nos. 2 and 4 in Table 2). In the duo-polymer system the cationic PAE is introduced first and quickly adsorbs on the negatively-charged fibers. The anionic CMC is then added and finds attractive sites for adsorption on the PAE. We have shown previously that during drying covalent bonds are formed between PAE and the fiber or between PAE and CMC. In the present experiment we carried out the sequence differently. Cationic PAE only was added to the furnish and sheets were formed, pressed, and dried as usual. The dried sheets were then dipped in a CMC solution whose concentration was chosen to produce a 0.4% pick-up based on the o.d. pulp. The dipped sheets were passed through a squeeze roll and then dried on a steam drum as usual. This procedure should allow very little of the CMC to penetrate into the areas bonded during the first drying. Opportunities for enhanced bonding (PAE plus CMC) would occur along the periphery of the previously bonded areas and possibly in previously unbonded regions. The results (set no. 10 in Table 2) can be compared with those for set nos. 2 and 4 in that table. The trends are not entirely clear. The properties of the sheets which were formed with PAE, then dipped in CMC are equal or better than those with no CMC. This indicates that CMC external

to the originally bonded area can contribute to the strength. Again, the advantages of treating the fibers with CMC before formation compared with treating the formed sheet with CMC (set nos. 4 and 10, respectively) are uncertain. Part of the ambiguities is because the sheets with CMC (set no. 4) are only slightly stronger than those without (set no. 2). These experiments will be repeated and extended with a classified pulp where the advantage of the duopolymer treatment compared with PAE alone is obvious.

External Treatment with Latex

One potential method to achieve improved moisture tolerance in paper and board is to use an additive that is itself hydrophobic. One of the pigment binders used in paper coating is SBR latex. This material is typically chosen to be rather flexible at room temperature to give the proper printing characteristics. However, the ratio of styrene to butadiene in the SBR latex can be varied during manufacture to give a variety of materials whose rigidity ranges from soft and rubbery to hard and glassy. A latex is a suspension in water of small spherical particles. Upon evaporation of the water, if the ambient temperature is above their glass transition temperature (Tg), the particles can flow and coalesce to form a film. For application as a material to confer strength and rigidity at room temperature and high humidity, we chose a latex with a Tg of 65°C and an average particle size of 0.2 m. At room temperature this material will be rigid but at typical paper drying temperatures it will be above its Tg and the individual particles will merge to form a continuous structure.

To prevent disruption of fiber-fiber bonding and to achieve high dosages without concern for retention, the latex was applied by dipping

already formed and dried sheets into a tray of the latex. The concentration of latex in the tray was adjusted to give pick-ups of either 1,3,5, or 10% based on the o.d. fiber. The dipped sheets were passed through a squeeze roll to remove the excess and dried on a steam drum at 105°C for 7 minutes. Because both the latex and the pulp fibers carry a negative charge and tend to repulse each other, some of the sheets were initially formed incorporating 0.1% PEI. This material is strongly cationic at the pH of use here (4.5) and provides positively-charged patches to attract the latex particles.

The results are presented in Table 3. Overall, the strength improvements appear quite promising. There seems to be no advantage to pretreating the fibers with PEI prior to exposure to the latex. The surface tension forces during water removal (drying) draw the latex into contact with the fiber surfaces. The fact that the PEI does not enhance the strength suggests that the interaction of the dried latex film with the fibers is a purely mechanical interlocking of the SBR with the fibrils. No intermediary surface treatment is necessary.

All of the mechanical properties exhibit marked improvement with increasing latex content. In particular, stiffness as reflected by Et and STFI compressive strength (both dry and moist) reach values at 10% latex that are higher than those we previously found for internal strength additives. As might be expected, since no chemical bonding occurs between the latex and the fibers, the enhancement of wet strength is modest. The internal strength additives (such as PAE/CMC) are much more effective in providing wet strength. Since the strength and rigidity results for this latex are encouraging, further work to clarify its mode of action will be pursued.

Table 3. The effect of external addition of an SBR latex softwood unbleached kraft - whole pulp.

Set No.	Additives, % Based on Fiber	Basis Weight, gm^2	Apparent Density, g/cc	Dry Strength Properties: Breaking Length, km		TEA kgm/m2		Et, kg/cm		Stretch, %	
				Av.	SD	Av.	SD	Av.	SD	Av.	SD
11	0% P-SBR	65.0	0.480	5.27	0.395	6.26	0.896	400	18.7	2.67	0.210
12	1% P-SBR	65.4	0.485	5.38	0.498	5.60	1.227	430	19.6	2.32	0.296
13	3% P-SBR	63.9	0.482	6.16	0.346	6.56	0.787	453	15.1	2.46	0.175
14	5% P-SBR	64.5	0.482	6.45	0.430	8.53	1.761	445	20.3	3.00	0.473
15	10% P-SBR	66.5	0.490	7.41	0.486	8.49	1.206	530	25.4	2.59	0.259
16	0.1% PEI, 0% P-SBR	63.5	0.475	4.90	0.266	5.38	1.161	365	29.6	2.56	0.402
17	0.1% PEI, 1% P-SBR	62.9	0.474	5.64	0.140	6.55	0.648	402	24.4	2.88	0.287
18	0.1% PEI, 3% P-SBR	63.8	0.479	6.27	0.378	7.46	1.335	441	8.6	2.74	0.330
19	0.1% PEI, 5% P-SBR	66.0	0.478	6.51	0.497	8.47	1.456	455	29.3	3.02	0.323
20	0.1% PEI, 10% P-SBR	65.7	0.490	7.33	0.313	10.06	1.068	478	19.5	3.12	0.262

Table 3 continued. The effect of external addition of an SBR latex softwood and unbleached kraft - whole pulp.

Set No.	Additives, % Based on Fiber	Moisture Content, % (at 91-93% RH)	Moist Strength Properties: Breaking Length, km Av.	Breaking Length, km SD	TEA kgm/m2 Av.	TEA kgm/m2 SD	Et, kg/cm Av.	Et, kg/cm SD	Stretch, % Av.	Stretch, % SD	Moist Tensile Factor
11	0% P-SBR	15.0	3.08	0.067	4.46	0.176	161	5.9	3.41	0.169	1.00
12	1% P-SBR	14.6	3.40	0.071	5.28	0.425	175	5.0	3.67	0.236	1.10
13	3% P-SBR	14.3	3.53	0.204	5.39	0.461	177	14.5	3.75	0.239	1.15
14	5% P-SBR	14.1	4.12	0.167	6.38	0.769	206	11.3	3.79	0.369	1.34
15	10% P-SBR	13.5	4.71	0.251	7.74	0.721	222	9.8	3.95	0.203	1.53
16	0.1% PEI, 0% P-SBR	14.7	3.03	0.207	4.25	0.604	155	4.4	3.34	0.250	0.984
17	0.1% PEI, 1% P-SBR	14.6	3.40	0.194	4.93	0.229	165	16.3	3.59	0.204	1.10
18	0.1% PEI, 3% P-SBR	14.2	3.76	0.394	5.96	0.911	176	16.2	3.92	0.290	1.22
19	0.1% PEI, 5% P-SBR	13.9	4.02	0.138	6.49	0.457	197	14.8	3.57	0.663	1.31
20	0.1% PEI, 10% P-SBR	13.7	4.75	0.333	7.14	1.055	243	18.9	3.66	0.346	1.54

Table 3 continued. The effect of external addition of an SBR latex softwood and unbleached kraft - whole pulp.

Set No.	Additives, % Based on Fiber	Wet Breaking Length, km Av.	SD	Wet Tensile Factor	Dry STFI Compressive Strength, lbF/in. Av.	SD	Moist Compressive Strength, lbF/in. Av.	SD	Moist Compressive Strength Factor
11	0% P-SBR	0.204	0.0096	1.00	8.43	0.880	3.83	0.309	1.00
12	1% P-SBR	0.331	0.0172	1.62	8.92	0.744	3.81	0.518	0.995
13	3% P-SBR	0.481	0.0162	2.36	10.16	0.718	4.33	0.420	1.13
14	5% P-SBR	0.577	0.0374	2.83	10.92	0.954	4.71	0.359	1.23
15	10% P-SBR	0.803	0.0064	3.94	12.47	1.382	5.77	0.375	1.51
16	0.1% PEI, 0% P-SBR	0.263	0.0183	1.29	8.24	0.496	3.80	0.311	0.992
17	0.1% PEI, 1% P-SBR	0.438	0.0100	2.15	8.56	0.860	3.83	0.276	1.00
18	0.1% PEI, 3% P-SBR	0.610	0.0463	2.99	10.08	0.882	4.39	0.380	1.15
19	0.1% PEI, 5% P-SBR	0.691	0.0364	3.39	11.23	0.934	4.97	0.414	1.30
20	0.1% PEI, 10% P-SBR	0.889	0.0453	4.36	11.89	0.901	5.79	0.438	1.51

External Addition of Duopolymer Systems

There is some interest in being able to apply a strength additive to linerboard or medium at a size press without adversely affecting the subsequent corrugating process, i.e., good glueability must be maintained. To make a duoplymer system feasible both components must be added at the same station. This requires that the two components form a homogeneous mixture. The combination PAE/CMC is ruled out because it forms a gummy mass. This is the expected result when two polyelectrolytes of moderate and opposite charge are mixed together. Two other systems examined, PAE/pearl starch and PAE/CMPS (carboxymethylated potato starch), gave homogeneous mixtures. The much lower charge density of the starches compared with the CMC is thought to be responsible for their success. These two duopolymer mixtures were tested for their ability to improve strength under conditions of both internal and external addition.

For internal addition the two polymers were mixed together and then added to the pulp slurry. Sheets were formed, pressed and dried as usual. For external addition the two polymers were mixed together at a concentration appropriate to give the desired pick-up when dried previously-formed sheets were dipped into it. The dipped sheets were passed through a squeeze roll and dried on a steam drum at 105°C for 7 minutes.

The results are presented in Table 4. In general, strength improvements are good when compared with the untreated pulp (set no. 1, Table 2). An exception may be those properties related to the rigidity in the moist condition, i.e., moist Et and moist STFI compressive strength. Here the effect of the additives is negligible, if not detrimental. Except for the dry tensile strength, neither internal nor external addition offers an advantage over the other. Further work is planned with external addition utilizing the Keegan coater and a continuous web of linerboard and/or medium.

Table 4. Internal vs. external addition (softwood unbleached kraft - whole pulp)

Set No.	Additives, % Based on Fiber	Basis Weight, gm^2	Apparent Density, g/cc	Dry Strength Properties: Breaking Length, km Av.	Breaking Length, km SD	TEA kgm/m2 Av.	TEA kgm/m2 SD	Et, kg/cm Av.	Et, kg/cm SD	Stretch, % Av.	Stretch, % SD	Moisture Content, % (at 91-93% RH)
22	1% PAE, 1% pearl starch; internal	63.3	0.484	7.35	0.659	11.3	2.10	418	29.0	3.65	0.394	16.7
23	1% PAE, 1% CMPS, internal	62.7	0.487	7.46	0.650	10.6	1.62	419	20.2	3.46	0.239	16.8
24	1% PAE, 1% pearl starch, external	64.0	0.474	6.81	0.390	9.5	1.15	411	11.4	3.28	0.235	15.9
25	1% PAE, 1% CMPS, external	65.4	0.484	7.00	0.507	11.1	0.99	419	22.9	3.61	0.164	16.1

Set No.	Additives, % Based on Fiber	Moist Strength Properties: Breaking Length, km Av.	Breaking Length, km SD	TEA kgm/m^2 Av.	TEA kgm/m^2 SD	Et, kg/cm Av.	Et, kg/cm SD	Stretch, % Av.	Stretch, % SD	Wet Breaking Length, km Av.	Wet Breaking Length, km SD	Dry STFI Compressive Strength, lbF/in. Av.	Dry STFI Compressive Strength, lbF/in. SD	Moist STFI Compressive Strength lbF/in. Av.	Moist STFI Compressive Strength lbF/in. SD
22	1% PAE, 1% pearl starch, internal	4.66	0.191	8.20	0.668	185	11.4	4.45	0.181	1.83	0.090	10.0	1.02	3.47	0.355
23	1% PAE, 1% CMPS, internal	3.98	0.119	6.38	0.346	152	2.7	4.14	0.171	1.82	0.073	10.2	1.06	3.59	0.354
24	1% PAE, 1% pearl starch, external	4.44	0.246	8.29	0.396	177	7.5	4.66	0.140	1.55	0.067	10.1	0.77	4.70	0.418
25	1% PAE, 1% pearl starch, external	3.93	0.232	7.12	0.314	161	15.1	4.24	0.336	1.57	0.080	10.5	0.88	4.01	0.347

Status Report

INTERNAL STRENGTH ENHANCEMENT

Project 3526

PART TWO: Fundamentals of Bonding

Effect of Refining

We have measured the single fiber/fiber bond strength of fibers from the same pulp beaten to two levels of freeness: 570 and 345 mL CSF. The results listed in the first and last columns of Table 5 are surprising in that there is little, if any, difference in the values reported. The 10% increase in bonded area may be real, but a statistical analysis must be performed to verify it. These data imply that by refining to 570 mL CSF the maximum specific bond strength has already been developed. Further refining creates additional fines which can enhance sheet strength but do not contribute to specific bond strength.

Table 5. Average fiber/fiber bond parameters (softwood unbleached kraft pulp) as a function of degree of refining.

	Light, 570 mL CSF			Heavy, 345 mL CSF
Chemical Treatment	None	Covalent[a]	Ionic[b]	None
Breaking Load, g	0.73	1.44	1.51	0.68
Bond Area, μm^2	2070	2130	2050	2290
Specific Bond Strength, $\mu g/\mu m^2$	360	760	850	370

[a] 1% PAE, 0.4% CMC.
[b] 0.5% PDADMAC, 0.5 NaPSS.

Effect of Chemical Additives

Our earlier handsheet studies have shown that strength aids can enhance sheet strength by either covalent bond formation or ionic interactions. The former generally provide stronger sheets under dry and moist conditions.

As might be expected, they are much more effective as wet strength aids than are the purely ionic materials whose bonds dissociate when placed in water. It was of interest to determine how the individual fiber/fiber bonds were affected by the type of bonding supplied by the strength aids. The lightly refined fibers were treated with either the PAE/CMC combination (sequential addition) or the ionic PDADMAC/NaPSS combination. The average values are given in Table 5 in columns two and three; the strength aids' effectiveness may be judged by comparison with the values for the untreated fibers in the first column. Both additive combinations greatly improve the strength of the bonds. The difference between the two is not statistically significant. This finding confirms the handsheet results that covalent bond formation is not a prerequisite for substantial strength improvement.

Effect of Relative Humidity

It is well-known that both sheet and individual fiber properties are affected by the relative humidity (or moisture content). Specifically, both the tensile strength and the tensile modulus of these decrease with increasing relative humidity. Since sheet strength is a function of the properties of both the individual fibers and of the bonds between them, it was not evident whether the fiber/fiber bond was also influenced by moisture. Experiments were carried out, therefore, to ascertain this dependence on the same lightly refined fibers mentioned above. Individual fiber/fiber bonds were prepared as before. After installation in the FLER II for breaking load measurement, the bonded fibers were conditioned in a gentle stream of air regulated to either 75 or 88% RH. (The room is conditioned to 50% RH (72°F) for all the other measurements). The conditioning period of three minutes at the elevated relative humidity was judged sufficient for the sample to essentially attain moisture equilibrium.

The bond was then strained to failure as usual. The average strength values are listed in Table 6. Specific bond strength decreases with increasing relative humidity as do individual fiber strength and sheet strength.

Table 6. Effect of relative humidity on average bond parameters (lightly refined [570 mL CSF] softwood unbleached kraft fibers).

	Relative Humidity, %		
	50	75	88
Breaking load, g	0.73	0.60	0.42
Bond area, μm^2	2070	2260	2220
Specific Bond Strength, $\mu g/\mu m^2$	360	290	210

Handsheets were also formed from these same (classified) fibers and were tested at 50, 75, and 92% RH. The strength results are presented in Table 7. The trends are similar to those for the individual fiber/fiber bonds. Whether the decrease in sheet properties with increasing RH is a result of the similar decrease in fiber strength or in bond strength cannot be determined from the data in hand. Likely, both contribute.

Table 7. Effect of relative humidity on sheet properties (lightly refined [570 mL CSF] softwood unbleached kraft pulp-classified)

	Relative Humidity, %		
	50	75	92
Moisture Content, %	--	10.5	15.5
Breaking Length, km	4.5	3.2	2.2
TEA, kgm/sqr m	4.0	3.8	2.6
Et, kg/cm	350	230	140
Stretch, %	2.1	2.8	2.8
STFI, lbs F/inch	7.2	4.4	3.3

Data Analysis

We have amassed a great deal of additional data on the fiber/fiber single bonds discussed above and in the previous status report. Currently, this data is being entered into a microcomputer for further analysis including statistical analysis.

THE INSTITUTE OF PAPER CHEMISTRY

Appleton, Wisconsin

Status Report

to the

PAPER PROPERTIES AND USES

PROJECT ADVISORY COMMITTEE

Project 3469

STRENGTH IMPROVEMENT AND FAILURE MECHANISMS

September 11, 1987

PROJECT SUMMARY

PROJECT NO. 3469: STRENGTH IMPROVEMENT AND FAILURE MECHANISMS

STAFF: J. Waterhouse, W. Whitsitt September 11, 1987

PROGRAM GOAL:

Identify critical parameters which describe converting and end-use performance and promote improvements in cost/performance ratios.

PROJECT OBJECTIVE:

Establish practical methods for enhancing strength properties (especially compressive strength) during paper manufacture and to evaluate deformation behavior as it relates to sheet composition and structure.

PROJECT RATIONALE, PREVIOUS ACTIVITY and PLANNED ACTIVITY FOR FISCAL 1987-88 are on the attached 1987-88 Project Form.

SUMMARY OF RESULTS LAST PERIOD: (October 1986 - March 1987)

(1) A paper "Morphological Factors in the Refining of Eucalypt and Pinus Radiata Fiber" was presented at PIRA's Advances in Refining Technologies International Conference, Birmingham, England, December 1986. A copy of this paper is included in Appendix 1.

(2) A number of 16 mm x 16 mm wood coupons (230) of white spruce have been prepared and characterized and will be used primarily to determine the effects of lignin content on compressive strength.

(3) Capital has now been authorized for the purchase of the major components for the API/IPC formation tester which include an x-y table, optical equipment and a beta source.

(4) Commercial samples of newsprint, tissue and fine papers and their furnishes have been obtained for the API/IPC formation study. Noble and Wood's and Formette handsheets have been made for these furnishes. An extensive property evaluation of the commercial and handsheet samples has also been completed.

(5) A series of Formette handsheets have been made and characterized, for the purpose of determining the effects of fiber orientation and furnish composition on the variation of internal stress and properties in the thickness direction of paper.

(6) In student related work Tom Bither's doctoral research is entitled "Strength Development through Internal Fibrillation and Wet Pressing. Tom has established a suitable method for wet pressing and restrained drying of his handsheets, and has measured changes in pore size distribution as a result of refining and wet pressing.

(7) In student related work Maripat Franke master's research is entitled "Z-direction variation of internal stress and paper properties". This project will be completed during this winter quarter.

SUMMARY OF RESULTS THIS PERIOD: (April 1987 - September 1987)

(1) A paper entitled, "The Effect of Supercalendering on the Strength Properties of Paper" has been prepared for presentation at "The International Paper Physics Conference Auberge Mont Gabriel, Quebec, Canada, September 15-18, 1987.

(2) The design of the API/IPC Formation Tester has been completed and its fabrication is expected to be completed by the end of September 1987.

(3) A numerical procedure for determining the variation of residual stress in the Z-direction from curvature and elastic property measurements is being developed.

(4) In student related work Hilda Cedegren is exploring fiber techniques as part of her master's research project, "The effect of Lignin and Hemicellulose Removal on the Short Span Compressive Strength Potential of White Spruce".

(5) In student related work Tom Bither is making fracture toughness measurements using a modified IPC in-plane tear tester as part of his Ph.D. research entitled, "Strength Development through Internal Fibrillation and Wet Pressing".

PROJECT TITLE: Strength Improvement and Failure Mechanisms

PROJECT STAFF: J. Waterhouse/W. Whitsitt

PRIMARY AREA OF INDUSTRY NEED: Properties related to end use

Date: 1/14/87
Budget: $90,000
Period Ends: 6/30/88
Project No.: 3469

PROGRAM AREA: Improved converting processes and converted products

PROGRAM GOAL:

Identify critical parameters which describe converting and end-use performance and promote improvements in cost/performance ratios.

PROJECT OBJECTIVE/GOAL:

To evaluate deformation behavior and its relationship to sheet composition and structure, and to establish practical methods for enhancing strength properties (especially compressive strength).

PROJECT RATIONALE:

Deformation and strength properties are important in predicting end use performance. An improved understanding of failure mechanisms and ways to improve certain strength properties are important to nearly all grades. The recognized importance of compressive strength in linerboard and corrugating medium to box performance provides impetus for research in this area. The approach is to meet the objectives through new papermaking strategies.

RESULTS TO DATE:

We have shown that compressive strength of paper is highly related to a product of in-plane and out-of-plane elastic stiffnesses. The relationship holds for commercial and experimental sheets made under a variety of conditions. This development suggests it will be possible to monitor compressive strength in the mill using ultrasonic techniques.

Compressive strength is enhanced by high densification, which increases bonding, and high fiber axial compressive stiffness. Thus compressive strength increases with refining and wet pressing. Within a practical range, higher CD compressive strength can be achieved by decreased fiber orientation, loose draws, and/or increased CD restraint during drying. Where limitations to increased refining and wet pressing exist, low levels of polymer addition could be used as a viable means to improve compressive strength. The effect of pulp type and additives on the stiffness-compressive strength correlation has been investigated. A technique involving small wood coupons and mini handsheets has been developed to measure the compressive strength potential of wood fibers.

We have developed a torsion mode technique for measuring the out-of-plane shear stress-strain behavior, and studied ZD shear straining on compressive strength. Internal stress variations have been determined in the thickness direction together with the variation of in-plane and out-of-plane properties. Measure-

ments of the relative losses in elastic and strength properties due to super-calendering have been made. The layer removal technique has been used to determine the Z direction variation of residual stress.

PLANNED ACTIVITY FOR FY 1987-88.

Non-destructive characterization of wood coupons, pulped wood coupons, and mini handsheets made from them, will be used to estimate the compressive strength potential of certain softwood and hardwood species as a function of lignin removal.

Work will continue on measuring the deformation behavior of board when subjected to combined stresses, an important aspect of a number of converting processes.

Complete construction of a formation tester capable of the simultaneous measurement of light transmittance, reflectance and beta particle absorption; and provide suitable software for formation analysis.

STUDENT RELATED RESEARCH

T. Bither, Ph.D.-1988; H. Cedergren, M.S. - 1988.

Status Report

STRENGTH IMPROVEMENT AND FAILURE MECHANISMS

Project 3469

INTRODUCTION

This project is an outgrowth of two earlier projects namely Project 3469 "Compressive Strength Improvement" and Project 3500 "Shear Deformation and Failure", and embraces the following areas: Compressive Strength Improvement, Formation Measurements, Combined Stress Measurements and Internal Stresses in Paper and Board. The project advisory committee has expressed an interest in all of these areas, however they have recommended that Formation Measurements should receive priority if a choice has to be made because of manpower or funding limitations.

1. COMPRESSIVE STRENGTH IMPROVEMENT

The possibility of using small wood coupons (15 mm x 15 mm) and mini-handsheets (19 mm diameter) to determine the effects of species and yield on compressive strength has been demonstrated in earlier work. The main objective of this approach is to determine how the compressive strength potential of the fibers in the wood coupon, and their subsequent modification through chemical and mechanical treatments is realized in paper and board. A flow diagram outlining the steps in this procedure is shown in Fig. 1.

Characterization of the wood coupons before and after delignification includes the measurement of elastic constants using out-of-plane longitudinal wave propagation techniques. Following fiber separation, mini-handsheets are made. Characterization of these includes measurement of apparent density, elastic constants, and compressive strength.

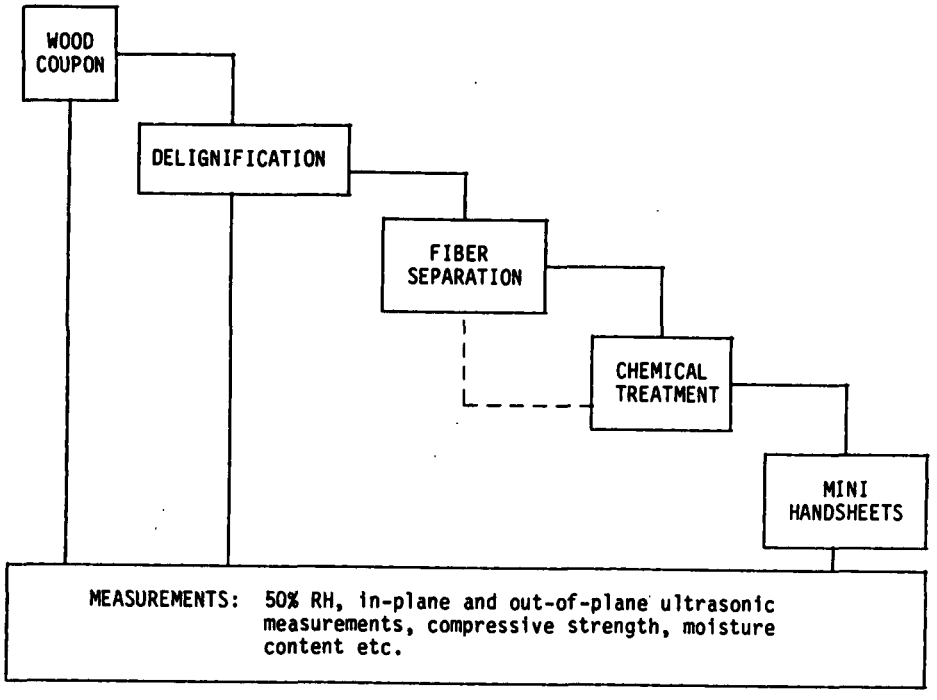

Figure 1. Flow diagram for determining Compressive Strength Potential.

Results to date, using white spruce wood coupons which have been delignified using an acid chlorite procedure, indicate that the elastic constants of the wood coupons increased significantly with increasing wood density and delignification. Furthermore the elastic constants of the handsheets were significantly higher than those predicted using the wood coupon measurements, and assuming a handsheet having a random fiber orientation.

Further work in this area is now being undertaken by Hilda Cedergren in a student related project. This will involve the preparation of wood coupons at different yields and the development of suitable methods of fiber separation to minimize fiber damage.

2. FORMATION MEASUREMENTS

It is not surprising that the recent emphasis on improving paper quality has led to a renewed interest in formation. A single precise definition

of formation is elusive, however it can be argued that a number of definitions are possible and the problem is to select the definition most appropriate to the quality problem under consideration whether it be concerned with the operation of the paper machine or associated with the converting or end use characteristics of paper. Even this task is not easy and printing provides a good example. Although formation has long been recognized as important to printing there is still not a satisfactory definition or measurement of formation which can be related to printability. Nevertheless we understand formation to be concerned with small scale variations in properties which might include optical, mass, compressibility, roughness, and porosity. Initially our main concern will be with small scale optical and mass related property variations.

We are currently undertaking for API an evaluation of both off line and on line commercial formation measuring instruments. In addition as a joint effort with API we are building a new formation tester capable of making light transmission and reflectance measurements, as well as beta particle absorption measurements. The instrument layout is shown diagramatically in Fig. 2 and a general view of it is shown in Fig. 3.

The instrument utilizes where possible off-the-shelf components. Presently the collimating source frame and adjustable detector arm are being fabricated, and we expect completion of the assembly by the end of September. The system for making light transmission measurements is currently being evaluated. Advice on, and a specification for a suitable promethium source was obtained courtesy of Wiggins Teape (Peter Herdman). The source we are attempting to purchase is a 50 millicurie source on a 5 mm aluminium disk with 2 micron window. This source type would enable us to greatly reduce the dwell time required

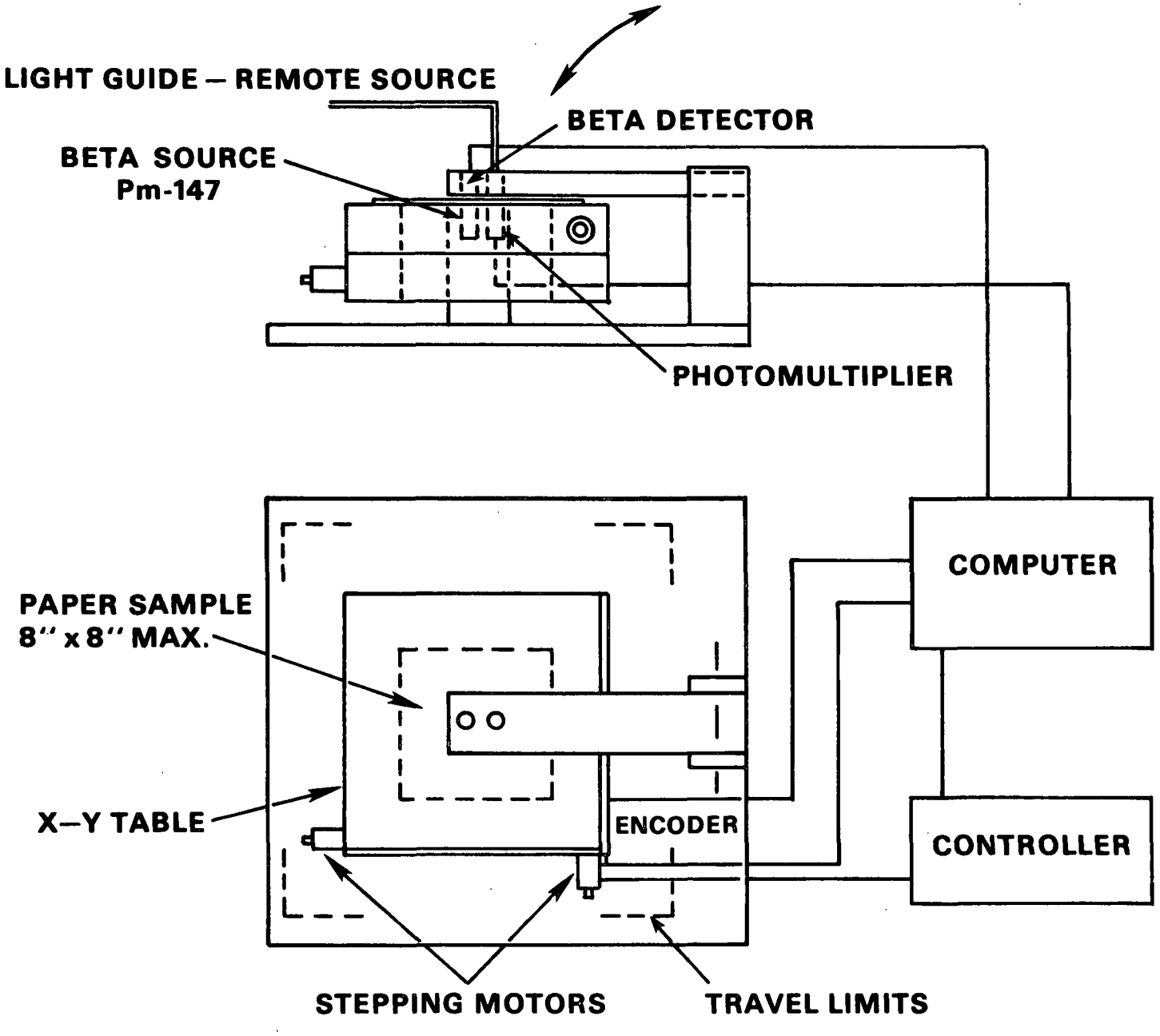

Figure 2. Schematic layout of formation tester.

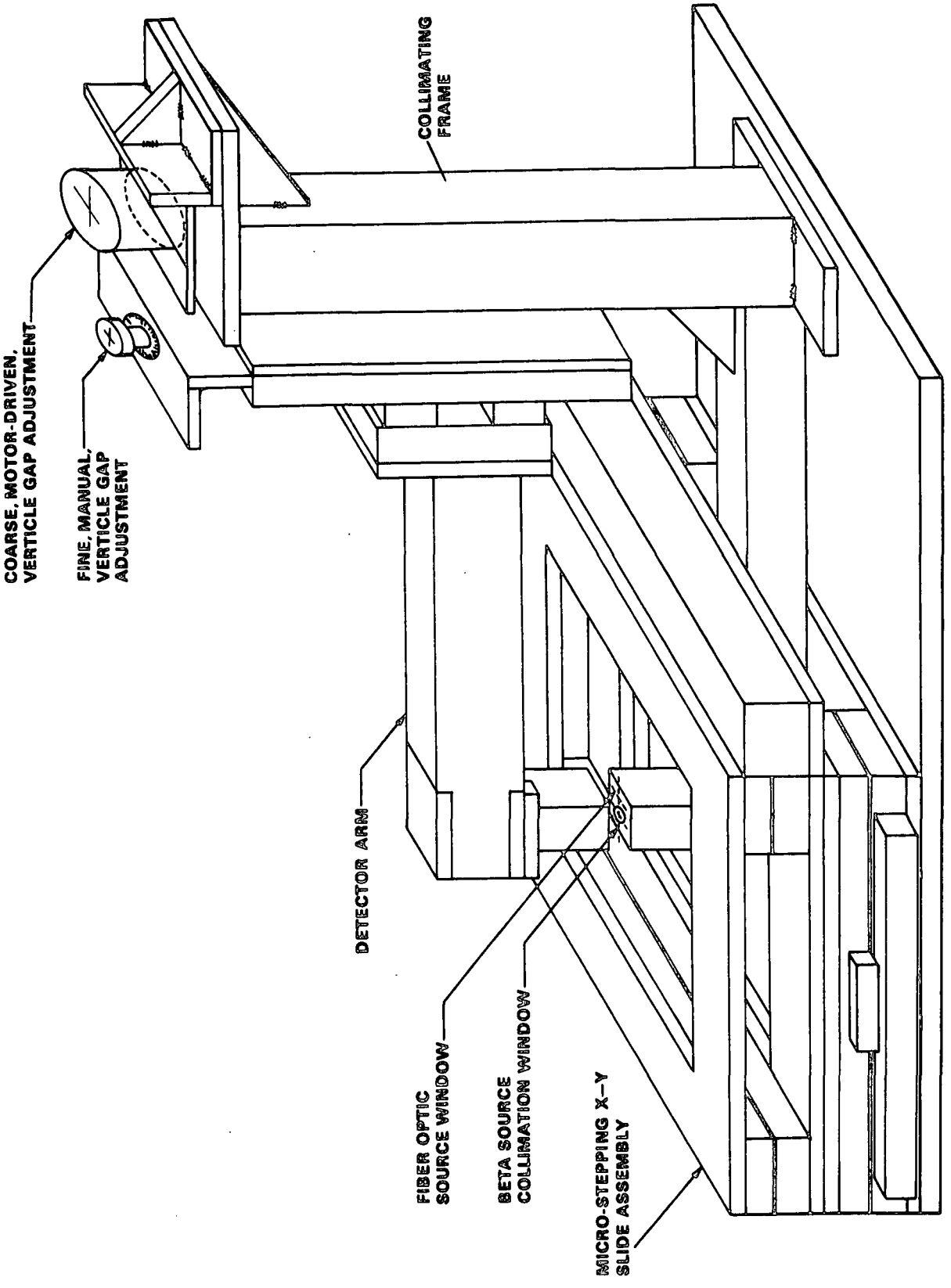

Figure 3. General view of formation tester.

for beta particle counting. However we recently learned from Amersham International, the sole proprietors of promethium 147, that it would no longer be available in four years time unless alternative sources can be located, e.g., Russia or China. This would mean that a source might only be available for the next six years (i.e. the half life of promethium 147 is 2.7 years). Amersham, at this point in time, are not anxious to secure new business.

We are also in the process of developing the necessary software for the formation tester and investigating packages for texture and image analysis as part of our output of formation information.

3. COMBINED STRESS MEASUREMENTS

Combined stresses, particularly combinations of out of plane stresses, occur in a number of converting processes such as corrugating and calendering. In past work we have investigated out-of-plane shear deformation behavior and in student related work we have investigated supercalendering as an example of combined out-of-plane stresses consisting principally of a normal stress and a cyclic shear stress. No significant progress has yet been made towards the building of an instrument to measure the deformation behavior of paper and board when subjected to combined out-of-plane stresses. However a paper has been prepared on the effects of supercalendering on the elastic and strength properties of paper (see Appendix 1) for presentation at the International Paper Physics Conference, Mont Gabriel, Quebec, Canada. It is clear from writing this paper that more work is necessary to determine more precisely the reasons for the large losses in elastic properties which are produced by supercalendering.

4. INTERNAL STRESSES IN PAPER AND BOARD

Internal stresses in paper and board are an important factor in their converting and end use behavior. These stresses which are generated during the

papermaking process may be modified during converting, and can play an important role in dimensional stability related problems such as curl, and some elastic and failure properties. Currently we are investigating the layer removal technique as a means of measuring internal stresses (residual stresses) and in-plane and out-of-plane property variations in the thickness direction of paper. A series of Formette handsheets have been made to determine the effects of fiber orientation and furnish composition variations in the thickness direction on property and residual stress distributions in the thickness direction. The overall composition and properties of these handsheets are given in Table 1.

Grammage, caliper, in-plane and out-of-plane elastic constants and curvature measurements have been made on a series of surface ground samples obtained from the handsheets shown in Table 1.

Loss tangent measurements using the technique developed by Chuck Habeger have also been made on these samples.

Presently a numerical procedure is being developed to determine the variation of residual stress in the thickness direction from the curvature and elastic property measurements.

STUDENT RELATED WORK

1. "Strength Development through Internal Fibrillation and Wet Pressing" is the title of Tom Bither's doctoral research and Tom will report on his work at the forthcoming PAC Meeting.
2. "The effect of lignin and hemicellulose removal on the short span compressive strength potential of white spruce" is the title and subject matter of Hilda Cedergren's Masters research project. This work has already been commented on in the section Compressive Strength Improvement.

Table 1. Summary of sheet properties for residual stress and properties study.

Sheet Structure & Furnish*	Fiber Orient.	Apparent Density g/cm	Mean In-plane Constant (km/sec)	Out-of-plane Constant (km/sec)
100% S.W.	1.19	0.830	9.21	0.273
	1.74	0.834	9.29	0.264
50% S.W./ 50% unbl. S.W.	1.12	0.806	9.34	0.244
	1.73	0.790	8.77	0.246
25% S.W. / 50% unbl. S.W. / 25% S.W.	1.19	0.801	9.30	0.266
	1.85	0.809	9.42	0.276
25% unbl. S.W. / 50% S.W. / 25% unbl. S.W.	1.15	0.790	9.57	0.253
	1.90	0.804	9.80	0.266

*CSF: S.W. 641 ml., unbl. S.W. 443 ml., 50% S.W./50% unbl. S.W. blend 569 ml.

THE EFFECT OF SUPERCALENDERING ON THE STRENGTH PROPERTIES OF PAPER

L. A. CHARLES and J. F. WATERHOUSE

THE INSTITUTE OF PAPER CHEMISTRY
APPLETON, WISCONSIN 54912

ABSTRACT

This investigation is concerned with how supercalendering affects certain strength and elastic properties of paper, and how these changes are affected by wet pressing and fiber orientation.

Formette handsheets were made at three levels of fiber orientation and three levels of wet pressing; they were then subjected to four levels of supercalendering using a laboratory supercalender. A reduction in both in-plane and out-of-plane elastic properties was found with increased supercalender loading. The highest rate of reduction was in the out-of-plane moduli (i.e., longitudinal and shear), and increased with increased wet pressing. The in-plane CD modulus was more severely affected than the MD modulus, with the loss in CD modulus increasing with increased fiber orientation.

The in-plane elastic anisotropy of the sheet decreased with increased densification by wet pressing, and increased with increased densification by supercalendering. This effect, together with a reduction in out-of-plane elastic moduli, strongly suggests a bond breaking process is occurring, despite the reduction in scattering coefficient with increased supercalendering.

Tensile and compressive strength losses are not as great as might be expected from the losses in elastic moduli due to supercalendering. In fact, no significant loss in failure properties was found at the highest level of wet pressing. Consequently, the correlation obtained between these strength properties and elastic moduli for wet pressing is altered by supercalendering.

INTRODUCTION

Calendering and supercalendering are important unit operations, whose main function is to improve the surface characteristics of paper, such as smoothness and gloss. Strength and other properties may also be affected during these operations. However, research to date has been mainly concerned with understanding how the surface characteristics of paper are modified by calendering and supercalendering.

Strength related properties are important with regard to the converting and end-use performance requirements of paper. For example, the gradual reduction in grammage in some fine paper grades and the need to retain stiffness places greater emphasis on minimizing stiffness and other strength losses occurring during calendering and supercalendering. Strength maintenance is also important with regard to press room runnability.

The impact of calendering and supercalendering on the strength properties of paper has been investigated by a number of researchers [1-15], with the main emphasis on the calendering of newsprint [4-6,8,10-11]. Data taken from Rance [12] given in Table I, illustrate that supercalendering can either improve or adversely affect strength properties, depending on the grade of paper involved.

Table I. Effect of supercalendering on the strength properties of some grades of paper.

Properties	NEWSPRINT		MACHINE COATED		GLASSINE	
	Before	After	Before	After	Before	After
Grammage, g/m^2	54	--	105	--	32	--
Density, g/cm^3	0.41	0.63	0.91	1.16	0.8	1.32
Breaking length, MD (km)	2.2	2.2	4.6	1.1	1.1	2.3
Tear, MD (mN)	19	16	55	47	17	15

Peel and Hudson [2], in summarizing the impact of supercalendering on strength properties for a variety of grades, found slight losses in tensile and burst strength of 0 to 10%, a loss in tear strength of 10 to 15%, and an improvement in fold endurance of 10 to 40%. Losses in specific tensile modulus with calendering have been reported by Lyne [6] and Back and Mataki [13].

Ways to circumvent the loss of properties in calendering, particularly loss in bulk, has led to the concept of gradient calendering, e.g., temperature, Kerekes and Pye [5], and Crotogino [11]; and moisture, Lyne [6]. Taking advantage of the viscoelastic nature of paper, improvement in surface properties is accomplished by treating the surface layers of the paper without

affecting its inner core. In addition to bulk preservation, strength properties are less affected when gradient calendering is employed. Clearly, it is of importance to understand the reason for these changes if we are to exercise better control over calendering and supercalendering.

The action of the supercalender and its impact on surface finish has been a controversial issue for a number of years. It now appears to be reduced to one of semantics, i.e., the debate between microslip and replication as proposed by Peel and Hudson [2] and Pfeiffer [9], respectively. By action we mean: what stresses does the paper web experience during passage through the supercalender nip? These stresses not only act to change the surface properties of the sheet, but can also affect strength and other bulk properties. According to Peel and Hudson [2] the principal stresses involved are a normal stress and a cyclic shear stress. Tension and bending stresses are also present. Van den Akker [1] stressed the importance of shear in the action of the supercalender. The relative contribution from shear and normal stresses will be controlled by a number of factors including the characteristics of the soft roll, particularly its Poisson's ratio.

The objective of the present study is to determine how the elastic and strength properties of paper are modified by the action of supercalendering.

EXPERIMENTAL

The main purpose of these experiments was to compare the densification of an uncoated web by wet pressing and supercalendering. Preliminary work [15] with commercial coated two side (C2S) samples convinced us that we first needed to understand the response of an uncoated base material to the action of supercalendering before considering the effects of coating.

Handsheets with three levels of fiber orientation (approximately a 1:1, 2:1, and 3:1 MD/CD elastic constant ratio measured ultrasonically) were made on the Formette Dynamique. The market pulp, which was a bleached kraft southern pine, was beaten to 600 CSF in a valley beater. After the sheets were formed (using a five shed wire 84 x 68 mesh) and couched, they were wet pressed (0 pli, 281 pli, 750 pli) to produce three levels of densification, using The Institute of Paper Chemistry's press and dryer combination. The purpose of this arrangement is to be able to produce handsheets dried as close as possible to conditions of full restraint. The dryer can surface temperature was 195°F. In order to measure any dimensional changes the sheet may undergo during wet pressing, drying, or supercalendering, the sheets were marked after couching in both the MD and CD directions.

After preconditioning (30% RH, 73°F, for 48 h) and conditioning (50% RH, 73°F, for 48 h) various nondestructive and destructive tests were performed on one handsheet from each condition. The conditioned basis weight of the handsheets was 214.8g/m^2 with a standard deviation of 3.7g/m^2.

The handsheets were supercalendered using the laboratory facilities at Wartsila-Appleton Machine Co. (now Valmet Inc.). The single nip supercalender described by Agronin [16] consisted of a 10-inch diameter iron roll and a 13.48-inch diameter AMCO 80# White cotton filled roll. The speed and temperature of the iron roll were held constant at 300 fpm and 160°F, respectively. The filled roll temperature was 153°F plus or minus 5°F. The roll surface temperatures were measured using an infrared pyrometer. This device has a bracket which holds a blackened Teflon strip in front of the thermometer lens. The Teflon strip is held in contact with the roll and the temperature of the Teflon is measured. This eliminates any other environmental effects on the temperature being read.

The Formette handsheets (approximately 36 inches x 8.5 inches) were aligned in the machine direction and hand fed into the single supercalender nip, with the wire side facing the steel roll. The sheets were supercalendered in the order of increasing load, at levels of 0 pli (< 100 pli), 1000 pli, 1500 pli, and 2000 pli. In addition, one control sheet was exposed to the environment of the supercalendering laboratory (35% RH and 72°F) but was not supercalendered. After supercalendering the samples were immediately placed in plastic bags and brought back to our laboratory for preconditioning and conditioning as noted above.

After conditioning, both nondestructive and destructive property measurements were again performed. The samples were measured for MD and CD dimensional changes after wet pressing and drying, and after supercalendering. Other nondestructive tests included soft [17] and hard platen caliper, Parker Print-Surf smoothness at a land pressure of 10 Kgf/cm^2, Gurley porosity (seconds to displace 100 mL), in-plane and out-of-plane measurement of elastic constants [18-19], and scattering coefficient. Tensile deformation behavior and STFI compressive

strength measurements were also made. Tests were performed according to TAPPI standards where appropriate.

RESULTS AND DISCUSSION

Supercalendering is one important converting process where paper is subjected to combined out-of-plane stresses. The effects of densification by wet pressing and supercalendering are compared in Figures 1 through 11. The expected improvement in surface smoothness by supercalendering is shown in Figure 1. Smoothness appears to be slightly impaired by increased wet pressing.

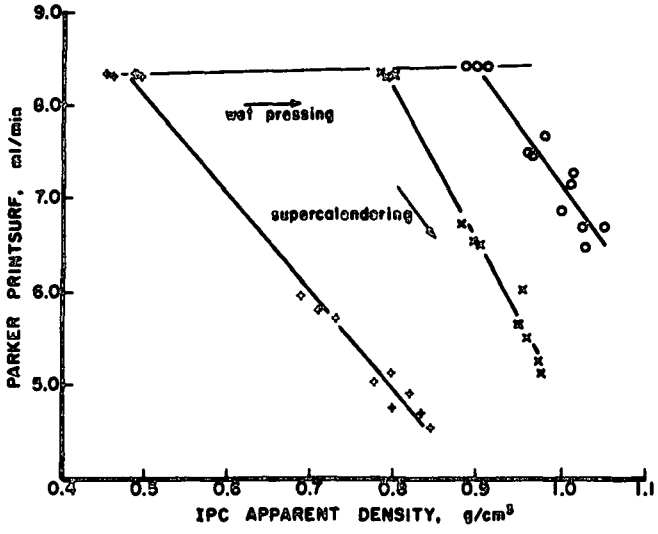

Fig. 1. Effects of wet pressing and supercalendering on Parker Print-Surf smoothness.

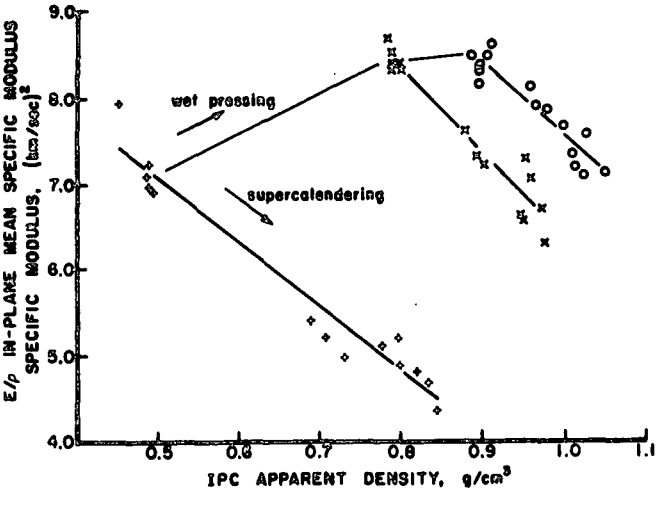

Fig. 2. Effects of wet pressing and supercalendering on in-plane mean specific modulus.

The effects of wet pressing and supercalendering on in-plane and out-of-plane elastic moduli are shown in Figures 2 through 5. We note, in general, that the moduli are improved by wet pressing, but a significant loss results from supercalendering.

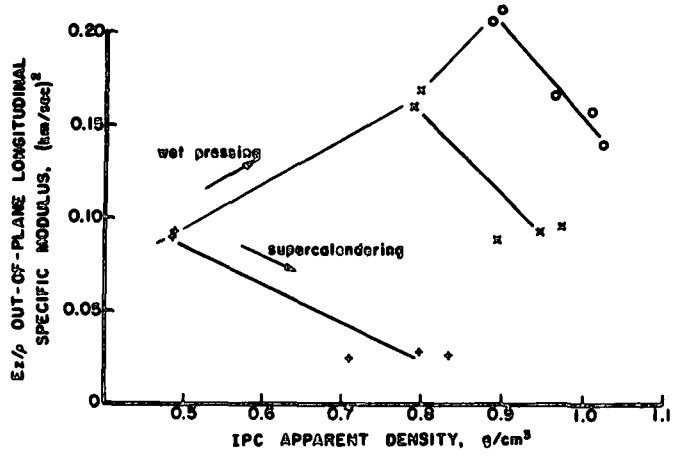

Fig. 3. Effects of wet pressing and supercalendering on out-of-plane longitudinal specific modulus.

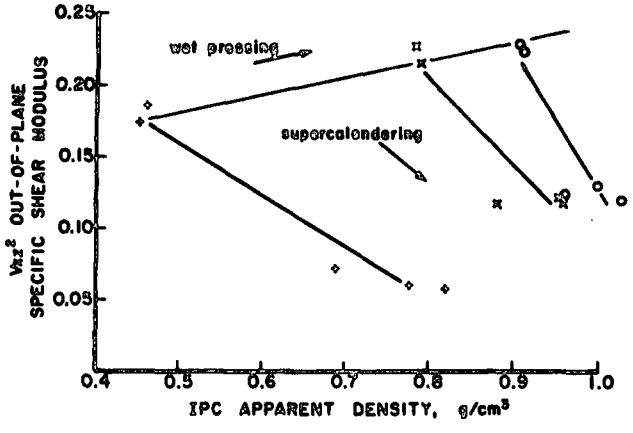

Fig. 4. Effects of wet pressing and supercalendering on out-of-plane specific shear modulus V_{xz}^2.

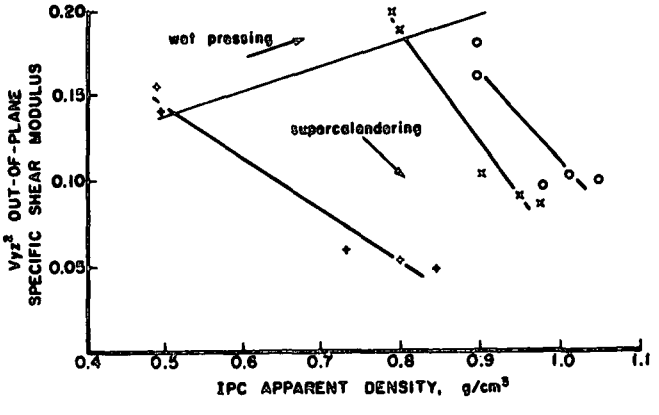

Fig. 5. Effects of wet pressing and supercalendering on out-of-plane specific shear modulus V_{yz}^2.

According to the regression line data shown in Table II, the rate of loss in elastic properties with increased supercalendering appears to

be dependent on the level of wet pressing. Its dependence is particularly strong for the out-of-plane moduli, and surprisingly the rate of loss increases with increased wet pressing.

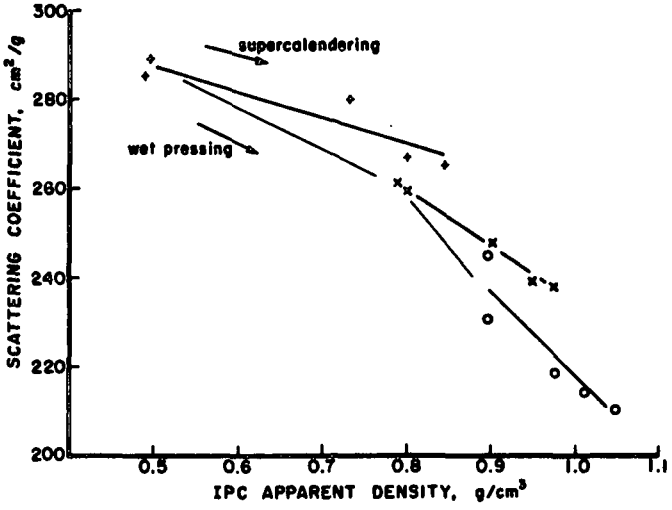

Fig. 6. Effects of wet pressing and supercalendering on scattering coefficient.

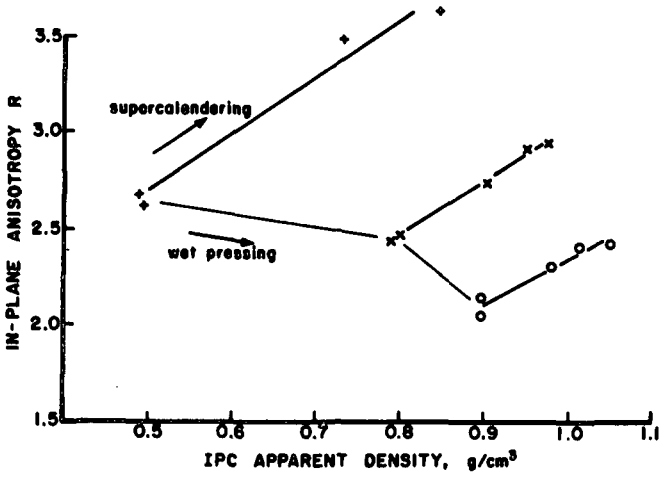

Fig. 7. Effects of wet pressing and supercalendering on in-plane anisotropy.

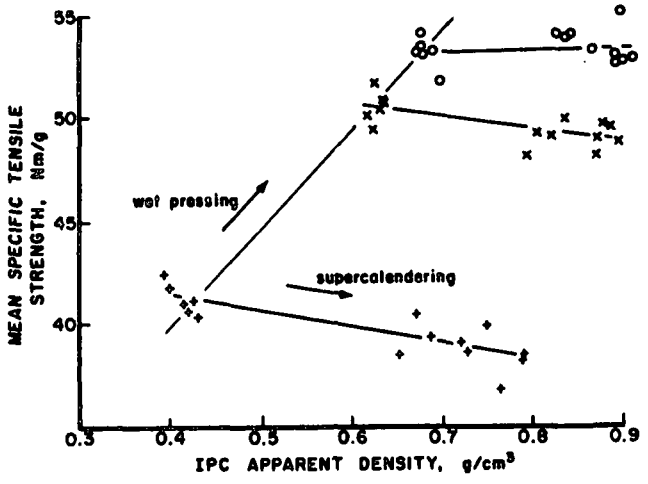

Fig. 8. Effects of wet pressing and supercalendering on mean specific tensile strength.

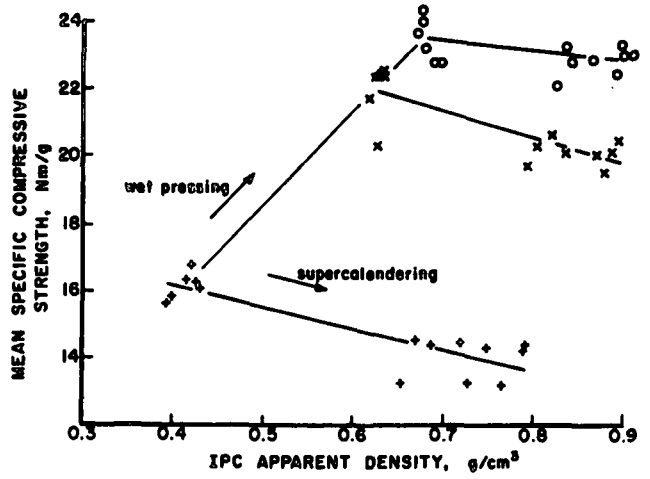

Fig. 9. Effects of wet pressing and supercalendering on mean specific compressive strength.

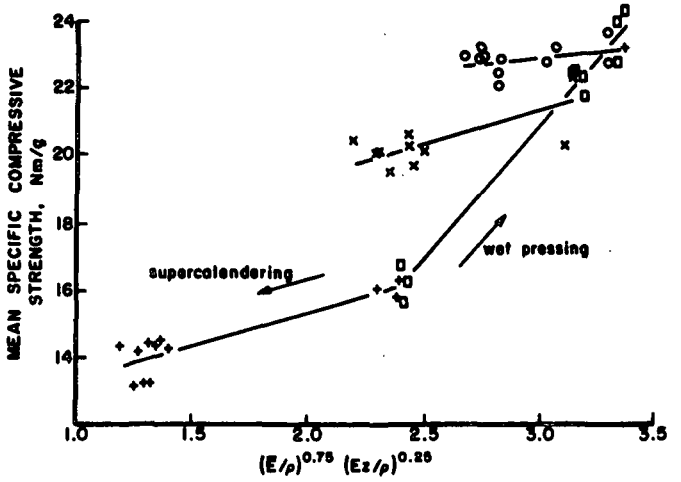

Fig. 10. Effects of wet pressing and supercalendering on mean specific compressive strength and $E/\rho^{0.75} \times E_z/\rho^{0.25}$ relationship.

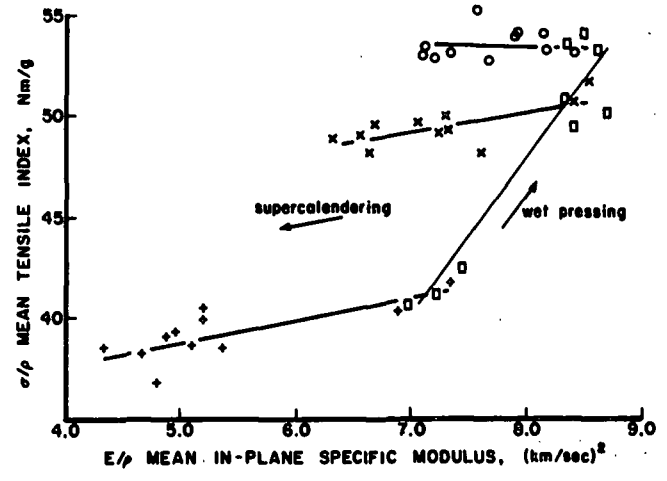

Fig. 11. Effects of wet pressing and supercalendering on mean tensile index and mean in-plane specific modulus relationship.

Table II. Slopes of regression lines for supercalendering at three levels of wet pressing.

	Low WP	Med WP	High WP
E/ρ	-7.55	-10.1	-8.78
G/ρ	-2.05	-2.99	-2.25
E_z/ρ	-0.205	-0.428	-0.491
G_{xz}/ρ	-0.362	-0.610	-0.949
G_{yz}/ρ	-0.315	-0.527	-0.523

There is little published data on the effects of calendering or supercalendering on elastic properties. In his investigation of the effects of moisture on the calendering of newsprint furnishes, Lyne [6] found a loss in mean extensional stiffness and strength properties of newsprint with increased calender loading. Back and Matuki [13] also found a loss in specific modulus with the calendering of a highly filled rotogravure paper. Furthermore, they also reported a loss in Scott bond which suggests that there may also have been a loss in out-of-plane stiffness.

The elastic properties of paper are dependent on network, interfiber bonding, and fiber properties. It is clear, therefore, that supercalendering, leaving aside for the moment network considerations (e.g., changes in fiber orientation and formation), has modified either interfiber bonding or fiber properties or both.

Let us first consider interfiber bonding. The variation of scattering coefficient (which is commonly used as a measure of unbonded surface area in paper) with densification by wet and supercalendering is shown in Figure 6. It is seen that both these processes reduce the scattering coeffficient as the sheet is densified, implying that there is an increase in bonded area. Wet pressing appears to be more effective in developing bonded area than supercalendering. However, it is possible that the reduction in scattering coefficient with supercalendering does not represent a real increase in bonded area, i.e., optical contact does not imply that the surfaces are sufficiently close to each other to establish bonding. Furthermore, since interfiber bonding according to Page and Seth [20] affects sheet modulus by its contribution to load transfer at fiber ends, this may also be a factor which is adversely affected by supercalendering. Lyne [6] also found a small reduction in scattering coefficient with calendering, and when the surface layers of the sheet were plasticized by the application of heat or surface moisture, strength losses were not as great and the scattering coefficient was further reduced. Lyne [6] suggests that the reduction in scattering coefficient may be due to a loss of intrafiber surface area as a result of web heating during supercalendering.

An interesting consequence of the effect of wet pressing and supercalendering on elastic properties is the change in the in-plane elastic anisotropy ratio shown in Figure 7. We note, that whereas wet pressing decreases the anisotropy ratio, supercalendering increases it. In unpublished work we have found that processes which are expected to improve interfiber bonding, e.g., refining, wet pressing, and certain chemical additives, reduce the anisotropy ratio, and possible bond breaking processes such as calendering tend to increase it. In processes such as calendering and supercalendering, we cannot ignore the fact that this effect may also be due, in part, to changes in fiber structure. The effect of increased bonding on elastic anisotropy, however, is in agreement with the theoretical predictions of Perkins [21].

In determining the effects of calendering and supercalendering on the recycling behavior of paper, Gottsching and Sturmer [7] found significant fiber damage as a result of increased calendering, but, none was found as a result of supercalendering. The indicators of fiber damage were changes in the long fiber fraction and a reduction in water retention value. It is possible that part of the damage may have occurred during the redispersion of the fibers.

Another aspect of fiber damage we might consider is the possibility that supercalendering may induce axial compression in the fibers. This effect could certainly contribute to a reduction in in-plane moduli, while the direction of change in out-of-plane moduli is less certain. The loss in the out-of-plane shear moduli, Figures 3, 4, and 5, suggests that bond breaking is also occurring. Leporte [3] found that web shrinkage occurred during supercalendering and increased with increasing basis weight. This suggests that supercalendering might produce a Clupak effect, evidence of which might include increased stretch and tensile energy absorption, Rance [12], Ihrman and Ohrn [22]. However, we find very little change in MD and CD stretch values as a result of increased supercalendering. Lyne [6] found that mean stretch values were significantly reduced as a result of calendering. We note that the optimum Clupak process takes place at a much higher web moisture content than used in these experiments [12]. The Clupak process has been suggested as

a means of improving newsprint runnability, see Hamrick [23].

The effects of fiber orientation and wet pressing on the reduction of in-plane machine and cross machine direction elastic moduli due to supercalendering are summarized in Table III. The reduction is defined as the ratio of the specific modulus at the highest nip loading (2000 pli) to the specific modulus prior to supercalendering.

Table III. The effect of fiber orientation and wet pressing on the reduction of in-plane MD and CD elastic moduli.

Fiber Orient. ($=E_x/E_y$)		1:1	2:1	3:1
Low dens.	E_x/ρ	0.638	0.721	0.733
	E_y/ρ	0.634	0.578	0.528
Med. dens.	E_x/ρ	0.805	0.820	0.842
	E_y/ρ	0.817	0.745	0.692
High dens.	E_x/ρ	0.814	0.887	0.908
	E_y/ρ	0.921	0.776	0.817

The decrease in the elastic moduli is greatest for the low density sheets and diminishes with increasing densification by wet pressing. Furthermore, as fiber orientation increases, we see a greater loss in the cross machine direction than the machine direction. This is consistent with the increase in plane elastic anisotropy shown in Figure 7, which we have already discussed.

An improvement in both tensile and compressive strength with increased wet pressing is shown in Figures 8 and 9. The change in strength due to supercalendering is not as great as found with the elastic properties. In fact, at the highest level of wet pressing, there is no significant loss in tensile strength as a result of supercalendering. (This result is not inconsistent with the possibility of interfiber bond damage occurring during supercalendering, since if paper is strained beyond its yield point and interfiber bonds are partially broken, its ultimate strength is not usually affected.) Moffatt, Beath, and Mihelich [4] investigated the effects of mass distribution, fiber type and orientation on the strength properties of calendered newsprint. They found that as the severity of calendering increased, the locus of failure moved from a zone where the local grammage was below the sheet average to a zone where it was significantly above. It was argued that higher grammage areas would be subjected to more damage during calendering. Initially, they found no loss in tensile strength, but as the severity of calendering increased, there was a rapid drop in tensile strength. A similar result was also found by Berger [14] who investigated the effects of temperature and pressure on the calendering of linerboard. Further work would be required to determine if the formation effect, reported by Moffatt et al. [4] is a significant factor in the present study. It is possible that the high basis weight and good formation of the Formette handsheets used in this study would preclude that effect. Furthermore, as we have already noted, Gottsching and Sturmer [7] did not find any evidence of fiber damage as a result of supercalendering.

It is surprising that compressive strength, Figure 9, is not more adversely affected by supercalendering in view of its strong dependence on both in-plane and out-of-plane elastic constants, as demonstrated by Habeger and Whitsitt [24]. The correlation of mean specific compressive strength with the product of in-plane and out-of-plane elastic moduli (one form of their correlation) is shown in Figure 10. We note that the correlation obtained for wet pressing is altered by supercalendering. Another important factor, (which we usually assume to be constant), in the Habeger and Whitsitt model is the "roughness-weakness" factor RW given below. Compressive stength is inversely proportional to RW.

$$RW = \frac{(\text{initial curvature amplitude})\quad(\text{elastic stiffness})}{(\text{lamina thickness})(\text{shear strength})}$$

We speculate, in view of the fact that tensile strength is not as adversely affected as the elastic properties, that changes in out-of-plane shear strength would also be small. This would decrease the "roughness-weakness" factor and thus partly offset the reduction in elastic constants due to supercalendering. Therefore, a change in the correlation is not unexpected.

It is also interesting to note, as shown in Figure 11, that the correlation between mean tensile index and mean in-plane specific modulus is also altered by supercalendering. We have also checked the correlation between the in-plane specific modulus measured using Instron and ultrasonic techniques, and find that it is unaffected by supercalendering. Therefore, caution must be exercised in drawing conclusions about the failure properties of paper and board from elastic constant measurements when processes such as calendering and supercalendering are involved.

CONCLUSIONS

Our investigation has been concerned with how supercalendering affects certain strength and elastic properties of paper, and how these changes are affected by wet pressing and fiber orientation. A reduction in both in-plane and out-of-plane elastic properties was found with increased supercalender loading. The largest reduction was in the out-of-plane moduli (i.e., longitudinal and shear), and increased with increased wet pressing. The in-plane CD modulus was more severely affected than the MD modulus, with the loss in CD modulus increasing with increased fiber orientation.

The in-plane elastic anisotropy of the sheet decreased with increased densification by wet pressing, and increased with increased densification by supercalendering. This effect, together with a reduction in out-of-plane elastic moduli, strongly suggests a bond breaking process is occurring, despite the reduction in scattering coefficient with increased supercalendering.

Tensile and compressive strength losses are not as great as might be expected from the losses in elastic moduli due to supercalendering. In fact no significant loss in failure properties was found at the highest level of wet pressing. Consequently, the correlations obtained between these strength properties and elastic moduli for wet pressing is altered by supercalendering.

ACKNOWLEDGMENTS

The authors wish to thank Betty John for preparing the Formette handsheets, and Laura Schumacher and the Editorial staff of IPC for their contribution in preparing this paper. The authors would also like to express their gratitude to Wartsila for the use of their laboratory supercalendering facilities. This paper is based on a Masters degree research project performed by Laurine A. Charles while a student at The Institute of Paper Chemistry.

REFERENCES

1. VAN DEN AKKER, J. A. The Possible Role of Shear in Calendering, The Paper Industry and Paper World, April, 1946:57-59.
2. PEEL, J. D. and HUDSON, F. L. Application of Elasticity Theory to a Supercalender Nip. Paper Technology 7(5):460-470 (October, 1966).
3. LEPORTE, L. E. Observations Regarding Web Behavior in a Supercalender Nip. Tappi 52(8):1495-1497 (1969).
4. MOFFATT, J. M., BEATH, L. R. and MIHELICH, W. G. Major Factors Governing Newsprint Strength. The fundamental properties of paper related to its end uses. Trans. of Symposium held at Cambridge (1973).
5. KEREKES, R. J. and PYE, I. T. Newsprint Calendering and Experimental Comparison of Temperature and Loading Effects. Pulp Paper Canada 75(11):65-72 (1974).
6. LYNE, M. B. The Effect of Moisture and Moisture Gradients on the Calendering of Paper. Fiber-Water Interactions in Papermaking, Trans. 6th Fundamental Research Symposium, held at Oxford, 1977, Fund. Res. Comm., Tech. Div. Brit. Paper Board Ind. Fed., London, 1978 Vol. 2, 641-669.
7. GOTTSCHING, L. and STURMER, L. The Effect of Calendering and Supercalendering on the Properties of Secondary Fibers. Fiber-Water Interactions in Papermaking, Trans. 6th Fundamental Research Symposium, held at Oxford, 1977, Fund. Res. Comm., Tech. Div. Brit. Paper Board Ind. Fed., London, 1978 Vol. 2, 877-897.
8. MITCHELL, J. G. Calendering Alternatives for Reducing the Bulk of TMP Newsprint. Pulp Paper Canada 81(4):T102-107 (1980).
9. PFEIFFER, J. D. Supercalendering - 1980 Update. TAPPI Proceedings, Paper Finishing and Converting Conference (1980):19-31.
10. CROTOGINO, R. H. Machine Calendering - Recent Advances in Theory and Practice Trans. Tech Sect. CPPA (December 1981): TR75-87.
11. CROTOGINO, R. H. Temperature Gradient Calendering. Tappi J. 65(10):97-99 (1982).
12. RANCE, H. F., Handbook of Paper Science, Vol. 1, Elsevier Scientific Publishing Company (1982):279-291.
13. BACK, E. L. and MATAKI, Y. Potentials of Hot Calendering for Printing Papers. Svensk Papperstid. 12:R83-R93 (1984).
14. BERGER, B. The Effects of Heat and Pressure on the Machine Calendering of Linerboard. A-190 Masters Independent Study Project, The Institute of Paper Chemistry (1985).
15. CHARLES, L. A. The Effect of Supercalendering on the Strength Properties of Paper. A-190 Masters Independent Study Project, The Institute of Paper Chemistry (1985).
16. AGRONIN, R. D. TAPPI Paper Finishing and Converting Conference Proceedings, Wausau, WI., October 2-5, 1978:69-80.
17. WINK, W. A. and BAUM, G. A. Tappi 66(9):131 (1983).

18. BAUM, G. A. IPC Technical Paper Series No. 119, Dec., 1981.

19. HABEGER, C. C. and WINK, W. A. J. Applied Polymer Science 32:4503-4540 (1986).

20. PAGE, D. H. and SETH, R. S. The Elastic Modulus of Paper. II. The importance of fiber modulus, bonding and fiber length. Tappi 63(3):113-116 (1980).

21. PERKINS, R. W. NSF Workshop on Solid Mechanics Related to Paper, August 1986, Blue Mountain Lake, N.Y.

22. IHRMAN, C. B. and OHRN, O. E. Extensible Paper by the Double-roll Compacting Process. Cambridge Symposium, Consolidation of the Paper Web, Vol. 1: 410-434 (1966).

23. HAMRICK, H. L. Extensible Newsprint by the Compaction Process. Paper 184(1):12-16, 24 (1975).

24. HABEGER, C. C. and WHITSITT, W. J. A Mathematical Model of Compressive Strength in Paperboard. Fiber Science & Technology 19:215-239 (1983).

THE INSTITUTE OF PAPER CHEMISTRY

Appleton, Wisconsin

Status Report

to the

PAPER PROPERTIES AND USES

PROJECT ADVISORY COMMITTEE

Project 3332/3613

ON-LINE MEASUREMENT OF PAPER MECHANICAL PROPERTIES

September 11, 1987

PROJECT SUMMARY

PROJECT NO. 3332: ON-LINE MEASUREMENT OF PAPER MECHANICAL PROPERTIES

PROJECT STAFF: C. C. Habeger, G. A. Baum, M. S. Hall September 11, 1987

PROGRAM GOAL: Develop ways to measure and control manufacturing processes.

PROJECT OBJECTIVE:

To develop the capability to measure elastic parameters on a moving paper web. Current emphasis is on out-of-plane measurements.

PROJECT RATIONALE, PREVIOUS ACTIVITY, AND PLANNED ACTIVITY FOR FISCAL 1987-88 are on the attached 1987-88 Project Form.

SUMMARY OF RESULTS LAST PERIOD: (October 1986 - March 1987)

(1) Improved wheel transducers have been designed and constructed. These will be mounted in a frame and subsequently tested for application in the laboratory moving web device.

(2) A caliper gage for use on moving webs has been designed and is currently under construction. The approach is similar to the soft rubber platen measurement scheme. This device will be used with the (low speed) laboratory moving web system, but is also expected to be applicable to the on-machine system.

(3) In DOE work, we intend to attempt to incorporate the above advances into the on-machine system. In addition we are simultaneously developing a second type of transducer wheel, employing a disk type piezoelectric device made from PVDF.

(4) Dr. Maclin Hall has been hired to serve as Project Manager of the DOE project.

(5) In student work, Dennis Macdonald is studying the impact of changes in jet-to-wire speed differentials on sheets properties as a prerequisite to machine control of this variable.

SUMMARY OF RESULTS THIS PERIOD: (April 1987 - September 1987)

(1) A laboratory instrument for automatically profiling caliper and longitudinal out-of-plane velocity has been constructed and is ready to be evaluated.

PROJECT TITLE: On-Line Measurement of Paper Mechanical Properties

Date: 1/21/87

Budget: $75,000

PROJECT STAFF: C. Habeger/G. Baum/M. Hall

Period Ends: 6/30/87

PRIMARY AREA OF INDUSTRY NEED: Properties related to end uses

Project No.: 3332

PROGRAM AREA: Control of manufacturing processes

PROGRAM GOAL: Develop ways to measure and control manufacturing processes

PROJECT OBJECTIVE/GOAL:

To develop the capability to measure elastic parameters on a moving paper web. Current emphasis is on out-of-plane measurements. Project 3332 is concerned with development of a laboratory device. Project 3613 is a related DOE sponsored project concerned with measurements on the paper machine and subsequent control of the papermaking process.

PROJECT RATIONALE:

The ability to measure mechanical properties on the paper machine is valuable from several standpoints. It provides a non-destructive way to assess product quality on a continuous basis. It also provides a potential means for control of process variables.

RESULTS TO DATE:

Developed theory of ultrasound propagation in paper, and developed devices for measuring paper and board in-plane elastic parameters on-machine. Successfully tested devices in mill environments. Constructed and tested a version useful for light weight grades which is also self-calibrating. Developed cross correlation technique for use with in-plane velocity measurements, and initiated work relating to on-line measurements of z-direction properties. Developed a high-frequency, low impedance out-of-plane transducer using a plastic film piezoelectric material which is superior to commercial ceramic transducers. Developed equipment for measuring moisture and temperature effects on paper elastic properties. The feasibility of ZD signal transfer between rubber faced transducers at high speeds has been demonstrated with ceramic transducers. Several plastic piezoelectric wheel transducers have been designed; two wheels with a continuous active element around the circumference and one with only a short active segment (or button) have been constructed. Apparatus has been designed and constructed to provide a practical laboratory instrument for profiling caliper and ZD velocity by feeding a paper web sample through the nip between two wheel-type transducers.

PLANNED ACTIVITY FOR THE PERIOD:

We will complete the laboratory equipment to make out-of-plane ultrasonic measurements on stepping-motor-driven paper web samples. We will continue the

development of high frequency, broad banded, and low impedance wheel-type transducers. Hardware and software for a high speed data acquisition system will be completed. Work with the "Dynamic ZD Test" equipment is complementary to the DOE sponsored research program, since this laboratory unit will also be used to evaluate wheel-type transducer designs and caliper and ZD velocity measurement techniques that may be used at the higher speeds encountered on-line.

The first phase of the DOE project requires the development of a ZD sensor capable of measurements at machine speeds. Later, this will be integrated into a system capable of making both in-plane and out-of-plane measurements at machine speeds, for the purpose of controlling the paper machine.

STUDENT RELATED RESEARCH:

Bernie Berger, Ph.D.-1988, Dennis Mcdonald, M.S.-1987.

Status Report

ON-LINE MEASUREMENT OF PAPER MECHANICAL PROPERTIES

Projects 3332/3613

INTRODUCTION

These projects are founded on earlier IPC work which dealt with on-line measurements of the in-plane elastic stiffnesses of paper and board. The current effort is concerned with measurements of z-direction elastic stiffnesses. The IPC funded portion (Project 3332) deals with such measurements in the laboratory on a strip of paper, driven by a stepping motor at relatively slow speeds. Such equipment is needed for rapid measurements on MD and CD sample strips.

With a recognized potential for significant savings in energy by on-machine measurement and control of certain paper mechanical properties, the Department of Energy is supporting on-machine sensor development (Project 3613) through Contract DE-AC05-86CE40777. This is a four year program which is just completing the first year. This report reviews the background for these projects, recent developments and current status.

REVIEW OF TECHNICAL APPROACH

Research at the Institute of Paper Chemistry[1] has demonstrated that it is possible to use ultrasound velocity techniques to make nondestructive measurements of certain paper sheet properties that are indicators of product quality and also can be correlated with the end-use strength specifications used in the paper industry.

The sheet properties of interest are the elastic stiffnesses in the plane of the paper and in the thickness direction of the paper. The elastic stiffnesses are fundamental parameters which describe the stresses developed in

the paper as it is subjected to various strains. They are of particular interest, because: (a) they are very sensitive to changes in paper machine operating variables and thus provide a measure of paper machine performance; (b) they are measures of product quality and in fact are highly correlated with many of the measures of product quality now used to characterize paper (e.g., tensile strength, bursting strength, and internal bond strength); and (c) they can be obtained nondestructively and thus may be measured on the moving web during the manufacturing process.

Because of their sensitivity to paper machine variables, and the desire to use the measurements to actually control the paper manufacturing process, sensors that measure elastic stiffnesses would be mounted on the dry end of the paper machine just ahead of the reel. We envision that these sensors would be mounted along side the basis weight gage and moisture gage now used on most paper machines and would scan the web just as those devices do. In fact it will be desirable to have the basis weight and moisture at each location as inputs to our sensors, so that the elastic stiffnesses may be adjusted to constant temperature and moisture content conditions. Such adjusted values could then be compared directly with values obtained independently in a conditioned test laboratory, if desired.

Ultrasonic sensors capable of measuring elastic stiffnesses in the plane of the paper have already been developed by IPC[2] and have been licensed to a number of instrument manufacturers. Part I of this project is specifically concerned with the development of a sensor to make on-machine measurements of elastic stiffnesses in the thickness direction of the paper and the integration of this sensor with one of the earlier sensors. It is important to be able to measure elastic stiffnesses in both the plane and thickness directions, because

this will enable us to separate the effects of different paper machine variables. When this is done, it should be possible to monitor and control these variables independently.

Upon completion of Part I (Phases 1 and 2), we expect to be able to independently monitor the effects of refining, jet-to-wire speed ratios, and draws (and the related drying restraints) on paper properties. This means that we should be able to control these three machine variables continuously and independently during the manufacturing process. Part II of the project will then be concerned with the development of algorithms, hardware, and software necessary to control these variables on the paper machine in the machine direction (Phase 3) and the cross-machine direction (Phase 4). Project objectives call for a successful demonstration of the sensor and control scheme on a laboratory scale paper machine. Success would lead to further work on a pilot scale and eventual scale-up to a full size paper machine.

ULTRASONIC TRANSDUCER DEVELOPMENT FOR ON-LINE ZD MEASUREMENT

The first requirement for on-line ZD measurement is to devise a method of transmitting a pulse of ultrasonic energy through a sheet and detecting it on the opposite side, while the paper is moving at high web speeds. A practical gage would also need to measure caliper and determine the pulse transit time with no web present. To get decent resolution of the time-of-flight, the phase shift of the signal through the sample should be as large as possible. This is accomplished on thin specimens by operating at high frequency. The frequency used in the IPC laboratory ZD instrument is 1 MHz; thus, much greater than the 80 kHz used with the in-plane on-line gages.

The coupling requirements are also different in the two cases. The aluminum button used for web contact on the in-plane gage is not acceptable here. From our experience with laboratory ZD gages, we know a conformable coupling between the paper and the transducer is necessary for efficient transfer of energy in the z-direction. We also know that this is simpler to achieve with longitudinal waves than with shear waves; therefore, the first on-line ZD attempt was designed to generate longitudinal waves. The transducer-to-web coupling is done with 1/32 inch thick sheet of soft neoprene epoxied to the face of the transducer. This is the same neoprene used in the IPC thickness gage and in our laboratory longitudinal ZD instrument.

Acoustic transducers were made from two piezoelectric ceramic disks (1/10 inch thick P.Z.T. 5A) attached to a thin aluminum button. A 1/32 inch thick sheet of soft neoprene was epoxied to the face of this transducer to provide a conformable coupling to the paper web. These ceramic disk transducers, mounted in 5 inch aluminum wheels, were tested on 42-lb linerboard and a low basis weight bond paper, using the IPC web strainer. The signal quality was excellent even at a web speed of 2000 ft/min. This demonstrated the feasibility of transmitting and detecting an ultrasonic signal in the thickness direction at line speed. However, the resonant frequency of the transducer was not as high as needed to resolve the time-of-flight of a longitudinal ZD pulse.

To overcome the frequency limitations of the ceramic button-in-wheel transducers described above, a much different design was chosen for experimental evaluation. This design is modeled after the low-impedance, broadband, disk transducers which are key components in the IPC designed and built laboratory unit for static ZD measurements. The active piezoelectric elements in these transducers are polarized polyvinylidene fluoride (PVDF or Kynar) films. This

design, described in detail in the previous report, was extended to construct wheel transducers that are active around the entire circumference.

OUT-OF-PLANE ULTRASONIC MEASUREMENTS USING WHEEL TRANSDUCERS

We have constructed a laboratory instrument which measures the longitudinal out-of-plane velocity of sound in paper samples using wheel transducers. We hope this apparatus will achieve two purposes. The direct benefit is to provide a laboratory instrument which can rapidly profile the out-of-plane velocity and soft-platen caliper of a sample running in the nip between two wheel transducers. This is also the first step toward developing an on-line out-of-plane velocity gage. We will be able to simulate some of the on-line conditions and decide what modifications will be necessary to produce a gage suitable for on-line operation.

We are using the one inch wide PVDF wheel transducers described in earlier PAC reports on this instrument. The wheels, which are five inches in diameter, are covered with the same soft neoprene used in our standard out-of-plane transducers. They are of sufficient sensitivity to communicate a signal through thick board in a laboratory environment. Their variability in diameter is about 20 microns; and, except in the region where the neoprene and PVDF films are spliced, there is less than a ten percent variability in signal strength around the circumference. For on-line operation a more sensitive receiver may be needed, and we have built a new wheel which is active only in a short segment (one inch) of the circumference. This design does improve the signal-to-noise ratio, and this wheel will be evaluated for future use on line.

Figure 1 is the mechanical drawing for the mounting and wheel alignment apparatus. The top wheel is mounted on a slide; so that, it can move up

and down as the caliper of the paper in the nip changes. An L.V.D.T. is used to sense the movement of the slide relative to the stand and to infer sample caliper. Alignment of the wheels to a standard position on their circumference is accomplished with a mechanism employing wheels and slotted cams. The bottom wheel is driven by a computer-controlled stepping motor, allowing the sample to be transported between the transducers.

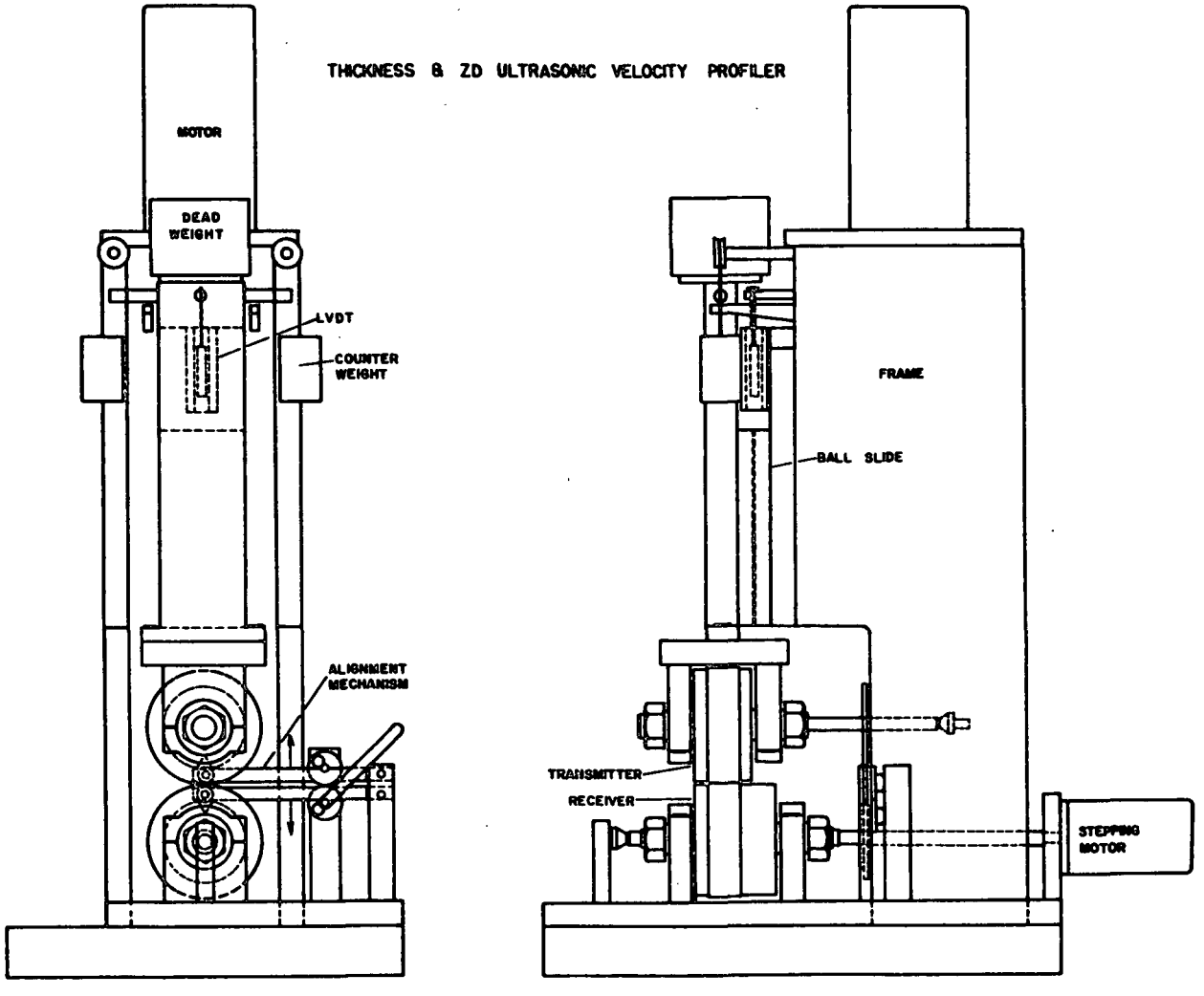

Figure 1. Schematic of out-of-plane wheel transducers and thickness measuring mounts.

Figure 2 is an operational schematic of the instrument. A Superior Electric model M063 stepping motor drives the wheels. It is connected to a Superior Electric 230 PTO motor controller, which receives instructions over a digital I/O line from the PC class AT computer, which operates the instrument. The L.V.D.T and amplifier are identical to those in our standard out-of-plane instrument and have been described in earlier PAC reports. The signal from the amplifier goes to an H.P. 3478A Multimeter. This is used as a high speed (up to 50 samples/second) digital voltmeter. It communicates the top wheel elevation to the computer over an I.E.E.E. bus. An acoustic signal sequence begins by triggering a Wavetek 143 function generator to output a single cycle sinusoidal signal. This is sent to an E.N.I. Model 240L RF Power Amplifier which drives the transmitter wheel through mercury slip rings. The receiver signal goes through mercury slip rings to Panametrics 5050AE Ultrasonic Preamplifer and then to a high speed analog-to-digital converter which communicates to the computer over the I.E.E.E. bus. The analog-to-digital converter is a LeCroy Model 8013A 100 MHz Transient Recorder. It is also equipped with a variable attenuator; so that, the computer can adjust the level of the input signal into the transient recorder to take full advantage of its eight bit resolution. The transient recorder, upon instructions from the computer, can begin the signal sequence through an external trigger output routed to the function generator.

The measurement will be accomplished in the following manner. First the caliper and delay time readings must be calibrated. After setting the wheel positions with the alignment mechanism, the first step in the calibration procedure is to place an 8 micron thick piece of aluminum foil in the wheel nip and activate the computer. The computer feeds the foil through the nip in half inch steps. At the completion of each step, the computer waits for a fixed time

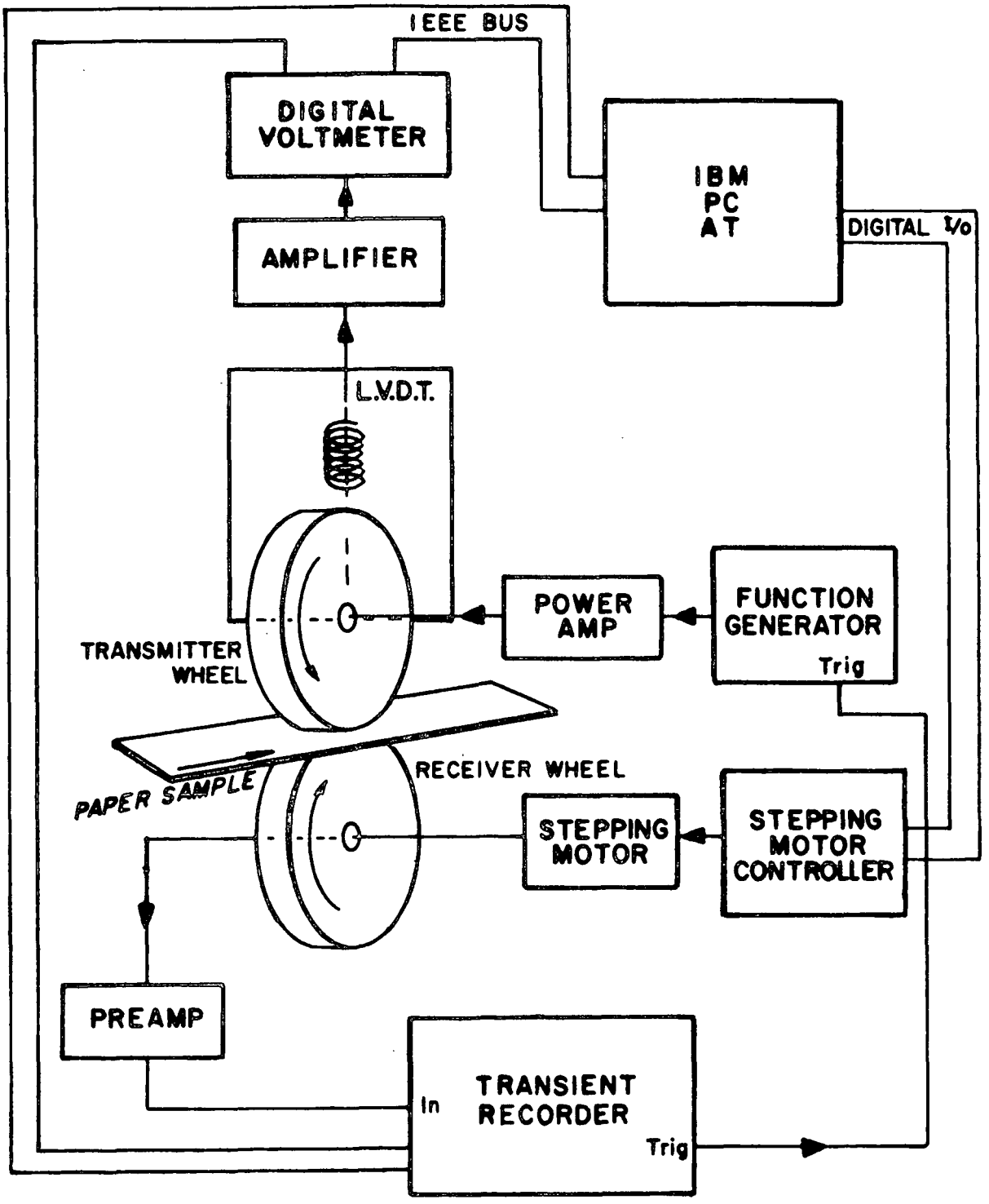

Figure 2. Schematic of laboratory out-of-plane wheel apparatus.

period (about 1/2 second) and reads the digital multimeter. It then fires an acoustic pulse and stores the resulting signal from the transient recorder in memory. Finally, it reads the multimeter again and stores the average of this reading and the first reading. This process is repeated for an operator adjusted number of times. Now, a thicker calibration sheet is placed in the nip of the manually aligned wheels. It has a known thickness, somewhat greater than the thickest sample to be tested. This is stepped between the wheels as before, but only the voltmeter readings are recorded.

Now a paper sample can be profiled. It is presented to the aligned wheels and computer manipulated between the wheels in exactly the same manner. The caliper at each position of the wheels is extrapolated from the calibration standard readings at that location. The time-of-flight is determined by cross-correlating the acoustic signal through the paper with the signal through the thin foil at the same location of the wheels.

At present, the mechanical and electronic construction of this instrument is complete. The first cut at the software is also complete, and we are ready to start checking out the operation. The phenomena which we intend to investigate is the effect of rolling rate on soft-platen paper caliper measurements.

After checking out the caliper and time-of-flight performance of the instrument, we will do a simulation of the on-line operation. For on-line work, we will not have position dependent calibration. We will simply average calibration and sample reading over several turns of the wheels and give an average reading for several feet of product. This will be accomplished on the laboratory instrument by inserting a spliced belt between the wheels and running

the stepping motor at a fixed speed. This can give us speeds of up to a few hundred feet per minute, and it provides an imitation of on-line testing without risking damage to the laboratory instrument. The results of this testing will lead to the construction of wheel transducers specifically built to operate at higher speeds on the IPC web strainer.

OTHER ACTIVITIES

To make evaluation of the wheel-type transducers more convenient, hardware has been designed to run a sample continuously through the nip in the form of a belt. This hardware is currently being made at a local shop.

Work is nearly complete on an improved design for in-plane transducers. Drawings have been completed for hardware to mount a drum unit (on hand from previous IPC work) onto the IPC web strainer. This drum will be used to hold the in-plane transducers for laboratory evaluation of their performance on a moving web. The drawings for the hardware to mount the drum have been taken to a local machine shop for construction.

REFERENCES

1. Mann, R. W., G. A. Baum, and C. C. Habeger, Tappi 62(8):115(1979).

2. Habeger, C. C., and G. A. Baum, Tappi 69(6):106(1986).